

AD-777 161

X-RAY EVALUATION OF CRYSTALS FOR
STELLAR SPECTROMETERS

Nikos G. Alexandropoulos

Aerospace Corporation

Prepared for:

Air Force Systems Command

29 March 1974

DISTRIBUTED BY:

NTIS

National Technical Information Service
U. S. DEPARTMENT OF COMMERCE
5285 Port Royal Road, Springfield Va. 22151

ACCESSION FOR	
RTIS	White Section <input checked="" type="checkbox"/>
P. 3	Buff Section <input type="checkbox"/>
UNCLASSIFIED	<input type="checkbox"/>
JUSTIFICATION	
BY	
DISSEMINATION AVAILABILITY CODES	
DECL.	AVAIL. AND/OR SPECIAL
A	

LABORATORY OPERATIONS

The Laboratory Operations of The Aerospace Corporation is conducting experimental and theoretical investigations necessary for the evaluation and application of scientific advances to new military concepts and systems. Versatility and flexibility have been developed to a high degree by the laboratory personnel in dealing with the many problems encountered in the nation's rapidly developing space and missile systems. Expertise in the latest scientific developments is vital to the accomplishment of tasks related to these problems. The laboratories that contribute to this research are:

Aerophysics Laboratory: Launch and reentry aerodynamics, heat transfer, reentry physics, chemical kinetics, structural mechanics, flight dynamics, atmospheric pollution, and high-power gas lasers.

Chemistry and Physics Laboratory: Atmospheric reactions and atmospheric optics, chemical reactions in polluted atmospheres, chemical reactions of excited species in rocket plumes, chemical thermodynamics, plasma and laser-induced reactions, laser chemistry, propulsion chemistry, space vacuum and radiation effects on materials, lubrication and surface phenomena, photo-sensitive materials and sensors, high precision laser ranging, and the application of physics and chemistry to problems of law enforcement and biomedicine.

Electronics Research Laboratory: Electromagnetic theory, devices, and propagation phenomena, including plasma electromagnetics; quantum electronics, lasers, and electro-optics; communication sciences, applied electronics, semi-conducting, superconducting, and crystal device physics, optical and acoustical imaging; atmospheric pollution; millimeter wave and far-infrared technology.

Materials Sciences Laboratory: Development of new materials; metal matrix composites and new forms of carbon; test and evaluation of graphite and ceramics in reentry; spacecraft materials and electronic components in nuclear weapons environment; application of fracture mechanics to stress corrosion and fatigue-induced fractures in structural metals.

Space Physics Laboratory: Atmospheric and ionospheric physics, radiation from the atmosphere, density and composition of the atmosphere, aurorae and airglow; magnetospheric physics, cosmic rays, generation and propagation of plasma waves in the magnetosphere; solar physics, studies of solar magnetic fields; space astronomy, x-ray astronomy; the effects of nuclear explosions, magnetic storms, and solar activity on the earth's atmosphere, ionosphere, and magnetosphere; the effects of optical, electromagnetic, and particulate radiations in space on space systems.

THE AEROSPACE CORPORATION
El Segundo, California

ib

UNCLASSIFIED

Security Classification

DOCUMENT CONTROL DATA - R & D		
<i>(Security classification of title, body of abstract and indexing annotation must be entered when the overall report is classified)</i>		
1. ORIGINATING ACTIVITY (Corporate author) The Aerospace Corporation El Segundo, California		2a. REPORT SECURITY CLASSIFICATION Unclassified
		2b. GROUP
3. REPORT TITLE X-RAY EVALUATION OF CRYSTALS FOR STELLAR SPECTROMETERS		
4. DESCRIPTIVE NOTES (Type of report and inclusive dates)		
5. AUTHOR(S) (First name, middle initial, last name) Nikos G. Alexandropoulos		
6. REPORT DATE 74 MAR 29	7a. TOTAL NO. OF PAGES 83	7b. NO. OF REFS 35
8a. CONTRACT OR GRANT NO. F04701-73-C-0074	9a. ORIGINATOR'S REPORT NUMBER(S) TR-0074(9260-02)-1	
b. PROJECT NO.		
c.		
d.	9b. OTHER REPORT NO(S) (Any other numbers that may be assigned this report) SAMSO-TR-74-83	
10. DISTRIBUTION STATEMENT Approved for public release; distribution unlimited		
11. SUPPLEMENTARY NOTES		12. SPONSORING MILITARY ACTIVITY Space and Missile Systems Organization Air Force Systems Command Los Angeles, California
13. ABSTRACT This report consists of three parts. The first part is an original piece of work done in collaboration with Dr. G. G. Cohen of Columbia University. It is an analysis of the principles involved in x-ray crystal evaluation and how they are applied to a number of crystals. The principles of crystal evaluation analysis as they apply to the special problems of x-ray astronomy are presented. A number of crystals were evaluated, and the energy dependence of the diffraction properties of (002) PET, (111) Ge, (101) ADP, (001) KAP, and (001) RAP are reported. The second part is a compilation of the diffraction properties of a number of crystals as reported by other authors. In the third part some technical details of a triple crystal spectrometer built by the author at Polytechnic Institute of Brooklyn are given. This spectrometer seems to be a most appropriate instrument for evaluation of crystal properties.		

UNCLASSIFIED

Security Classification

14

KEY WORDS

X-ray
Spectroscopy
Crystals
Stellar Spectrometers

Distribution Statement (Continued)

Abstract (Continued)

ia

UNCLASSIFIED

Security Classification

Air Force Report No.
SAMSO-TR-74-83

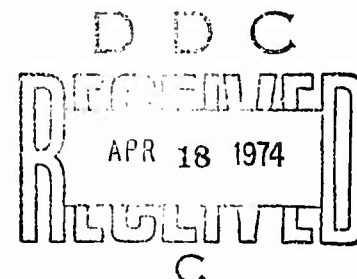
Aerospace Report No.
TR-0074(9260-02)-1

X-RAY EVALUATION OF CRYSTALS
FOR STELLAR SPECTROMETERS

Compiled by
N. G. Alexandropoulos
Space Physics Laboratory

74 MAR 29

Laboratory Operations
THE AEROSPACE CORPORATION



Prepared for
SPACE AND MISSILE SYSTEMS ORGANIZATION
AIR FORCE SYSTEMS COMMAND
LOS ANGELES AIR FORCE STATION
Los Angeles, California

Approved for public release;
distribution unlimited

-ic-

FOREWORD

This report is published by The Aerospace Corporation, El Segundo, California, under Air Force Contract No. F0470-73-C-0074, and NASA Contract No. NAS8-27404.

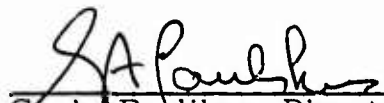
Part I of this report, "Crystals for Stellar Spectrometers", is an original piece of work done by the author in collaboration with Dr. Gabrielle G. Cohen, Columbia Astrophysics Laboratory, Columbia University, New York, New York. Dr. Cohen's research was supported by NASA under Contract NAS5-11362.

Part II, "Crystal Diffraction Properties", was compiled by the author from the works of other investigators.

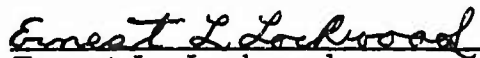
Part III, "Multi-Purpose Triple Crystal Spectrometer", presents some technical details of a spectrometer built by the author at Polytechnic Institute of Brooklyn.

This report, which documents research carried out from October 1972 through April 1973, was submitted on 27 February 1974 to Lieutenant Ernest L. Lockwood, DYAE, for review and approval.

Approved


G. A. Paulikas, Director
Space Physics Laboratory

Publication of this report does not constitute Air Force approval of the report's findings or conclusions. It is published only for the exchange and stimulation of ideas.


Ernest L. Lockwood
1st Lt., United States Air Force
Project Officer

ABSTRACT

This report consists of three parts. The first part is an original piece of work done in collaboration with Dr. G. G. Cohen of Columbia University. It is an analysis of the principles involved in x-ray crystal evaluation and how they are applied to a number of crystals. The principles of crystal evaluation analysis as they apply to the special problems of x-ray astronomy are presented. A number of crystals were evaluated, and the energy dependence of the diffraction properties of (002) PET, (111) Ge, (101) ADP, (001) KAP, and (001) RAP are reported. The second part is a compilation of the diffraction properties of a number of crystals as reported by other authors. In the third part some technical details of a triple crystal spectrometer built by the author at Polytechnic Institute of Brooklyn are given. This spectrometer seems to be a most appropriate instrument for evaluation of crystal properties₍₄₇₎

CONTENTS

FOREWORD	ii
ABSTRACT	iii
INTRODUCTION	1
PART I. CRYSTALS FOR STELLAR SPECTROMETERS	3
Introduction	3
Crystal Evaluation	5
Measurement of the Diffraction Properties of a Crystal	17
Results	21
References	37
PART II. CRYSTAL DIFFRACTION PROPERTIES	41
References	73
PART III. MUTI-PURPOSE TRIPLE CRYSTAL SPECTROMETER	75
Introduction	75
Construction of a Multi-Crystal Spectrometer	77
Applications	79

Preceding page blank

TABLE

1.	Properties of Crystals Frequently Used in X-ray Spectroscopy	42
----	--	----

FIGURES

1.	Spectral area in energy (upper scale) or in wavelength (bottom scale) covered by a single flat crystal spectrometer as a function of the crystal d spacing	6
2.	Normalized F.W.H.M. calculated according to Darwin's theory as a function of the Bragg angle θ	9
3.	Normalized crystal resolving power as a function of θ_{Bragg} (using Darwin's dynamical theory)	11
4.	The theoretical rocking curve for a (002) PET crystal at $\lambda = 8.34 \text{ \AA}$	13
5.	The alignment and orientation vectors characteristic to a double crystal spectrometer	19
6.	The measured F.W.H.M. $\sqrt{2}$ for a (002) PET crystal	22
7.	$\sqrt{2}$ (F.W.H.M.) obtained from a (002) PET crystal, similar to that used to obtain the results shown in Fig. 6 after it had been bonded to a crystal mount with urethane and vibrated according to a NASA Specification	24
8.	The F.W.H.M. for a perfect (002) PET crystal, a mosaic crystal with mosaic spread 1.5 min. and for a flat single crystal spectrometer using a mosaic PET crystal and a 1.5 min. collimator	25
9.	The calculated and the measured peak reflectivities for our best (002) PET crystal	26
10.	$\sqrt{2} \times \text{F.W.H.M.}$ for a (111) Ge crystal	27

FIGURES (Continued)

11.	The measured peak reflectivity for a (111) Ge crystal.	28
12.	$\sqrt{2} \times \text{F.W.H.M.}$ for a (101) ADP crystal.	29
13.	$\sqrt{2} \times \text{F.W.H.M.}$ of a (001) KAP crystal.	30
14.	$\sqrt{2} \times \text{F.W.H.M.}$ of a (001) RAP crystal	31
15.	Sift of the Bragg angle of Al $K\alpha$ radiation scattered by a (101) ADP crystal as a function of the crystal illumination by an incandescent lamp	33
16.	F.W.H.M. as a function of the illumination time for a (101) ADP crystal.	34
17.	The peak reflectivity for a (101) ADP crystal as a function of the illumination time	35
18.	Spectral region in energy (bottom scale) or in elements K-absorption edge (top scale) covered by a single flat crystal spectrometer as a function of 2d spacing for a number of crystals	49
19.	F.W.H.M. of (10 $\bar{1}$ 0) quartz	50
20.	The peak reflectivity of (10 $\bar{1}$ 0) quartz as a function of the Bragg angle (bottom) or as a function of x-ray energy (top).	51
21.	$\sqrt{2} \times \text{F.W.H.M.}$ of (10 $\bar{1}$ $\bar{1}$) quartz	52
22.	The peak reflectivity of (10 $\bar{1}$ $\bar{1}$) quartz.	53
23.	$\sqrt{2} \times \text{F.W.H.M.}$ of (111) silicon	54
24.	The peak reflectivity of (111) silicon	55
25.	$\sqrt{2} \times \text{F.W.H.M.}$ of (211) calcite in minutes as a function of the Bragg angle (bottom scale) or as a function of the x-ray energy (top) scale	56

FIGURES (Continued)

26.	$\sqrt{2} \times \text{F.W.H.M.}$ for calcite (211) at first, second, third, fourth and fifth order of reflection	57
27.	The peak reflectivity of (211) calcite	58
28.	The peak reflectivity of (211) calcite for a number of reflection	59
29.	The F.W.H.M. of (11 $\bar{2}$ 0) quartz	60
30.	The F.W.H.M. of (11 $\bar{2}$ 0) quartz	61
31.	The peak reflectivity of (11 $\bar{2}$ 0) quartz	62
32.	The peak reflectivity of (11 $\bar{2}$ 0) quartz	63
33.	The F.W.H.M. of (220) Germanium	64
34.	The peak reflectivity of (220) Germanium	65
35.	$\sqrt{2} \times \text{F.W.H.M.}$ of (220) silicon reported by Brogren et al ⁽¹³⁾	66
36.	The peak reflectivity of (220) silicon reported by Brogren et al ⁽¹³⁾	67
37.	$\sqrt{2} \times \text{F.W.H.M.}$ of (20 $\bar{2}$ $\bar{3}$) quartz in minutes reported by Adell et al ⁽⁸⁾	68
38.	The peak reflectivity of (20 $\bar{2}$ $\bar{3}$) quartz reported by Adell et al ⁽⁸⁾	69
39.	F.W.H.M. \times 2 of (22 $\bar{4}$ 3) quartz in minutes reported by Adell et al ⁽⁸⁾	70
40.	The peak reflectivity of (22 $\bar{4}$ 3) quartz reported by Adell et al ⁽⁸⁾	71
41.	Sideview of the Triple Crystal Multi-Purpose Spectrometer.	80
42.	Top View of Arm Ar ₂	81

INTRODUCTION

The need for compiled information on the diffraction properties of the crystals in designing an x-ray spectrometer is well appreciated by spectroscopists. However, only minor efforts have been made thus far in this direction, and a number of reports scattered throughout the literature are not easily available in an unified form to the designer. At the same time, a larger number of measurements performed by spectroscopists in their efforts to solve a specific problem never reach a publisher. The author's aim is to initiate the compilation of measured diffraction properties of crystals of some interest to the spectroscopist in a uniform way. He believes that it is possible to extend the present report to include previously unpublished data as well as future measurements that are not extensive enough to meet the standards of an original publication but which can be very handy in eliminating duplication of effort. Perhaps now is the time to create a data bank where measurements will be reported in a standard format and will be made generally available.

PART I. CRYSTALS FOR STELLAR SPECTROMETERS

INTRODUCTION

Recent interest in x-ray astronomy has turned from energy dispersive x-ray spectrometer such as scintillation and proportional counters, in the study of stellar and solar spectra to wavelength dispersive instruments, the crystal spectrometers. The configuration of these spectrometers runs from the simple geometry of a single flat crystal spectrometer to the more complicated systems using x-ray collecting optics together with a crystal analyser. The basic ideas used in the new technology are not new to the field of x-ray spectroscopy and x-ray crystallography, but many of the special problems that arise in astrophysical spectroscopy are not easily solved in the usual ways. It is the purpose of this paper to present a review of crystal evaluation analysis as it applies to instrumentation employed in x-ray astronomy, and to offer some suggested solutions to the problems that are commonly encountered. The methods can easily be applied to future astronomical applications. A general approach for selecting the most appropriate crystals for a given problem will be given here, also. The detailed proofs for our analysis can be found in the references.

Designing a crystal x-ray spectrometer has been more of an art than a systematic procedure, in contrast to the methods commonly applied to designing other instruments. In addition, difficulties arise because there is no organized source of information about spectrometer components. Therefore, one usually cannot predict the performance of a given spectrometer without making extensive measurements.

The needs of the research define the requirements of the spectrometer to be built. Typical considerations are: (a) the spectral region to be covered, (b) resolution; (c) sensitivity; (d) reproductibility (e) accuracy; (f) linearity; (g) intensity to be measured; (h) the spectrometer's physical dimensions, weight, power needs, etc.; (i) scanning pattern; and (j) size of the source.

Preceding page blank

Concerning the crystals to be used, the most pertinent information is the rocking curve as a function of energy, or at least the percent reflection (peak reflectivity), the rocking curve width at half maximum intensity and the coefficient of reflection (integral reflection coefficient). Other useful information includes: (a) the refractive index as a function of wavelength; (b) the crystal structure and the structure factor, $|F|$, for the specific reflections to be used; (c) the chemical stability and sensitivity to radiation damage; (d) the influence of surface treatment and corrosion on the diffraction properties; and (e) the mechanical properties of the crystal. Some of the above information can be found in the literature. Much more information is conveyed from investigator to investigator through private communications and never appears in print. For most crystals, the diffraction properties vary so widely with surface treatment that only actual crystal measurements are adequate.

Although studies of crystal perfection have become routine for several crystals, like silicon and germanium, for those wavelengths commonly used by crystallographers ($.497^{\circ}\text{A} - 2.29^{\circ}\text{A}$), considerable effort is needed in order to reach the same state of the art for the more complicated crystals and for the longer wavelengths of interest in x-ray astronomy.

CRYSTAL EVALUATION

After a tentative choice has been made as to the configuration of the spectrometer, the appropriate $2d$ spacing can be found from a diagram relating the spectral area to be covered to $2d$. Such a diagram is shown in Fig. 1. We have assumed a single flat crystal configuration and have used the relation:

$$\lambda_{\min} \leq 2d \left(1 - \frac{4d^2 \delta}{\lambda^2} \right) \sin \theta \leq \lambda_{\max} \quad (1)$$

where $\theta_{\min} \leq \theta \leq \theta_{\max}$. θ_{\min} and θ_{\max} are the specific angular limitations of the specific geometry, δ is the deviation of the refractive index from unity.

The index to the powder diffraction file of ASTM ⁽¹⁾ is a good starting point for preselecting a number of candidate crystals with a suitable $2d$ spacing. Some literature about these crystals can then be located from the same file. The crystal structure factor can be calculated using the extensive volumes Crystal Structures by Wyckoff ⁽²⁾ and the International Tables for Crystal Structure Analyses ⁽³⁾, but such calculations are often hard to perform for interesting crystals. However, if only the point group is known, the multiplicity for a given reflection follows and relative values of $|F|$ can be obtained from a powder pattern.

Before crystal diffraction measurements begin, some calculations as to optimum crystal performance can be made, as follows:

1) Dispersion, D .

$$D \equiv \frac{\delta \theta}{\delta \lambda} = \frac{1}{\lambda} \tan \theta \quad (2)$$

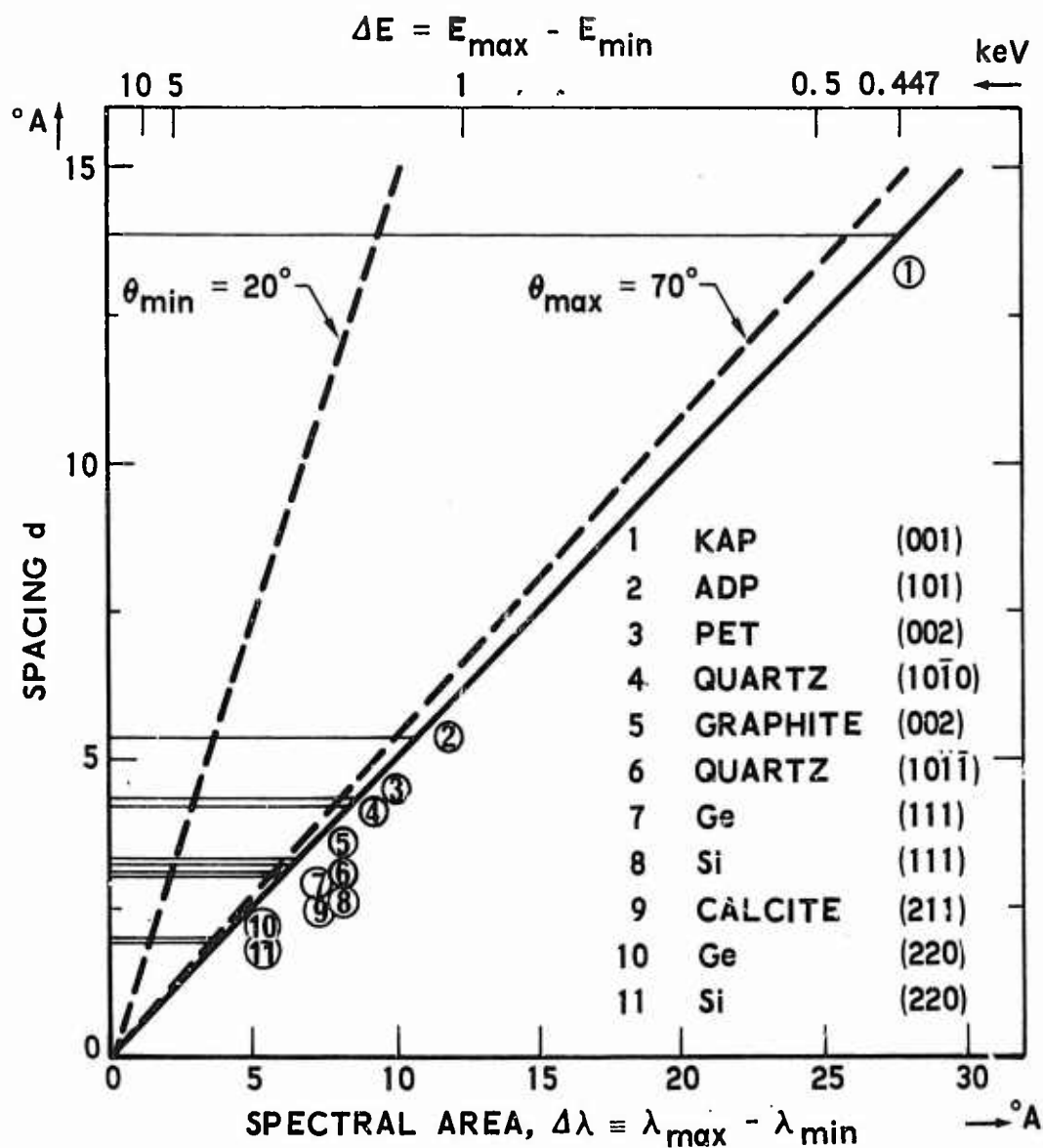


Figure 1. Spectral area in energy (upper scale) or in wavelength (bottom scale) covered by a single flat crystal spectrometer as a function of the crystal d spacing.

2) Resolution, S.

$$S \equiv \frac{\lambda}{\delta \lambda} = \frac{E}{\delta E} = \frac{\lambda D}{W} = \frac{\tan \theta}{W} \quad (3)$$

where W is the full width at half maximum (F.W.H.M.) of the recorded spectrum of a monoenergetic line and can be calculated from the crystal rocking curve, the collimator, and some geometrical factors. Let us call W_c the crystal rocking curve full width at half maximum, W_{col} the collimator angular divergence, and W_{mis} other miscellaneous uncertainties involved in defining the Bragg angle θ_B .

Although there is some disagreement about the correct relationship between W , W_c , W_{col} , and W_{mis} , we prefer the relation used by Ehrenberg and Mark.⁽⁴⁾ For the case of Gaussian distributions they give

$$W = \left(W_c^2 + W_{col}^2 + W_{mis}^2 \right)^{1/2} \quad (4)$$

a) Perfect Crystals

The FWHH = W_c (in radians) can be calculated, within the limits of Darwin's dynamical theory, from⁽⁵⁾

$$\begin{aligned} W_c &= r_o \frac{N |F| (1 + |\cos 2 \theta_B|)}{\pi \sin 2 \theta_B} \lambda^2 \\ &= 1.79 \times 10^{-5} N |F| d^2 (1 + |\cos 2 \theta_B|) \tan \theta_B \end{aligned} \quad (5)$$

For W_c in seconds

$$W_c = 3.695 N |F| d^2 (1 + |\cos 2 \theta_B|) \tan \theta_B \quad (6)$$

where d and λ are in Angstroms (\AA), N is the number of unit cells \AA^{-3} , $|F|$ is the absolute value of the structure factor in electrons and r_0 is the classical radius of the electron in \AA . The solid line in figure 2 shows

$$\left\{ \frac{W_c}{N|F|d^2} \right\} \text{ as a function of } \theta_B.$$

For W_c in electron volts, Eq. (5) becomes

$$W_c = 1.112 \times 10^{-1} N|F|d \cdot \frac{(1 + |\cos 2\theta_B|)}{\sin \theta_B} \quad (7)$$

The dashed line in figure 2 shows the quantity $\left\{ \frac{W_c}{N|F|d} \right\}$. It should be noted that this figure is general and applies to any crystal.

The other two components of equation (4), W_{col} and W_{mis} , to a first approximation, are independent of the incident radiation and their values can be larger or smaller than a given W_c . In many astronomical applications W_{col} is practically zero since the x-rays come from a "point source at infinity." W_{mis} depends on the satellite stability and it is feasible to make W_{mis} of the order of a few arc-seconds while W_c can be in tens of minutes. In the case of laboratory measurements W_{mis} is practically zero while with fine slits it is feasible to achieve a W_{col} of no more than a few seconds of arc.

For the sake of simplicity in deriving the spectrometer resolution, we suppose that

$$W_c^2 \gg W_{col}^2 + W_{mis}^2 \quad (8)$$

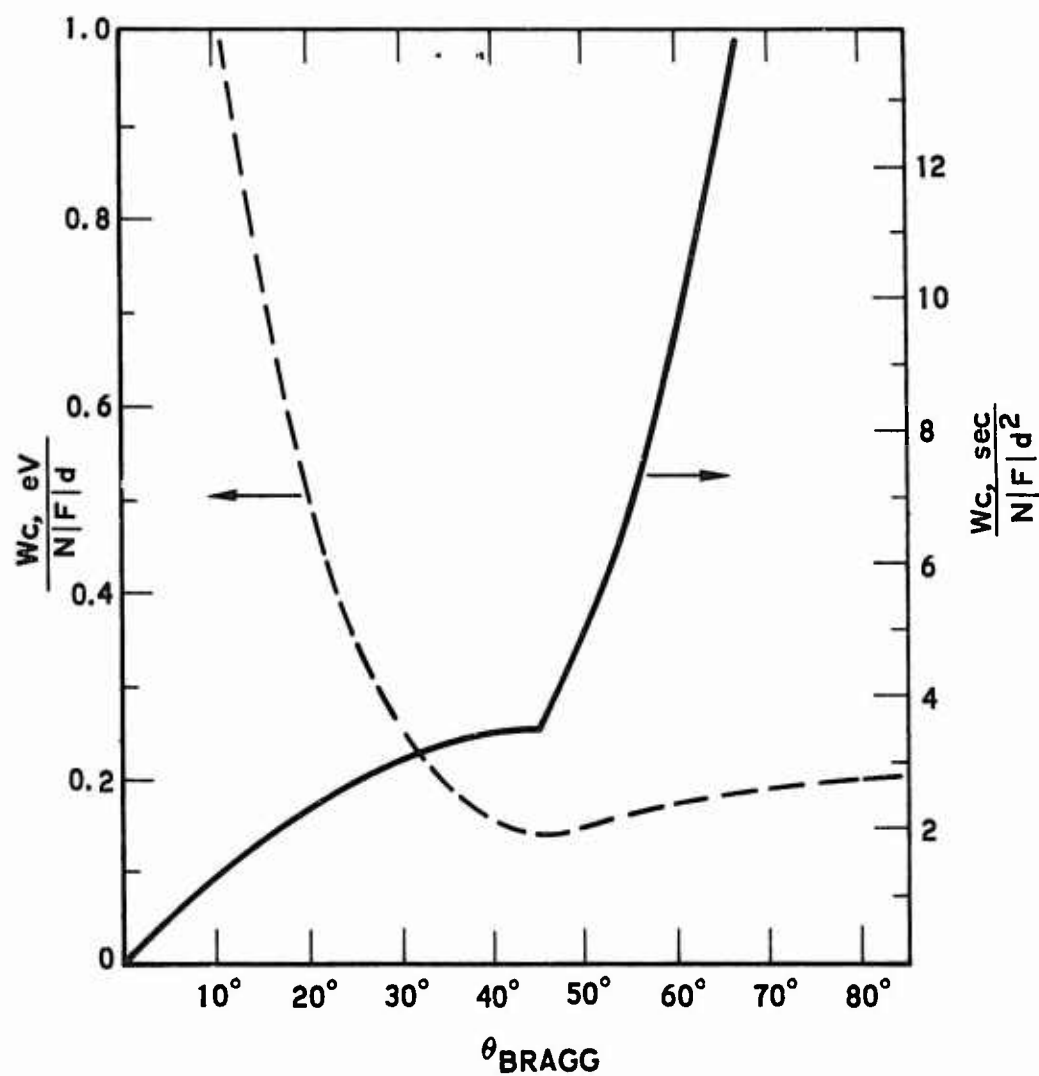


Figure 2. Normalized F.W.H.M. calculated according to Darwin's theory as a function of the Bragg angle. The solid line is in seconds (right scale) and the dashed line is in eV (left scale). This figure and figure 3 are applicable to any crystal.

In this case, the resolution can be calculated analytically and is given by

$$S = 5.574 \cdot \frac{10^4}{N |F| d^2} \cdot \frac{1}{(1 + |\cos 2 \theta_B|)} \quad (9)$$

Figure 3 shows $S \cdot N \cdot |F| \cdot d^2$ as a function of θ_B . When the approximation in equation (8) is dropped, then equation (9) is replaced by equation (3), and W is W_{tot} . It is important to note that the above discussion is largely a first-order approximation based on Darwin's theory, in which the peak reflectivity for a perfect crystal, independent of the crystal and the wavelength, is always set equal to unity. The integrated reflectivity is then proportional to W_c , being given by

$$R_c = \frac{8}{3\pi} r_o \frac{N \lambda^2 |F|}{\sin 2 \theta_B} \left\{ \frac{1 + |\cos 2 \theta_B|}{2} \right\} \quad (10)$$

It is more realistic to assume that some absorption can take place during diffraction. The peak reflectivity is then less than one, and the shape of the rocking curve is given by ⁽⁶⁾.

$$F(\ell) = \frac{1}{2} \left[\frac{(A + jB)/\delta}{\ell - j\frac{\beta}{\delta} \pm \left[(\ell - j\frac{\beta}{\delta})^2 - \left(\frac{A + jB}{\delta}\right)^2 \right]^{1/2}} \right]^2 + \frac{1}{2} \left[\frac{|\cos 2 \theta_B| (A + jB)/\delta}{\ell - j\frac{\beta}{\delta} \pm \left[(\ell - j\frac{\beta}{\delta})^2 - \left(\frac{A + jB}{\delta}\right)^2 \cos^2 2 \theta_B \right]^{1/2}} \right]^2 \quad (11)$$

where:

$$\ell \equiv \frac{\sin 2 \theta_B}{2 \delta} (\theta - \theta_B) - 1,$$

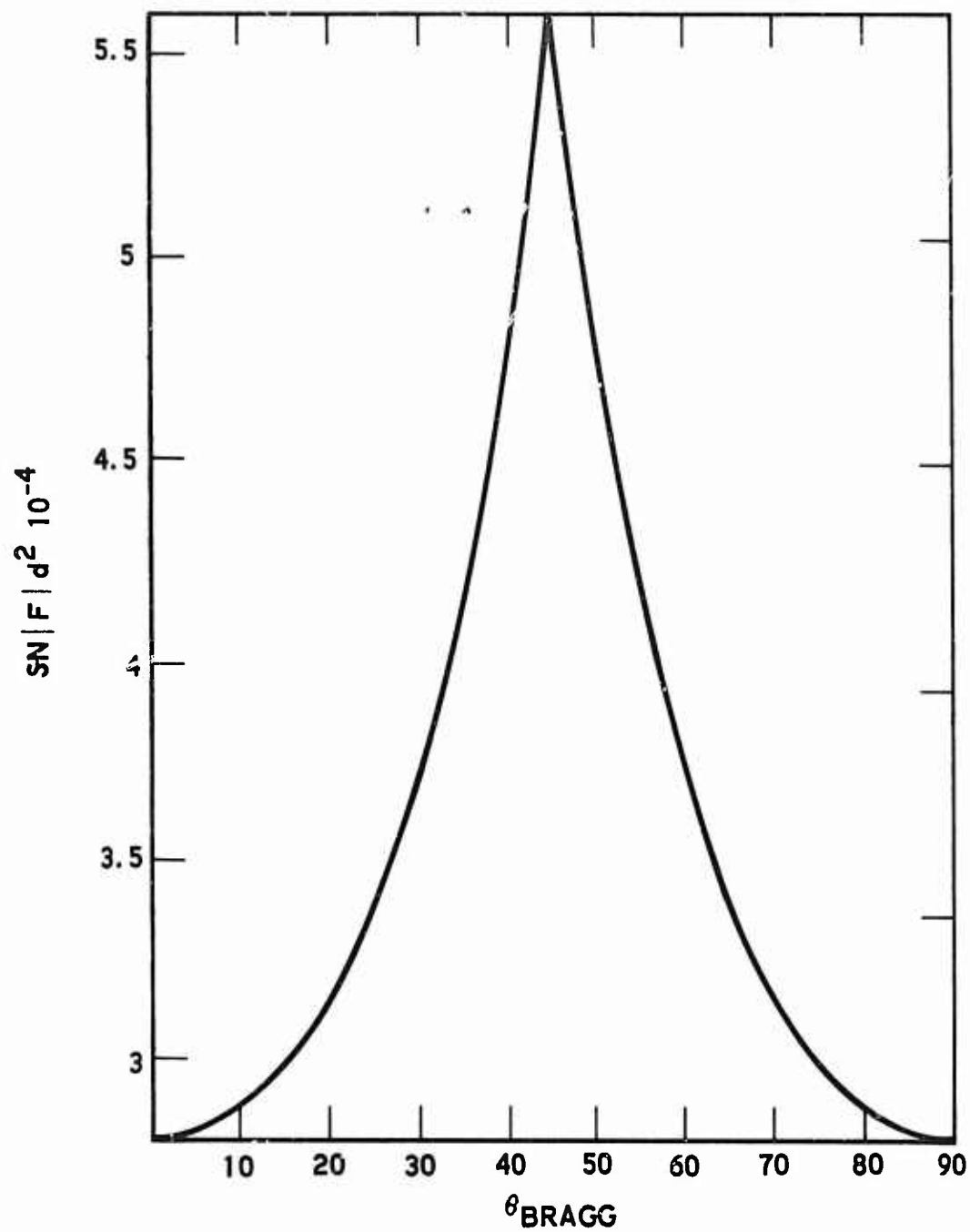


Figure 3. Normalized crystal resolving power as a function of θ_{Bragg} (using Darwin's dynamical theory).

A and B are the real and imaginary parts of structure factor, F and $\beta = (\lambda/4\pi)\mu_l$. (μ_l is the linear absorption coefficient). Relation (11) is not valid near the x-ray absorption edges of the chemical compounds of which the crystal is made. The peak reflectivity can be calculated from equation (11) since it is equal to $F(\ell_0)$. Figure 4 is the diffraction pattern for (002) PET as calculated using another form of eq. (11) for $\lambda = 8.34$ Å. In this particular case, the peak reflectivity is predicted to be $F(\ell_0) = .82$.

When calculations such as those used to prepared Figure 4 cannot practically be carried out for several of the wavelengths that will be analyzed by the crystal, then some idea of the energy dependence of the peak reflectivity can be obtained by comparing the absorption coefficients near and far from the Bragg angle. When a photon strikes a crystal, photoelectric absorption, incoherent scattering, or coherent scattering can take place. A measure of the incoherent scattering and the photoelectric absorption is the mass absorption coefficient μ , which is energy dependent. Far from an absorption edge, μ increases monotonically with λ^3 , independent of direction. Near a Bragg reflection, attenuation can be described by an equivalent absorption parameter τ . τ can easily be calculated for the case of a perfect crystal and is given by

$$\tau = \frac{1}{2} r_0 N \lambda |F| \quad , \quad \tau \gg \mu_l \quad (12)$$

The inverse of τ or μ_l determines the penetration depth. The penetration depth calculation predicts how much of the crystal will actually participate in each of the x-ray processes. When $\tau \rightarrow \mu_l$, the crystal is a poor reflector because a large proportion of the incident photons are absorbed by the crystal and re-emitted into 4π steradians, increasing the background. The crystal is then a poor analyzer crystal for this particular wavelength⁽⁷⁾.

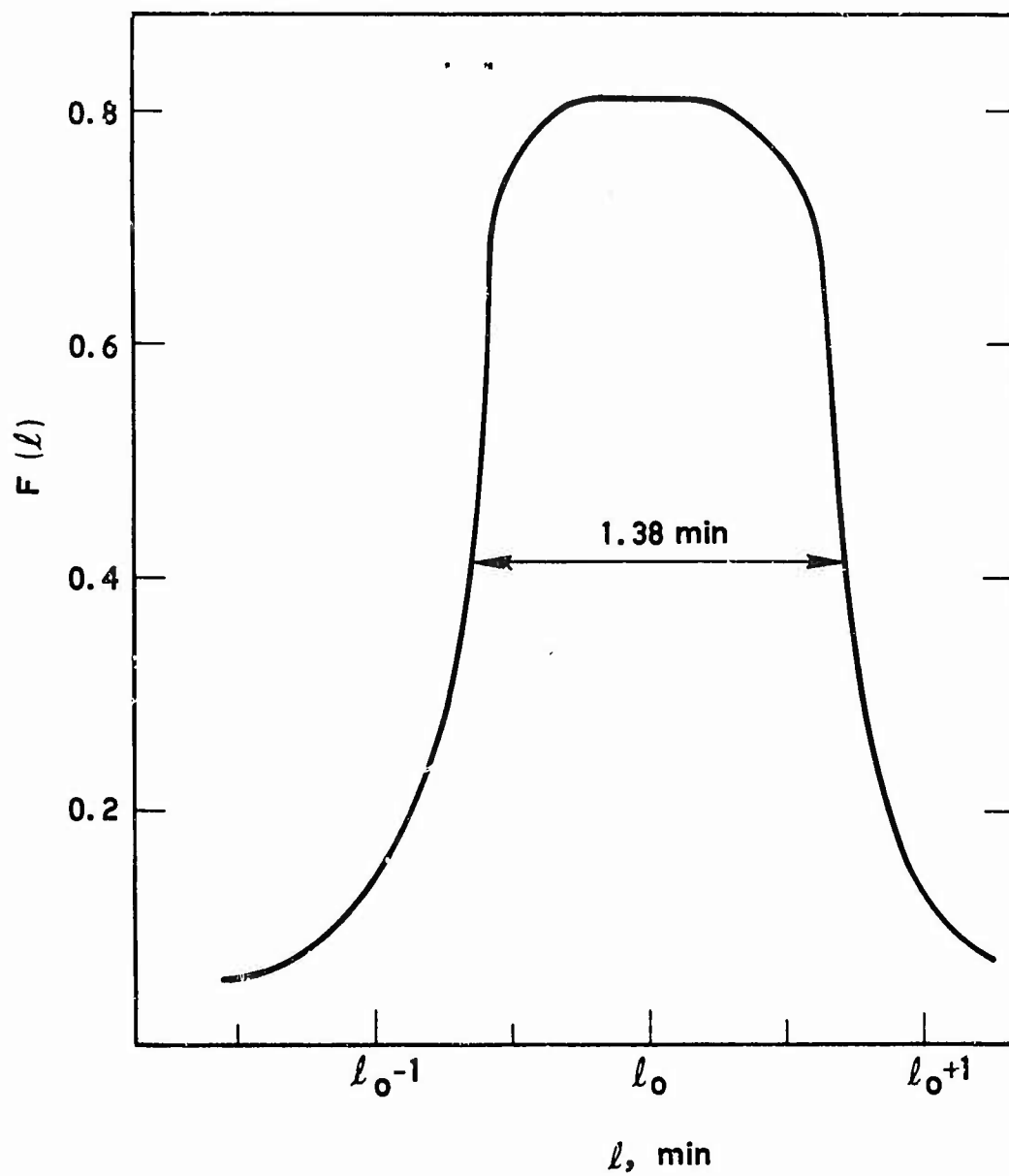


Figure 4. The theoretical rocking curve for a (002) PET crystal at $\lambda = 8.34 \text{ \AA}$.

b) Imperfect Crystals

The above analysis can be expected to hold to better than 1% when a spectrometer using perfect crystals is being designed. If imperfect crystals are chosen instead of perfect crystals, the only quantity that is well defined is the integrated reflectivity. The integrated reflectivity for an ideally imperfect crystal is given by ⁽⁵⁾.

$$R_c^i = \frac{1}{2\mu} r_o^2 \frac{N^2 \lambda^3 |F|^2}{\sin 2\theta} \left[\frac{1 + \cos^2 2\theta}{2} \right] \quad (13)$$

This relation is derived by applying kinematical theory to a small single crystal (crystallite), and it is valid for the ideally imperfect crystal, where it is assumed that each crystallite diffracts independent of its neighboring crystallites. The intensity is proportional to the number of crystallites diffracting at any given time. Nevertheless, the measured integrated intensity is always less than that predicted by equation (13). The deviation between the measured and the calculated intensities increase with increasing $|F|$ and increasing crystallite size. A measure of this deviation is given by the primary and secondary extinction.⁽⁸⁾ When equation (13) is used in crystal structure work, crystallographers avoid measuring the 10 strongest lines. This indicates the limited use of equation (13) for x-ray spectrometers where, usually, only the strongest reflections are employed. There is no simple relationship between the shape of the ideally imperfect crystal diffraction pattern and the predicted integrated intensity. The full width at half maximum, to a first approximation, depends only on the the crystal structure and the mosaic spread.

The above discussion can lead to the misleading conclusion that the ideally imperfect crystal, unlike its perfect counterpart, will be adequately analyzed if measurements of the diffraction pattern are made at one wavelength. Actually, due to the strong dependence of the penetration depth on wavelength, and the dependence of crystal perfection on the distance to

the surface, it is still necessary to measure crystal properties for a sampling of wavelengths over the energy band for which the spectrometer will be used.

c) Extra Reflection

Regardless of the perfection of the crystals, for crystals used in broad band spectrometers, care must be taken with respect to the three dimensional orientation of the crystals to the incoming beam, in order to avoid asymmetrical Bragg reflections from planes not parallel to the crystal surface.⁽⁹⁾ It is easy to identify higher order reflections from the planes $(nh\ nk\ nl)$ when the planes $(h\ k\ l)$ are parallel to the crystal surface. Indeed, the fact that higher order reflections occur may be very useful in identifying a questionable spectral feature that might otherwise be ignored. Higher order reflections are insensitive to a crystal rotation about the axis perpendicular to $(h\ k\ l)$. On the other hand, asymmetrical Bragg reflections from planes making an angle with the $(h\ k\ l)$ plane are difficult to identify, and are sensitive to the rotation mentioned above. This problem becomes more important in the single flat crystal geometry spectrometer when the detector is close to the crystal. The problem can be minimized by orienting the crystals so that reflections from planes other than $(h\ k\ l)$ do not reach the detector.

MEASUREMENT OF THE DIFFRACTION PROPERTIES OF A CRYSTAL

Theoretical predictions give only a first order approximation of what can be expected from a given crystal. It is clearly necessary to proceed to experimental measurements in order to decide which mode will be most useful for a specific crystal, or which crystal will be most advantageous given a necessary mode of operation. In this section, the techniques for measuring crystal diffraction properties are described.

In principle, it is possible to measure the rocking curve of a crystal by measuring the diffraction pattern using any diffractometer, provided that the shape of the incident radiation is well known. Using the superposition theorem⁽¹⁰⁾, the measured diffraction pattern $\Phi(\theta)$ is the convolution of the incident beam (angular) profile $\sigma(\phi)$, the energy spread of the beam $f(E)$, the actual crystal rocking curve $F(\ell)$, and $U(\phi, E)$ the apparatus profile. We can write

$$\Phi(\theta) = \sigma(\phi) * f(E) * F(\ell) * U(\phi, E) \quad (14)$$

where we wish to find $F(\ell)$. The practical problems are in knowing $f(E)$, which is nontrivial, and the accurate determination of $\sigma(\phi)$ and $U(\phi, E)$. Assuming that all of these computations can and are made, the process is a very tedious one. In addition, the experimental error propagates very rapidly during a deconvolution calculation, necessitating very accurate experimental data in order to obtain marginal information about $F(\ell)$.

In a nondispersive system, the measured diffraction pattern is independent of the shape $f(E)$, and $U(\phi, E)$ i.e., the relation (14) reduces to

$$\Phi(\theta) = \sigma(\phi) * F(\ell). \quad (15)$$

Preceding page blank

If $\sigma(\phi) = F(\ell)$, the problem reduces to its simplest form, and the FWHM of the measured diffraction line $\Phi(\ell)$ (assuming Gaussian shape) is $\sqrt{2}$ times the FWHM for $F(\ell)$.

It is clear from the above that the only straightforward way to measure $F(\ell)$ is through the use of a double crystal spectrometer in the parallel position, using two identical crystals. The reflection order should be the same for both crystals.⁽¹¹⁾ This is the only nondispersive system, and only in this way does $\sigma(\phi) = F(\ell)$.

Although the best and simplest method of obtaining $F(\ell)$ is through the use of a double crystal instrument in the nondispersive mode (1, -1), the actual measurements are very delicate, and special care⁽¹²⁾ is necessary in data interpretation. The angle between \vec{s} (the unit vector perpendicular to the crystal surface) and \vec{G} (the reciprocal lattice vector for the reflection planes) must be measured in advance, through one of the well-known crystallographic techniques, such as a back reflection Laue. If complicated corrections due to asymmetrical Bragg scattering and absorption are to be avoided, then the angle between \vec{s} and \vec{G} should be, to within a few seconds, equal to zero. The two crystals must be aligned so that \vec{k}_1 , \vec{k}_2 , \vec{k}_3 , \vec{G}_1 and \vec{G}_2 all lie in the same plane (see Fig. 5). If \vec{G}_2 forms an angle with the \vec{k}_1 , \vec{k}_2 plane, $(\vec{k}_1 = \frac{4\pi}{\lambda_1} \sin \theta_1)$, the wave vector of the i beam, then the measured FWHM will be artificially widened. The detailed alignment of a double crystal spectrometer depends on the specific instrument, but some general discussion along these lines and a detailed analysis of the errors involved are given in the literature.⁽¹³⁻²⁰⁾

In the present crystal study the double crystal vacuum spectrometer built by C. Howey and P. Metzger of the Space Physics Laboratory at The Aerospace Corporation was used. Most of the preliminary alignment is performed in air using a laser beam. The system consists of a 31.5-in diameter horizontal rotating table. The first crystal is supported by a model 10.553 Lansing mount on the axis of rotation. The incident x-ray beam \vec{k}_1 is

MEASUREMENT OF THE DIFFRACTION PROPERTIES OF A CRYSTAL

Theoretical predictions give only a first order approximation of what can be expected from a given crystal. It is clearly necessary to proceed to experimental measurements in order to decide which mode will be most useful for a specific crystal, or which crystal will be most advantageous given a necessary mode of operation. In this section, the techniques for measuring crystal diffraction properties are described.

In principle, it is possible to measure the rocking curve of a crystal by measuring the diffraction pattern using any diffractometer, provided that the shape of the incident radiation is well known. Using the superposition theorem⁽¹⁰⁾, the measured diffraction pattern $\Phi(\theta)$ is the convolution of the incident beam (angular) profile $\sigma(\phi)$, the energy spread of the beam $f(E)$, the actual crystal rocking curve $F(\ell)$, and $U(\phi, E)$ the apparatus profile. We can write

$$\Phi(\theta) = \sigma(\phi) * f(E) * F(\ell) * U(\phi, E) \quad (14)$$

where we wish to find $F(\ell)$. The practical problems are in knowing $f(E)$, which is nontrivial, and the accurate determination of $\sigma(\phi)$ and $U(\phi, E)$. Assuming that all of these computations can and are made, the process is a very tedious one. In addition, the experimental error propagates very rapidly during a deconvolution calculation, necessitating very accurate experimental data in order to obtain marginal information about $F(\ell)$.

In a nondispersive system, the measured diffraction pattern is independent of the shape $f(E)$, and $U(\phi, E)$ i.e., the relation (14) reduces to

$$\Phi(\theta) = \sigma(\phi) * F(\ell). \quad (15)$$

Preceding page blank

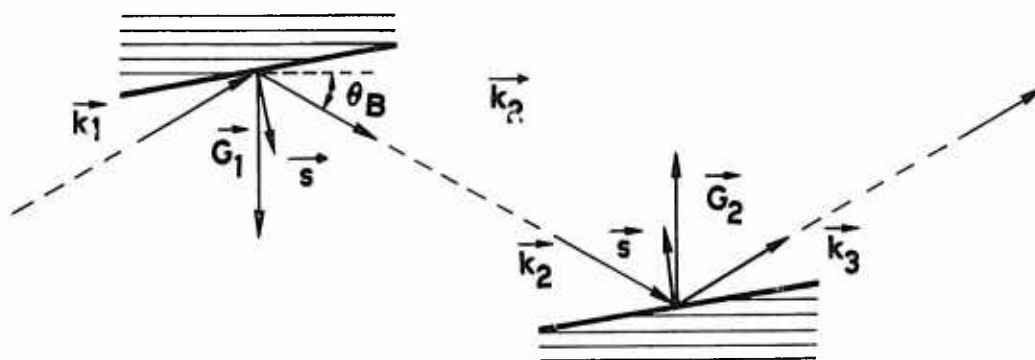


Figure 5. The alignment and orientation vectors characteristic to a double crystal spectrometer.

perpendicular to this axis. Using the table rotation around this vertical axis and the Lansing rotation about a horizontal axis, the \vec{k}_1 , \vec{k}_2 , and \vec{G}_1 vectors are brought into a horizontal plane (parallel to the plane of the table surface). On the same table, a second Lansing crystal mount can be made to slide in a precision motion along the table surface and perpendicular to the surface of the first crystal. The vector \vec{G}_2 is then brought into the horizontal plane using the second crystal Lansing rotation around the horizontal axis. A flow proportional counter rotates around the vertical axis of the table and can also be made to spin about its own axis. The peak and the integrated reflectivity are measured by manipulating the counter so that it first sees the intensity diffracted from the first crystal and then measures the diffracted intensity from the second crystal. Using a lead screw, different parts of the second crystal surface are illuminated. Since different portions of the crystal are brought into the diffraction position, the system can be used for a Berg-Barrett topography study. During the alignment process, the intensity of the Bragg peak is measured as \vec{G}_2 moves in a vertical plane. When \vec{G}_2 approaches the plane of \vec{k}_1 , \vec{k}_2 , and \vec{G}_1 , the peak intensity increases sharply.

RESULTS

Applying the methods described above, the diffraction properties of several crystals of specific interest to x-ray astronomy were measured for a number of wavelengths. The measurements were carried out on: (002) PET, (111) Ge, (101) ADP, (001) KAP, and (001) RAP. A complete analysis has been carried out for the PET, as an example of the problems that are encountered in preparing crystals for a flight instrument. Diffraction results, however, are given for all the crystals tested, and are shown in the graphs which follow.

Pentaerythritol, or PET, is a tetragonal crystal with a bimolecular unit which has the dimensions: $a_0 = 6.08 \text{ \AA}$ and $c_0 = 8.726 \text{ \AA}$. This is a body-centered grouping of $\text{C}(\text{CH}_2\text{OH})_4$ molecules, in which each molecule consists of a tetrahedral distribution of (CH_2OH) radicals about a central carbon atom. PET crystals were a popular crystal choice in the 1930's and 1940's because of their bending properties, large $2d$, and the relative ease of growing large crystals. They frequently found application in bent crystal spectrometers, where their intense (002) reflection was used. They dropped from favor when it was learned that they are highly temperature sensitive and that they suffered radiation damage when they were exposed for long periods of time to a relatively intense x-ray beam. Recently there has been renewed interest in these crystals because the $2d$ spacing (8.73 \AA) has made them suitable for application to x-ray astronomy. Stellar and solar fluxes are expected to be weak enough so that the radiation damage properties of these crystals will not come into play under conditions commonly found in a satellite-borne spectrometer. PET, then, is a useful choice for a sample material on which to demonstrate the problems that are faced in crystal analysis for x-ray astronomy.

Figure 6 shows the FWHM for the best PET crystal available to us, as a function of angle (bottom scale), or as a function of x-ray energy (top scale). The scale on the right indicates the FWHM in arc minutes, while

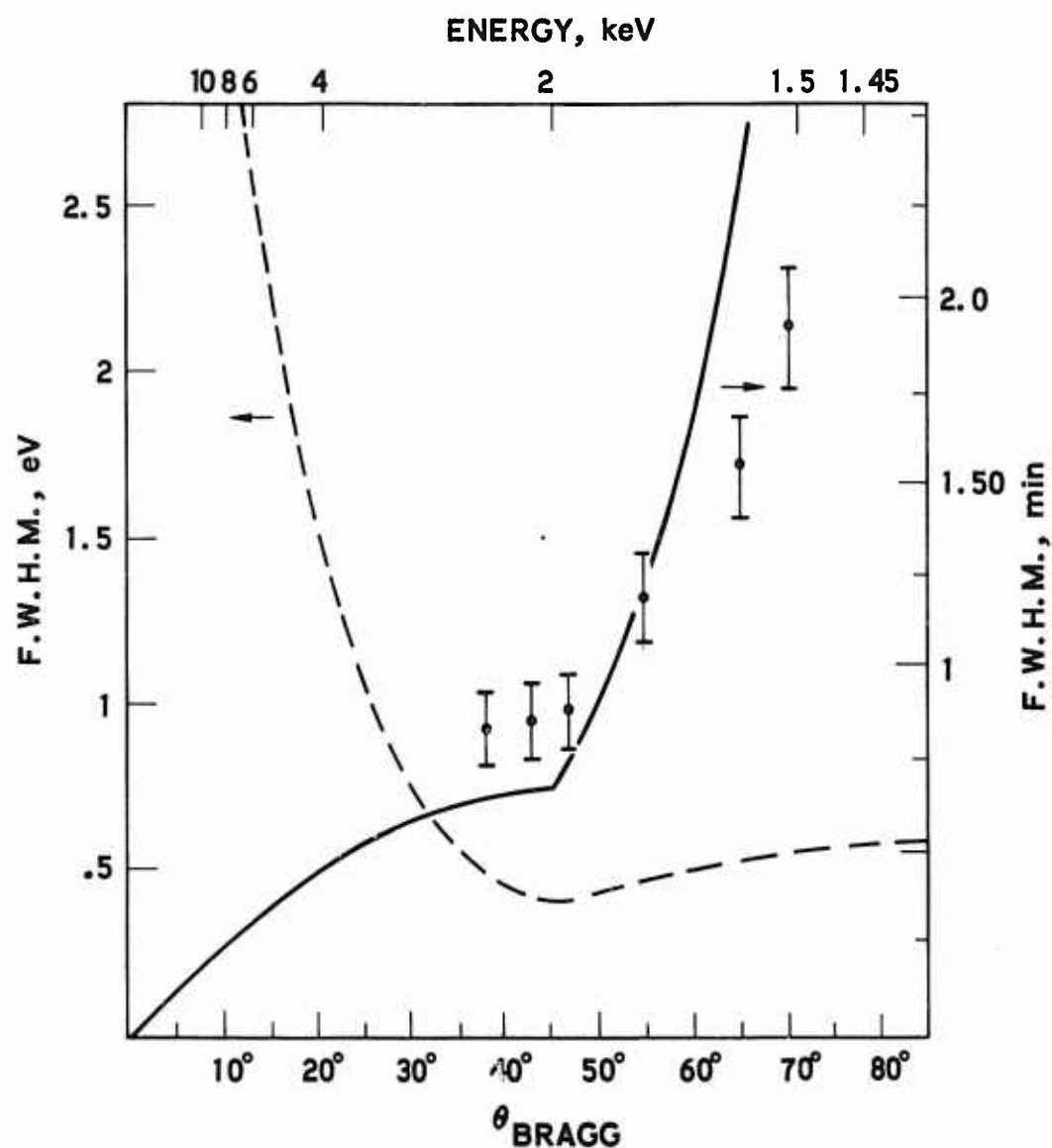


Figure 6. The measured F.W.H.M. $\sqrt{2}$. Theoretical predictions are shown by the solid line in min (right scale) and by the dashed line in eV (left scale) as a function of the Bragg angle (bottom) or as a function of x-ray energy (top). The experimental data were taken using the best (002) PET crystal available to us.

that on the left is the same for eV. The points indicate our measurements, which were performed in arc minutes, and corrected assuming Gaussian distributions for the beam. (Actually, a line shape somewhere between Gaussian and Lorentzian is closer to the fact. Any correction assuming a distribution other than Gaussian will result in a narrower FWHM, so these measurements can be regarded as maximum measured values.) The solid line and dashed line indicate theoretical predictions using equations (6) and (7) respectively. The measured values are compared only to equation (6).

Data were taken for pentaerythritol crystals for as many as ten different incident wavelengths. Original crystals were tested as well as crystals that had been treated in the following ways: (1) heated and cooled from -30 to $+50^{\circ}\text{C}$, (2) bonded with different vacuum-grade urethanes, and (3) bonded and then subjected to controlled vibration tests simulating launch conditions. The crystal that was heated and cooled showed an increase in the FWHM at all the wavelengths tested. Figure 7 shows the results obtained from a crystal, such as that used to obtain the results shown in Figure 6, after it had been epoxied to a crystal mount with Solithane and vibrated according to a NASA Specification. The crystal appears to be under considerable stress after epoxying and vibration. In Figure 8 we show the FWHM in eV for these crystals in a spectrometer assuming different treatments and a mosaic spread of 1.5 minutes. The calculated (dashed line) and measured peak (solid line) reflectivities for our best PET crystal is shown in Figure 9.

In the ensuing figures, we show results for the FWHM and peak reflectivity of (111) Ge (Figures 10 and 11); the FWHM of (101) ADP (Figure 12); the FWHM of (001) KAP (Figure 13); and the FWHM of (001) RAP (Figure 14).

The observation reported earlier⁽²⁴⁾ on the influence of the crystal illumination on crystal diffraction properties has been verified again for ADP and extended to PET. When a beam of visible light from an incandescent lamp is focused on a ADP or PET crystal, the reflecting properties of the crystal change significantly. The changes of Bragg angle, FWHM and

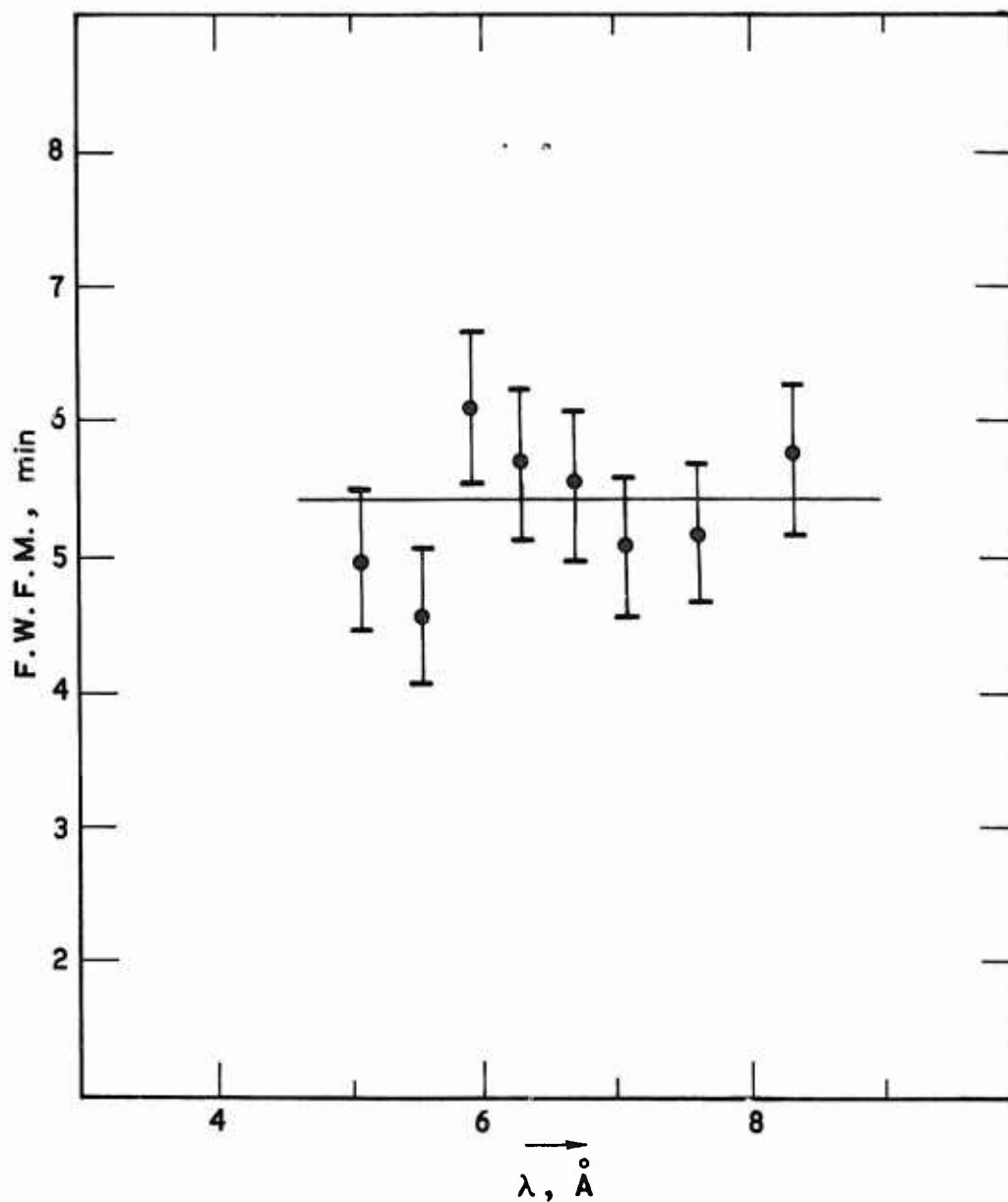


Figure 7. $\sqrt{2}$ (F.W.H.M.) obtained from a (002) PET crystal, similar to that used to obtain the results shown in Figure 6 after it had been bonded to a crystal mount with urethane and vibrated according to a NASA Specification.

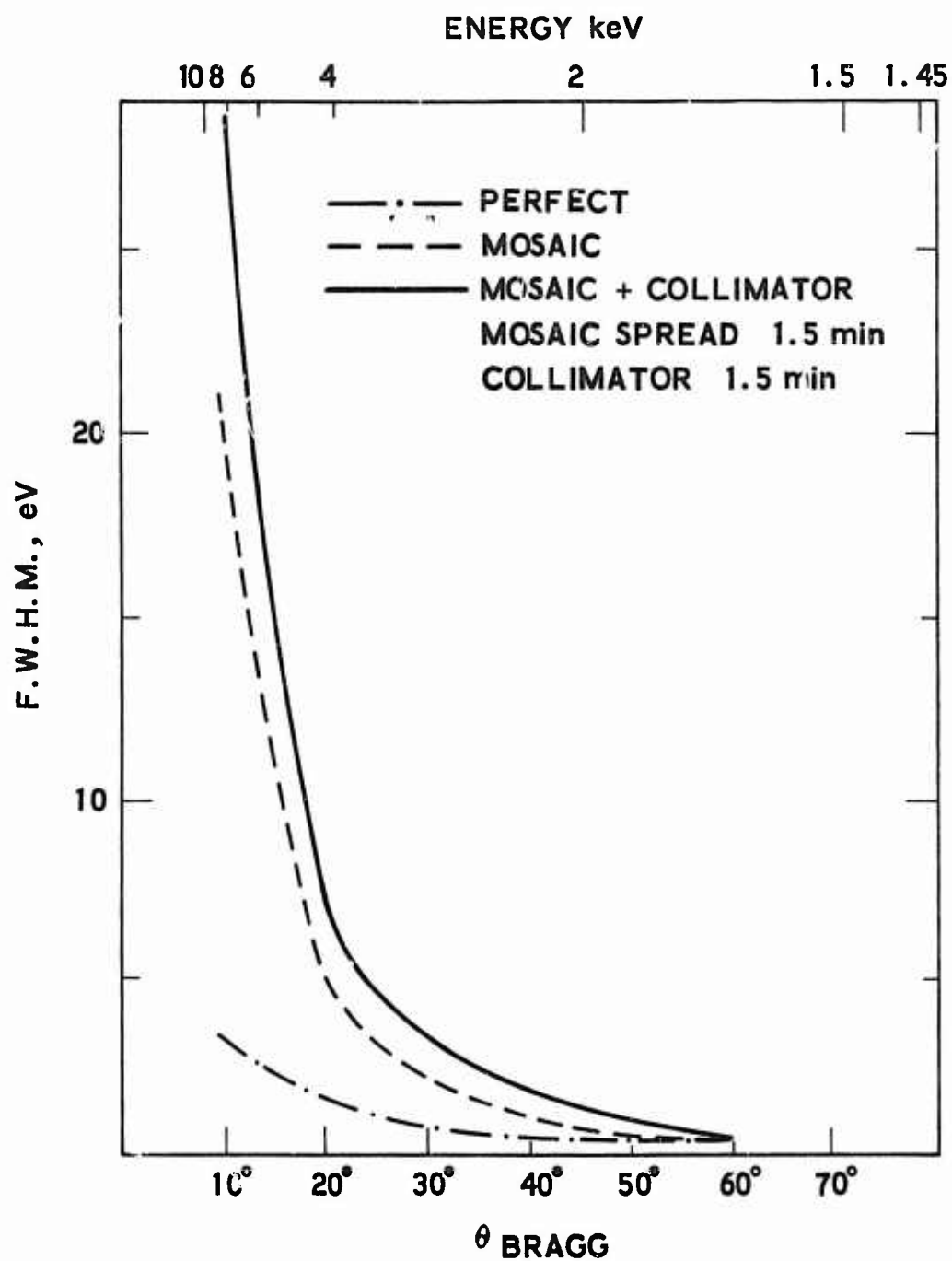


Figure 8. The F.W.H.M. for a perfect (002) PET crystal, a mosaic crystal with mosaic spread 1.5 min. and for a flat single crystal spectrometer using a mosaic PET crystal and a 1.5 min. collimator.

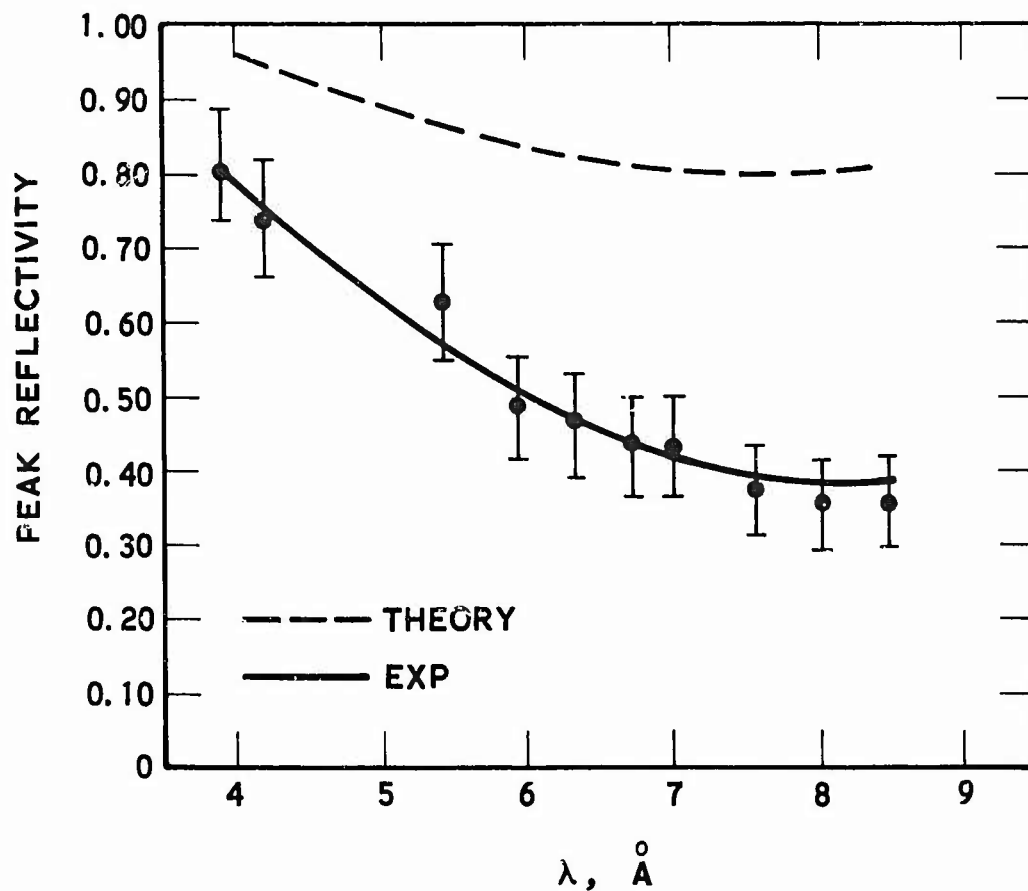


Figure 9. The calculated and the measured peak reflectivities for our best (002) PET crystal.

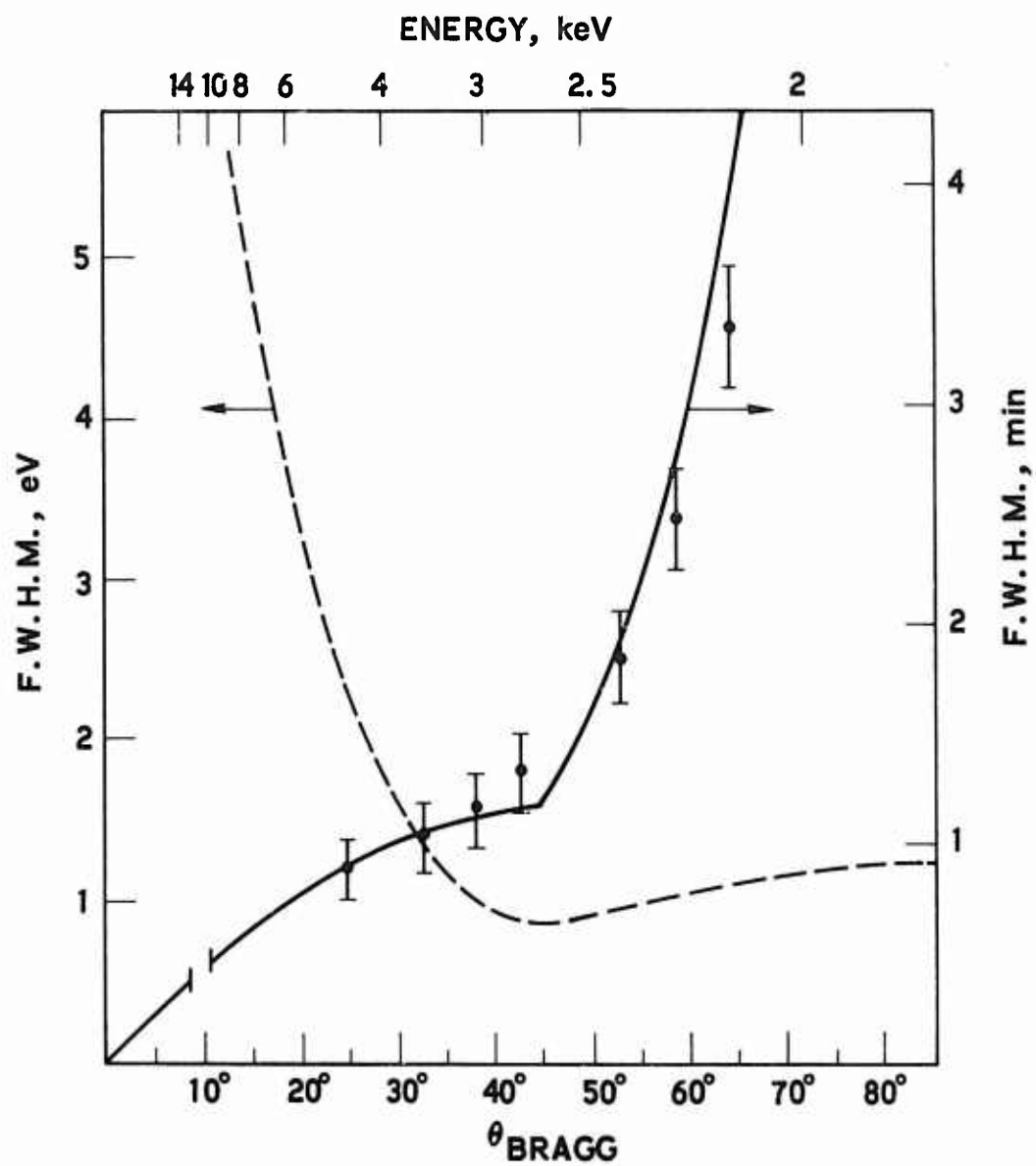


Figure 10. $\sqrt{2} \times \text{F.W.H.M.}$ for a (111) Ge crystal.

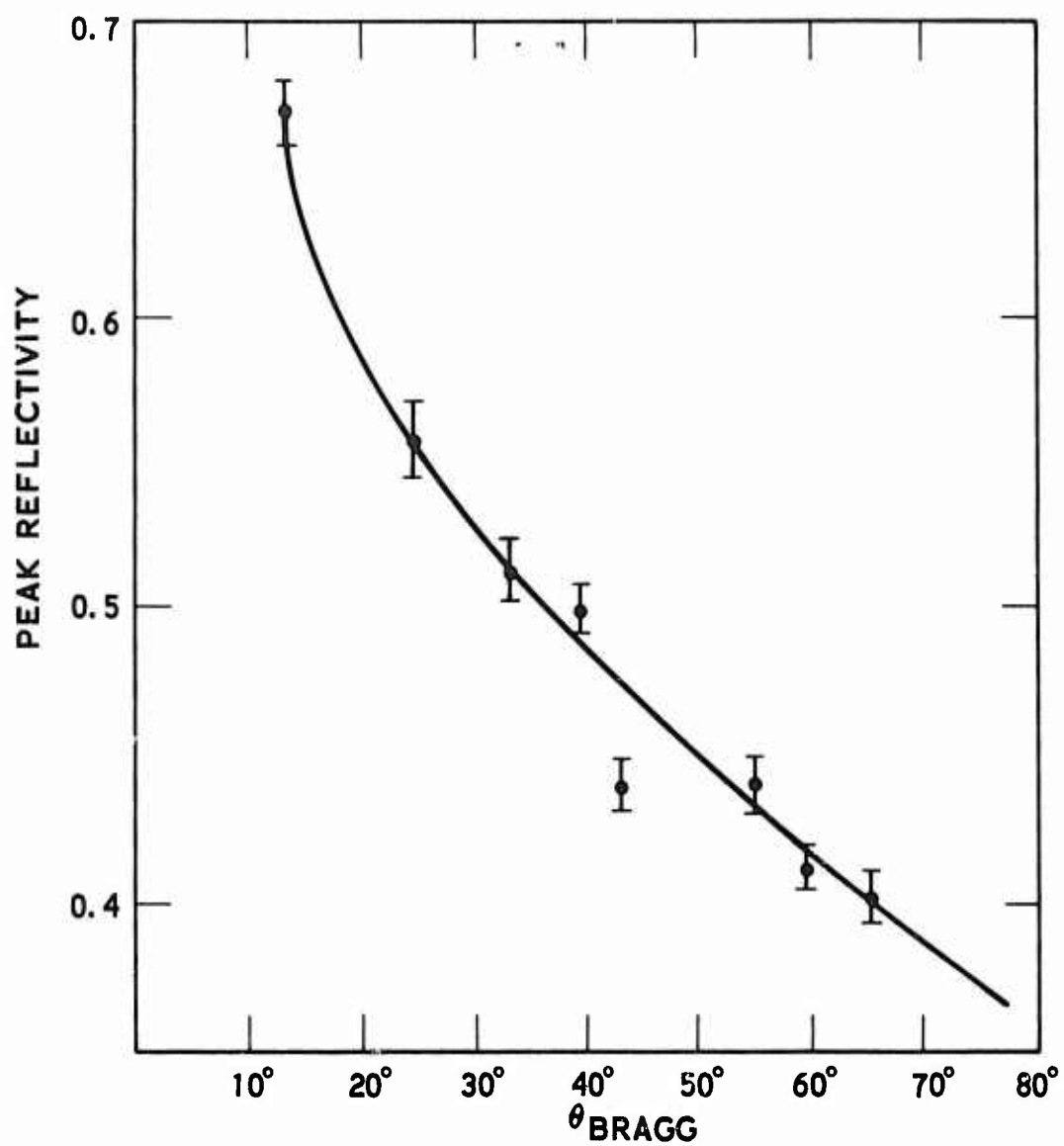


Figure 11. The measured peak reflectivity for a (111) Ge crystal.

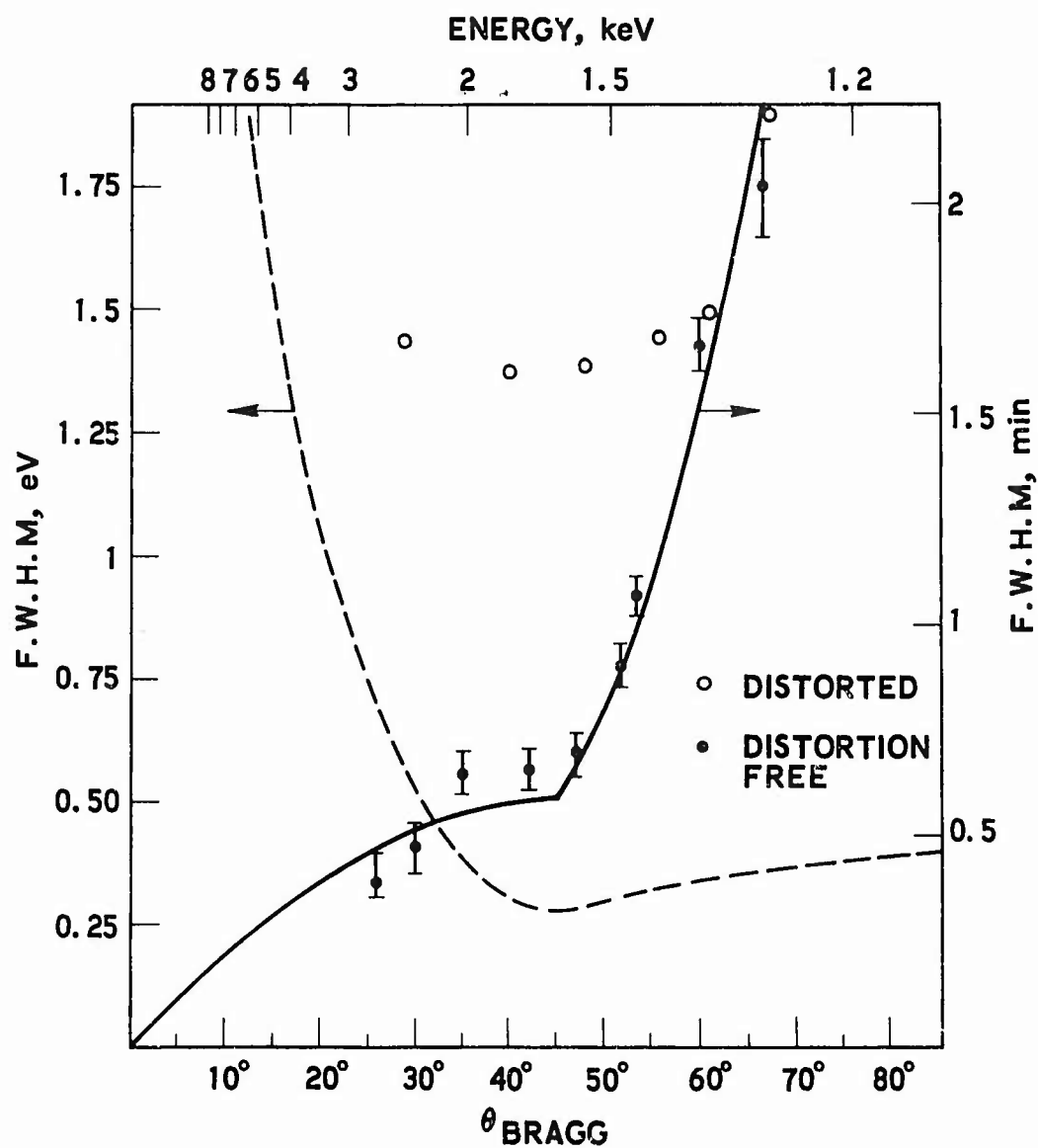


Figure 12. $\sqrt{2} \times \text{F.W.H.M.}$ for a (101) ADP crystal. The solid circles are experimental data on the best ADP crystal available to us. The open circles are data on a distorted ADP crystal.

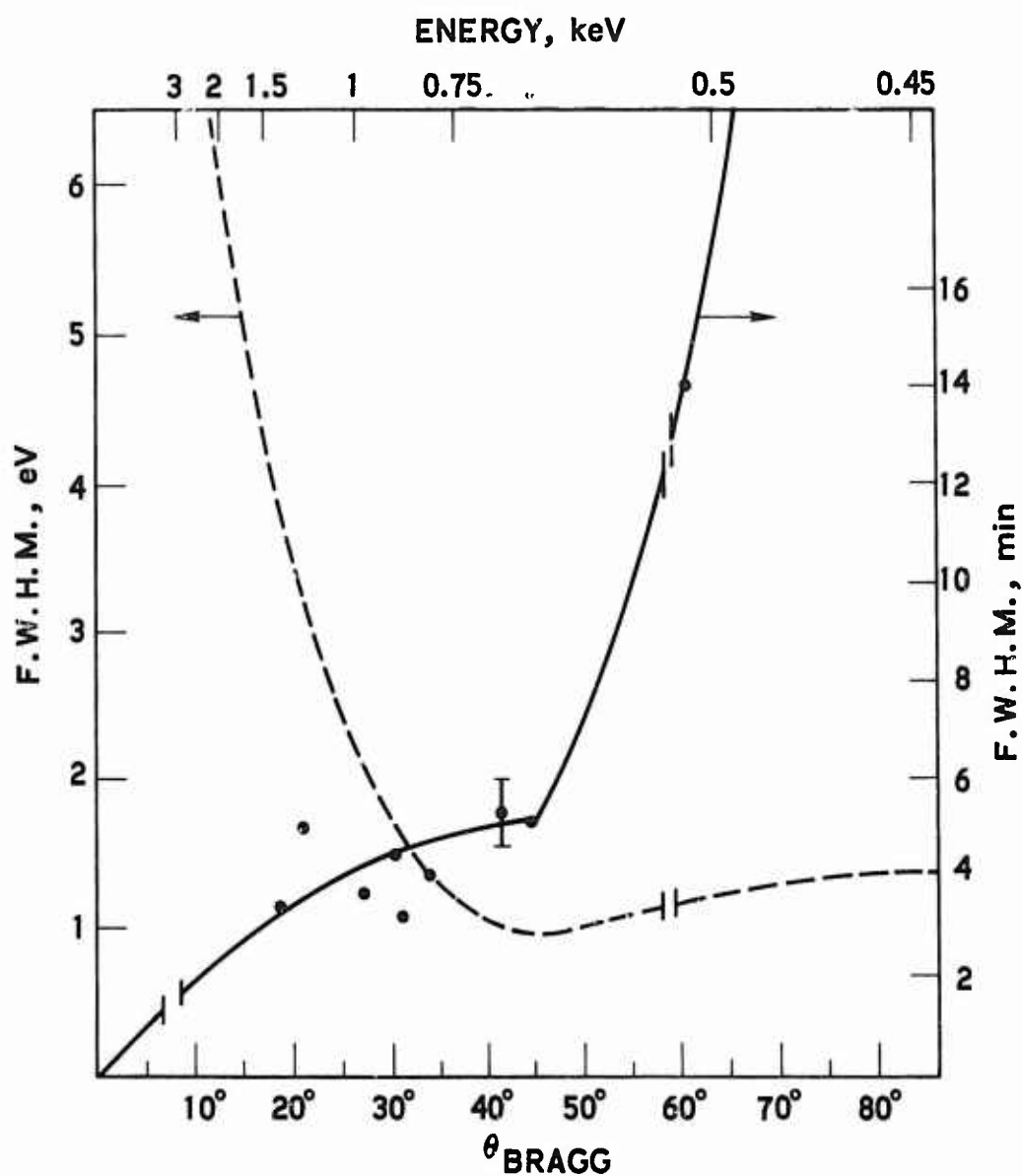


Figure 13. $\sqrt{2} \times \text{F.W.H.M.}$ of a (001) KAP crystal. The short vertical lines indicate a deleted region near absorption edges where the theory is invalid.

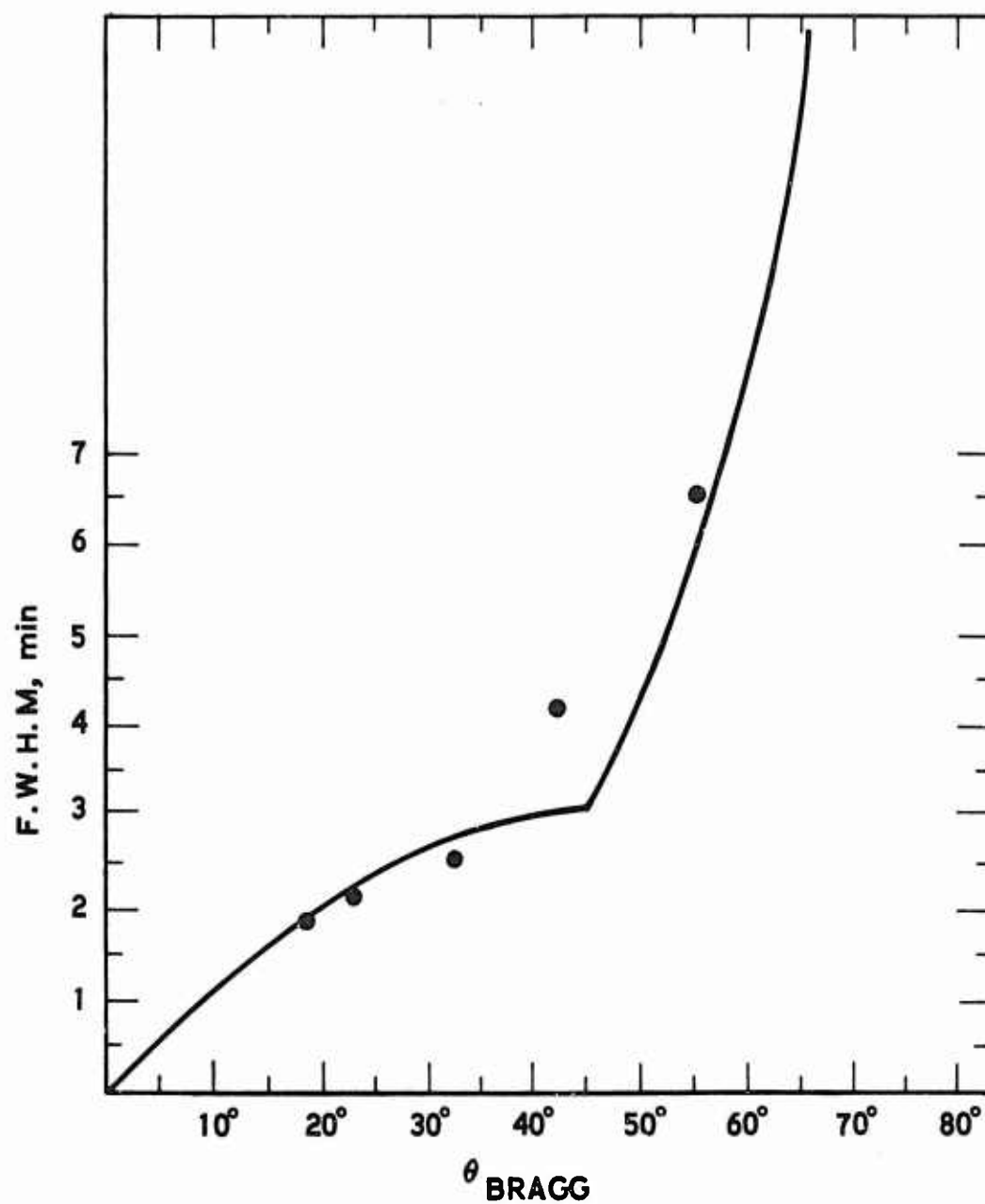


Figure 14. $\sqrt{2} \times$ F.W.H.M. of a (001) RAP crystal.

peak reflectivity for an ADP crystal as a function of illumination time are shown in Figures 15, 16, and 17. The distortion of the crystal diffraction properties are not permanent and returned to their original values after the crystal was allowed to relax for several minutes with the light off.

Although this observation has not been quantitatively explained, it is clear as it is related to a local heating effect. We report it for the following reasons: (1) The observed changes (under laboratory conditions) in the diffracting properties of a crystal are significantly smaller than the changes that can occur during the observations in space; (2) the changes disturb the recorded x-ray spectra considerably because the line position and intensity depends upon the length of time that the line has been observed; (3) to dramatize the need for measuring the crystal diffraction properties under actual flight conditions or in an in-flight calibration.

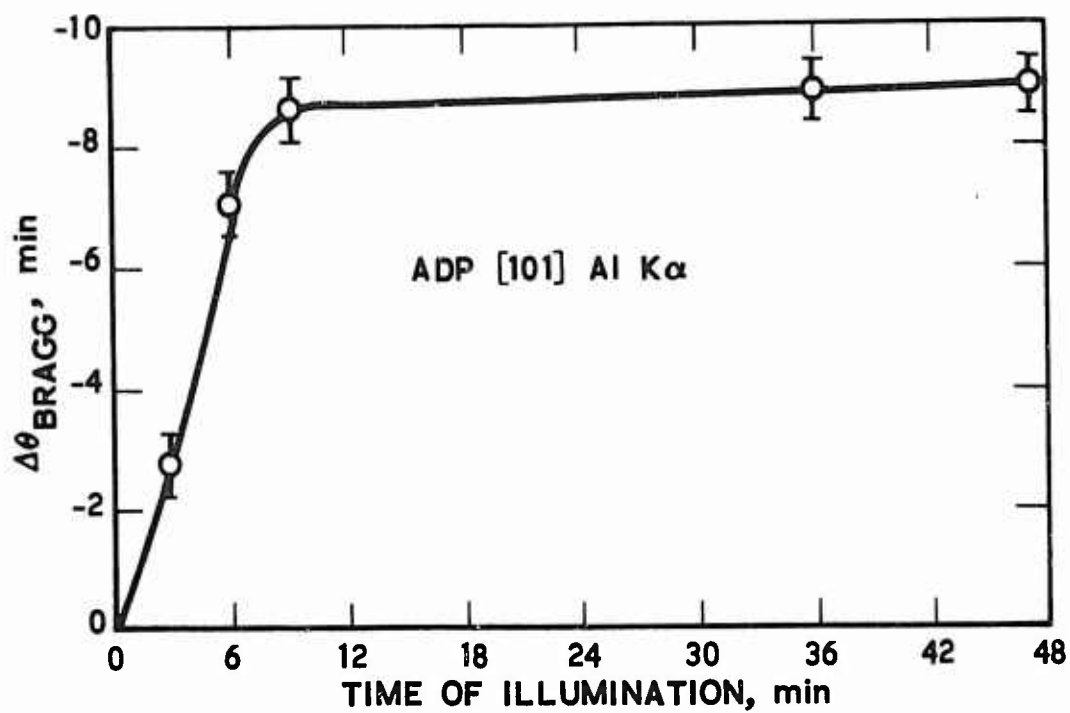


Figure 15. Shift of the Bragg angle of Al K α radiation scattered by a (101) ADP crystal as a function of the crystal illumination by an incandescent lamp.

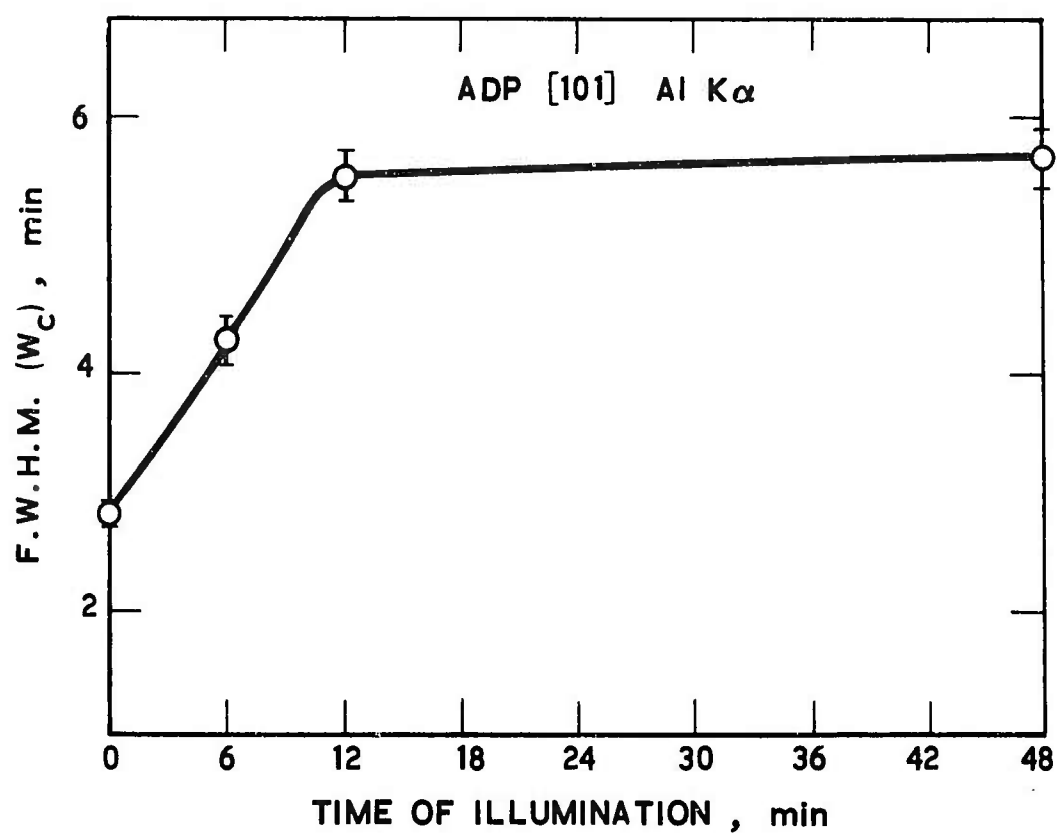


Figure 16. F.W.H.M. as a function of the illumination time for a (101) ADP crystal.

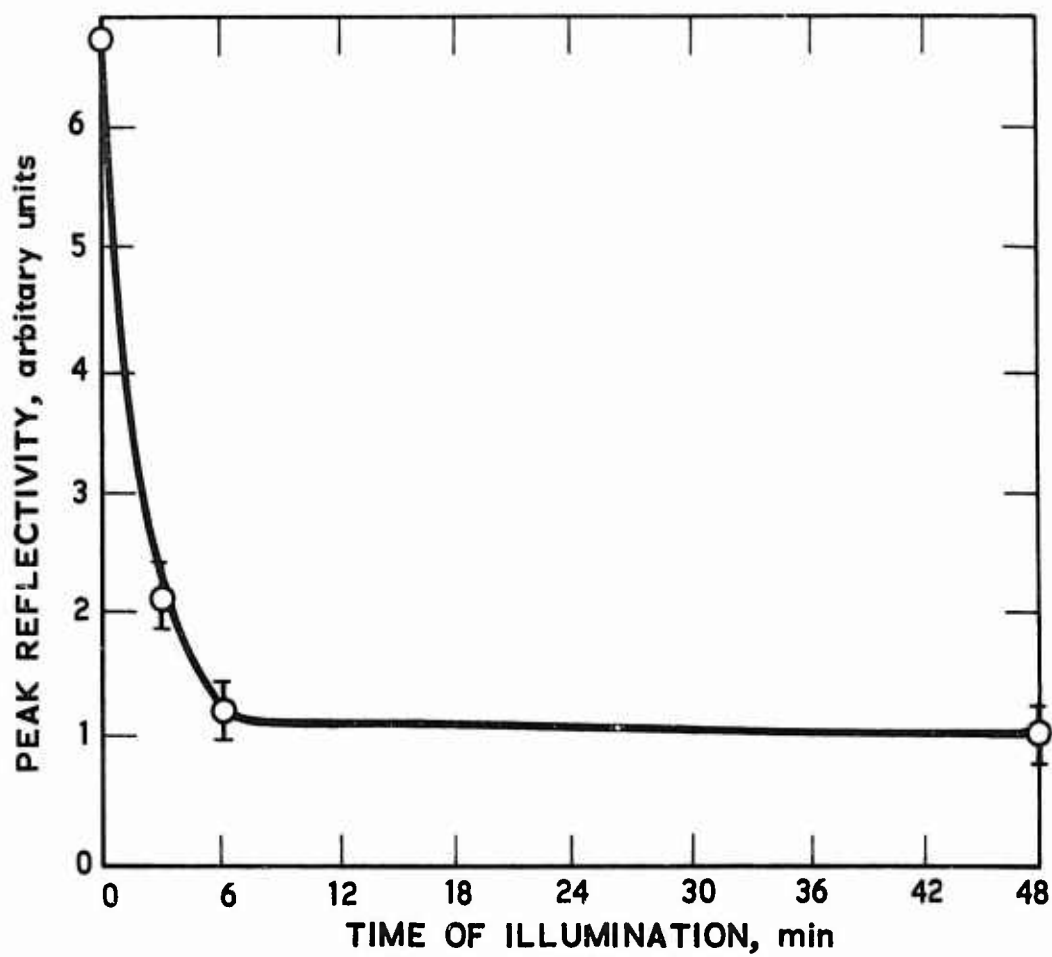


Figure 17. The peak reflectivity for a (101) ADP crystal as a function of the illumination time.

REFERENCES

1. American Society for Testing and Materials, 1916 Race Street, Phila. 3, Pa.
2. R. W. G. Wyckoff, Crystal Structures (Interscience Publishers Inc., New York), 2nd Ed. (1963).
3. International Tables for Crystal Structure Analysis (Kynoch Press, Birmingham, England 1952), Vol. I.
4. W. Ehrenberg and H. Mark, Z. Physik, 42, 807 (1927).
5. B. E. Warren, X-ray Diffraction (Addison Wesley Publishing Co.) (1969).
6. G. Brogren, Arkiv for Fysik, 6, 321-334 (1953).
7. In addition, it may be necessary to calculate that contribution to the total mass absorption coefficient arising from crystal impurities with absorption edges in the vicinity of the spectral region that will be under investigation.
8. A mosaic crystal is said to be ideally mosaic if primary as well as secondary extinction is negligibly small for all reflections. This condition is much more easily satisfied for weak than for strong reflections. Thus a crystal may be "ideally mosaic" only for its weak reflections.
9. N. Spielberg and T. Labell, J. Appl. Phys. 31, 1659-1664 (1960).
10. N. G. Alexandropoulos, Phys. Rev. 150, 610-613 (1966).
11. It is necessary to take the same order reflection from both crystals of the double crystal spectrometer because it is obvious from Eq. 5 that $W_c(\lambda_1) = W_c(n\lambda_0)$ for $1 = n_0$. In making precision measurements, special care is taken not to excite λ_0 . An arrangement using different crystals or different reflection order would be appropriate for topography or for unique defect imaging. It has sometimes been attempted to perform rocking curve measurements using two different crystals in a double crystal spectrometer. (Here we are discussing crystals of different $2d$). In this case the dispersion of a double crystal spectrometer in the parallel mode is given by

$$D = \frac{n_A}{2d_A \cos \theta_A} - \frac{n_B}{2d_B \cos \theta_B}$$

where n_A and n_B are the reflection orders of the first and second crystals, respectively. If two different crystals are used, one might still, somehow, be able to choose the $2d$ spacing and the reflection orders so that the above equation goes to zero. However, if $D \neq 0$, the resulting rocking curve will have to be corrected by deconvolution.

A. H. Compton, S. K. Allison, X-rays in Theory and Experiment (Van Nostrand Co., Inc., New York, 1935).

12. Suppose that, by some undesirable circumstance the crystal for which we wish to make rocking curve measurements is a piece of polycrystalline silicon, and it was assumed that the crystal is (111) single crystal silicon. If, for simplicity, we neglect absorption, this crystal is equivalent to a mosaic crystal with mosaic spread of 360 degrees, or to a (111) thin Si crystal that has been bent (uniformly stressed) into a cylinder. Let us determine the rocking curve of this Si sample using a well-collimated monochromatic incident beam (coming off a perfect flat Si crystal) and a stationary detector. The measured FWHM of this crystal is then 360° , because independent of the angle between the surface and the beam some part of the sample is always reflecting. We now replace the stationary detector with a detector that is rotating accurately in a $\theta - 2\theta$ motion. If the acceptance angle of this detector is of the same order as the divergence of the incident beam, and smaller than the rocking curve width of a perfect Si (111) crystal, then the measured FWHM of the cylindrical silicon (111) crystal is dependent only on the diffraction properties of a single stressed crystal domain. Going now to a flat crystal, it is clear from the above example that when stationary detectors with large acceptance angles are used, even with a well-collimated incident beam, the diffraction width that will be seen is that of the entire crystal. If the crystal is perfect, the width will be much narrower than that which will be seen for a similar crystal in its imperfect form. The above ideas are summarized in the following table.

Crystal	Detector	FWHM	Resolution S
Polycrystalline or cylinder	stationary collimated	360°	0
	rotating collimated	x sec	3000
	stationary large accept	$x < y < 360^\circ$	<3000
	rotating large accept	$x < y < 360^\circ$	<3000
Single flat	rotating large accept	x sec	~3000

13. L. G. Parratt, Phys. Rev., 41, 553-560 (1932).
14. G. Brogren, Arkiv, for Fysik, 3, 507-514 (1951).
15. H. W. Schnopper, J. Appl. Phys. 36, 1415-1423 (1965).
16. H. W. Schnopper, J. Appl. Phys. 36, 1423-1430 (1965).
17. R. D. Deslattes, Phys. Rev. 135, A 899 (1964).
18. R. D. Deslattes, Rev. Sci. Instr. 38, 815 (1967).
19. T. A. Bearden, T. G. Marzolf and T. S. Thomsen, Acta Cryst A 24, 295 (1968).
20. T. A. Bearden and T. S. Thomsen, T. Appl. Crystallogr. L, 130 (1971).
21. N. G. Alexandropoulos, J. F. Durana, A. G. Harper, C. K. Howey, P. H. Metzger, and A. B. C. Walker, Jr., Bull. Am. Phys. Soc. 18, 695 (1973).

PART II. CRYSTAL DIFFRACTION PROPERTIES

This second part of this report is composed of crystal diffraction properties for a number of crystals measured by other investigators. The FWHM is given in arc-minutes and in eV. For most of the crystals, the values expressed in eV were derived by converting the measured values of FWHM in arc-minutes or arc-seconds and not from direct measurements. In the absence of reported values for the integrated reflectivity, its value can be easily calculated assuming a Gaussian shape for the rocking curve with the known width and height. The table preceding the graphs is a summary of information coming from these graphs in addition to those collected from other sources.

Preceding page blank

Table I. Properties of Crystals Frequently Used in X-ray Spectroscopy

GENERAL INFORMATION								
No.	Ref.	Crystal	Chemical Composition	Crystal Structure	Lattice* Parameters	Perfection	Stability	Mechanical Properties
1	1 2 3	Potassium acid Phthalate KAP	$\text{KHC}_6\text{H}_4(\text{COO})_2$	Orthorhombic (tetramolecular cell)	a = 6.466 # b = 9.609 c = 13.857	Fair	Fair	Soft, easily cleaved
2	1	Rubidium acid Phthalate RAP	$\text{RbHC}_6\text{H}_4(\text{COO})_2$	Orthorhombic	a = 6.55 b = 10.02 c = 13.06	Fair	Fair	Soft
3	4	β Alumina	$\text{NaAl}_{11}\text{O}_{17}$	Hexagonal (unimolecular cell)	a = 5.595 c = 22.49	Almost Perfect	Good	Hard, brittle
4	4 5	Mica (Muscovite)	$\text{KA}[\text{Al}_2\text{Si}_3\text{O}_{10}][\text{OH}]_2$	Monoclinic	a = 5.19 b = 9.03 c = 20 $\beta = 95.77^\circ$	Almost Perfect	Perfect	Easily cleaved, bent
5	4 6	Gypsum	$\text{CaSO}_4 \cdot 2\text{H}_2\text{O}$	Monoclinic	a = 10.47 b = 15.15 c = 6.5 $\beta = 151.51^\circ$	Fair	Poor	Soft
6	4	β Alumina	$\text{NaAl}_{11}\text{O}_{17}$	Hexagonal (unimolecular cell)	a = 5.95 c = 22.49	Almost Perfect	Good	Hard, brittle
7	1 7	Ammonium dihydrogen phosphate ADP	$\text{NH}_4\text{H}_2\text{PO}_4$	Tetragonal (tetramolecular cell)	a = 7.510 c = 7.564	Good	Fair	Soft
8	6	Ethylene diamine-D-tartrate EDdT	$\text{C}_6\text{H}_{14}\text{N}_2\text{O}_6$	Monoclinic	a = 8.97 b = 8.808 c = 5.959 $\beta = 105.51^\circ$	Fair	Poor	Soft
9	1 6 4	Pentaerythritol PET	$\text{C}(\text{CH}_2\text{OH})_4$	Tetragonal (bimolecular cell)	a = 6.083 c = 8.726	Good	Poor	Soft, easily cleaved

*a, b, c, in Å as given by R. W. G. Wyckoff⁽¹⁶⁾

#The values given by A. T. Bearden et al⁽¹⁷⁾ are a = 6.47, b = 9.62, C = 13.3164

Table I. Properties of Crystals Frequently Used in X-ray Spectroscopy (Continued)

GENERAL INFORMATION								
No.	Ref.	Crystal	Chemical Composition	Crystal Structure	Lattice * Parameters	Perfection	Stability	Mechanical Properties
10	5, 8 9 10	α Quartz	SiO ₂	Hexagonal centrosymmetric	a = 4.913 c = 5.405	Perfect	Perfect	Hard. Can be bent
11	4 9	α Quartz	SiO ₂	Hexagonal centrosymmetric	a = 4.913 c = 5.405	Perfect	Perfect	Hard. Can be bent
12	11	Graphite	C	Hexagonal	a = 2.456 c = 6.696	Very Poor	Fair	Soft, brittle
13	4	Potassium bromide	KBr	Cubic	a = 6.60	Fair	Good	Hard
14	1 12	Germanium	Ge	Cubic	a = 5.6575	Perfect	Perfect	Hard. Can be bent
15	4 6 5	Calcium fluoride (Fluorite)	CaF ₂	Cubic	a = 5.451	Good	Good	Hard
16	6 13	Silicon	Si	Cubic	a = 5.43808	Perfect	Perfect	Hard. Can be bent
17	8 5 14	Calcium carbonate (calcite)	CaCO ₃	Hexagonal	a = 4.989 c = 17.026	Almost Perfect	Perfect	Easily cleaved, bent
18	4 6 5	Rock Salt	NaCl	Cubic	a = 5.64	Fair	Good	Hard

* a, b, c, in °A (Ref. 16)

Table I. Properties of Crystals Frequently Used in X-ray Spectroscopy (Continued)

GENERAL INFORMATION								
No.	Ref.	Crystal	Chemical Composition	Crystal Structure	Lattice * Parameters	Perfection	Stability	Mechanical Properties
19	8 10 15	α Quartz	SiO ₂	Hexagonal centrosymmetric	a = 4.913 c = 5.405	Perfect	Perfect	Hard. Can be bent
20	5 4	Aluminum	Al	Cubic	a = 4.049	Almost Perfect	Good	Soft
21	5	Topaz (AlSilicate)	Al ₂ Si ₂ O ₄ (F, OH) ₂	Orthorhombic	a = 4.64 b = 8.78 c = 8.37	Good	Good	Soft
22	5	α Quartz	SiO ₂	Hexagonal centrosymmetric	a = 4.913 c = 5.405	Perfect	Perfect	Hard. Can be bent
23	4, 5 6 11	Lithium fluoride	LiF	Cubic	a = 4.028	Almost Perfect	Perfect	Hard, plastically bent
24	12	Germanium						
25	5	Fluorite						
26	13	Silicon						
27	14	Calcite						

* a, b, c, in Å (Ref. 16)

Table I. Properties of Crystals Frequently Used in X-ray Spectroscopy (Continued)

DIFFRACTION PROPERTIES															
No.	Ref.	Crystal	Reflection	Spacing 2d, Å	E(keV)**		F.W.H.M at θ				S at θ_B^\dagger P at θ_B^\dagger R _c 10 ⁵ rad at θ_B^\dagger				Fig.
					Min.	Max.	Min.	Max.	Min.	Max.	Min.	Max.	Min.	Max.	
1	1	Potassium acid Phthalate (KAP)	001	27.714#	.454	2.577	2.26'	9.9'	1380	.01	.34	7.5	17.5	13	
	2				18.5°	60°	45°	57.22°	7.46°	7.46°	57.22°				
	3														
2	1	Rubidium acid Phthalate (RAP)	001	26.12	.482	2.738	1.3'	4.64'	1780		Not Available		14		
					18.79°	55°	33°								
3	4	β Alumina	0002	22.49	.560	3.176			Not Available						
4	4 5	Mica (Muscovite)	002	19.884	.633	3.59			Not Available						
5	4 6	Gypsum	020	15.168	.830	4.708			Not Available						
6	4	β Alumina	0004	11.24	1.120	6.353			Not Available						
7	1 7	Ammonium dihydrogen phosphate ADP	101	10.659	1.180	6.699	.27'	1.46'	10460	.25		Not Available	12		
	24.71°				65.76°	45°	51.50°								
8	6	Ethylene diamine-D- tartrate EDDT	020	8.808	1.429	8.107			Not Available						
9	1 6 4	Pentaerythritol PET	002	8.726	1.445	8.180	.58'	1.30'	7640	.38	.80	Not Available	6		
	37.96°				70°	45°	76.95°	27.28°							
												9			

The value given in Ref. 17 is 2d = 26.633 Å

Table I. Properties of Crystals Frequently Used in X-ray Spectroscopy (Continued)

DIFFRACTION PROPERTIES															
No.	Ref.	Crystal	Reflection	Spacing 2d, Å	** min	*** max	**** min	**** max	† max	†† min	†† max	††† min	††† max	Fig.	
10	5, 8 9 10	α Quartz	10 $\bar{1}$ 0	8.512	1.485	8.423	.032' 4.77°	.97' 70.99°	20500 52.69°	.065 51.80°	.72 7.29°	1.04 4.77°	11 70.99	19 20	
11	4 9	α Quartz	10 $\bar{1}$ 1	6.7153	1.89	10.72	.046' 4.8°	1.32' 71.55°	11100 20.03°	.22 71.55°	.79 10°	1.6 4.8°	13.9 71.55°	21 22	
12	11	Graphite	002	6.696	1.879	10.75	41.4' 66.8°	87' 30.1°	~300	← Not Available →					← →
13	4	Potassium bromide	200	6.60	1.91	10.85	← Not Available →					← Not Available →			
14	1 12	Germanium	111	6.5327	1.927	10.93	0.91' 25°	3.35' 65°	6100 43°	0.40 65°	.67 15°				10 14
15	4 6 5	Fluorite	111	6.28	2.049	11.37	← Not Available →					← Not Available →			
16	6 13	Silicon	111	6.271	2.078	11.39	0.072' 6.4°	.62' 54.07°	11000 23.30°	.43 44.17°	.73 11.72°	2 6.4°	10.3 14.17°	23 24	
17	8 5 14	Calcium carbonate (calcite)	211	6.069	2.084	11.799	.0615' 6.72°	1.5217' 73.83°	15400 18.30°	.43 62.01°	.73 11.72°	2.4 6.72°	30.3 73.83°	25/26 27/28	
18	4 6 5	Rock Salt	200	5.64	2.23	12.66	← Not Available →					← Not Available →			

Table I. Properties of Crystals Frequently Used in X-ray Spectroscopy (Continued)

DIFFRACTION PROPERTIES															
No.	Ref.	Crystal	Reflection	Spacing 2d, Å	E _{min} , keV	E _{max} , keV	**** W _{min}	**** W _{max}	† S _{max}	†† P _{min}	†† P _{max}	††† Rc _{min}	††† Rc _{max}	†††	Fig.
19	8 10 15	α Quartz	1120	4.912	2.563	14.537	.038' 6.53°	.46' 69.35°	31200 23.14°	.17 69.35	.55 18.22°	55 6.53°	3.24 69.35		25- 32
20	5 4	Aluminum	111	4.66	2.70	15.323				Not Available					
21	5	Topaz (Al Silicate)	200	4.638	2.715	15.393				Not Available					
22	5	α Quartz	2020	4.246	2.96	16.818				Not Available					
23	4, 5 6 11	Lithium fluoride	200	4.028	3.132	17.76				Not Available					
24	12	Germanium	220	4.00	3.147	17.85	.0731 7.2	.836' 57.8°	12800 16.15°	.42 16.15°	.68 20.37°	1.7	23.4 57.8°		33 34
25	5	Fluorite	022	3.84	3.279	18.59				Not Available					
26	13	Silicon	220	3.8399	3.279	18.59	.038' 7.5°	.231 51.55°	29200 30.3°	.49 7.5°	.68 22.62°	.89 7.5°	6.03 51.55°		35 36
27	14	Calcite	422	3.034	4.15	23.536	.0131 13.53°	0.651 64.97°	63946 30.5°	.241 64.97°	.491 13.59°	.37 13.53°	.91 64.59°		26 28

Table I. Properties of Crystals Frequently Used in X-ray Spectroscopy (Continued)

DIFFRACTION PROPERTIES													
No.	Ref.	Crystal	Reflection	Spacing $2d, \text{\AA}$	E_{\min} keV	E_{\max} keV	W _{min}	W _{max}	S _{max}	P _{min}	P _{max}	R _{c min}	R _{c max} Fig.
28	6	Lithium fluoride	220	2.848	4.421	25.07	←	←	←	Not Available	←	←	←
29	4 8	α Quartz	2023	2.806	4.487	25.45	.017' 11.73	.47' 40.58	87173 34.07	.52 40.58	.67 34.07	.31 11.73	.91 40.58 37 38
30	6 15	Topaz	303	2.712	4.643	26.331	←	←	←	Not Available	←	←	←
31	6	α Quartz	2240	2.451	5.137	29.134	←	←	←	Not Available	←	←	←
32	8	α Quartz	2243	2.024	6.221	35.28	.0083' 15.98°	.018' 38.97°	144000 32.22	.58 38.97	.61 15.98	.19 15.98	.45 38.97 39 40
33	14	Calcite	633	2.02	6.233	35.35	.018' 20.54°	.033' 49.56°	122000 49.56	.48 49.56	.49 20.54	.34 20.54	.63 49.56 26 28

** The value of the minimum (maximum) energy, assuming maximum (minimum) feasible Bragg angle 80° (10°).

*† The reported value of the FWHM in minutes (top); the Bragg angle θ_B at which the FWHM has been measured (bottom).

The resolution of a double crystal spectrometer $S(E/\Delta E)$ (top); θ_B (bottom).

‡ The peak reflectivity P (top); P_B (bottom).

The integrated reflectivity R_c in 10^{-5} radians (top); θ_B (bottom).

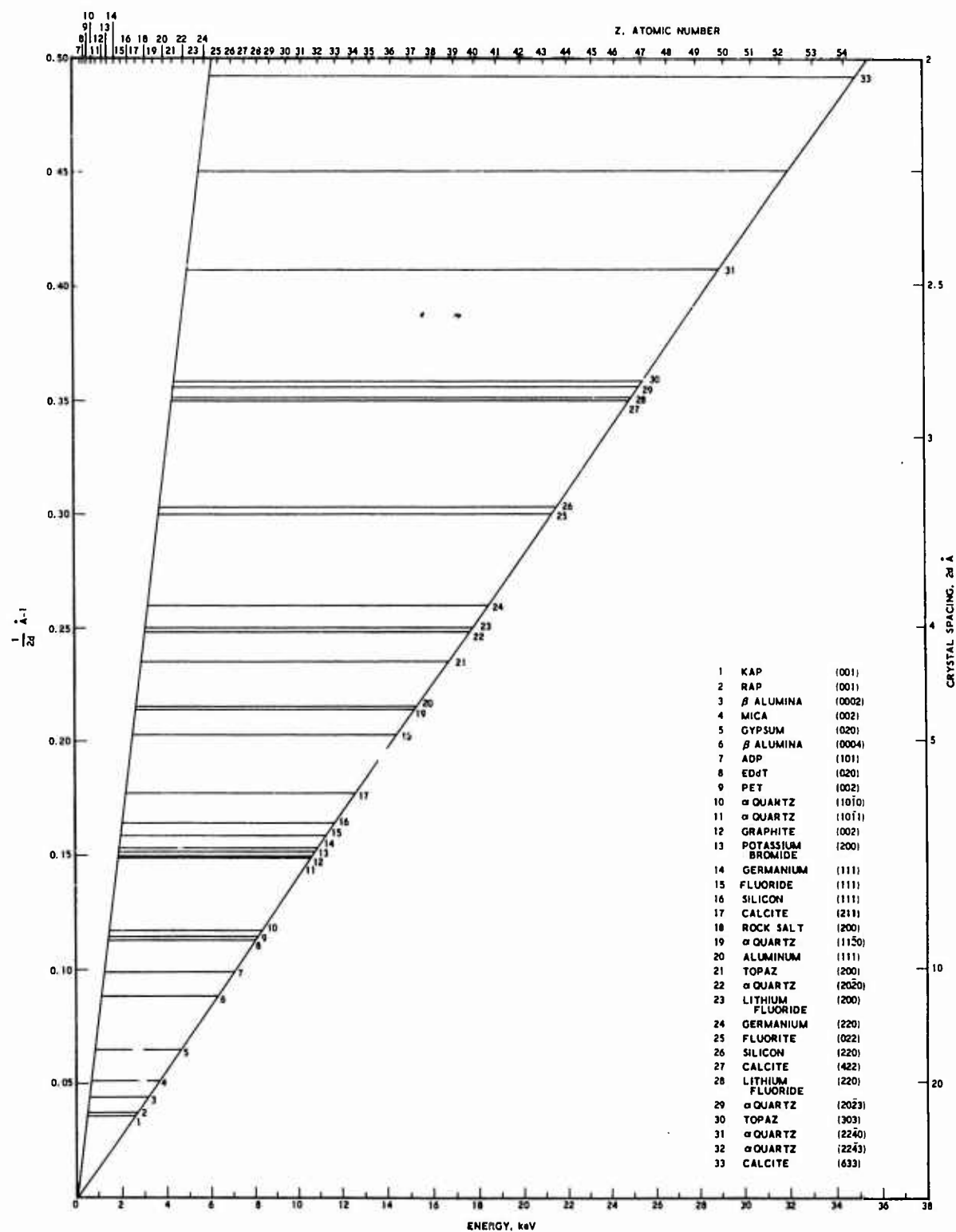


Figure 18. Spectral region in energy (bottom scale) or in elements K-absorption edge (top scale) covered by a single flat crystal spectrometer as a function of 2d spacing for a number of crystals.

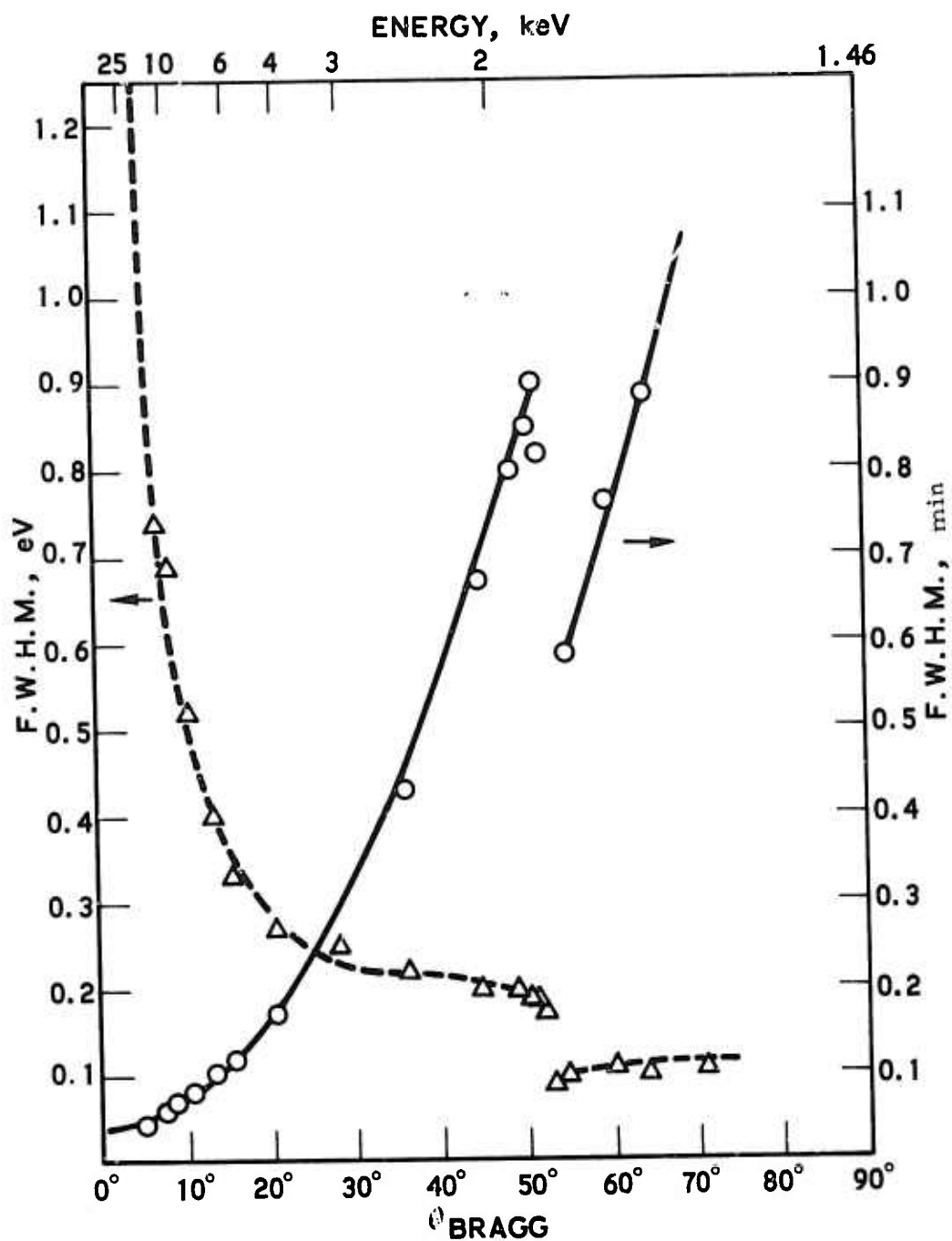


Figure 19. F.W.H.M. of (1010) quartz. Solid line in minute $\times \sqrt{2}$ (right-hand scale), dashed line in eV (left-hand scale) as a function of the Bragg angle (bottom) or as a function of x-ray energy (top). The experimental data are reported by G. Brogren⁽⁹⁾.

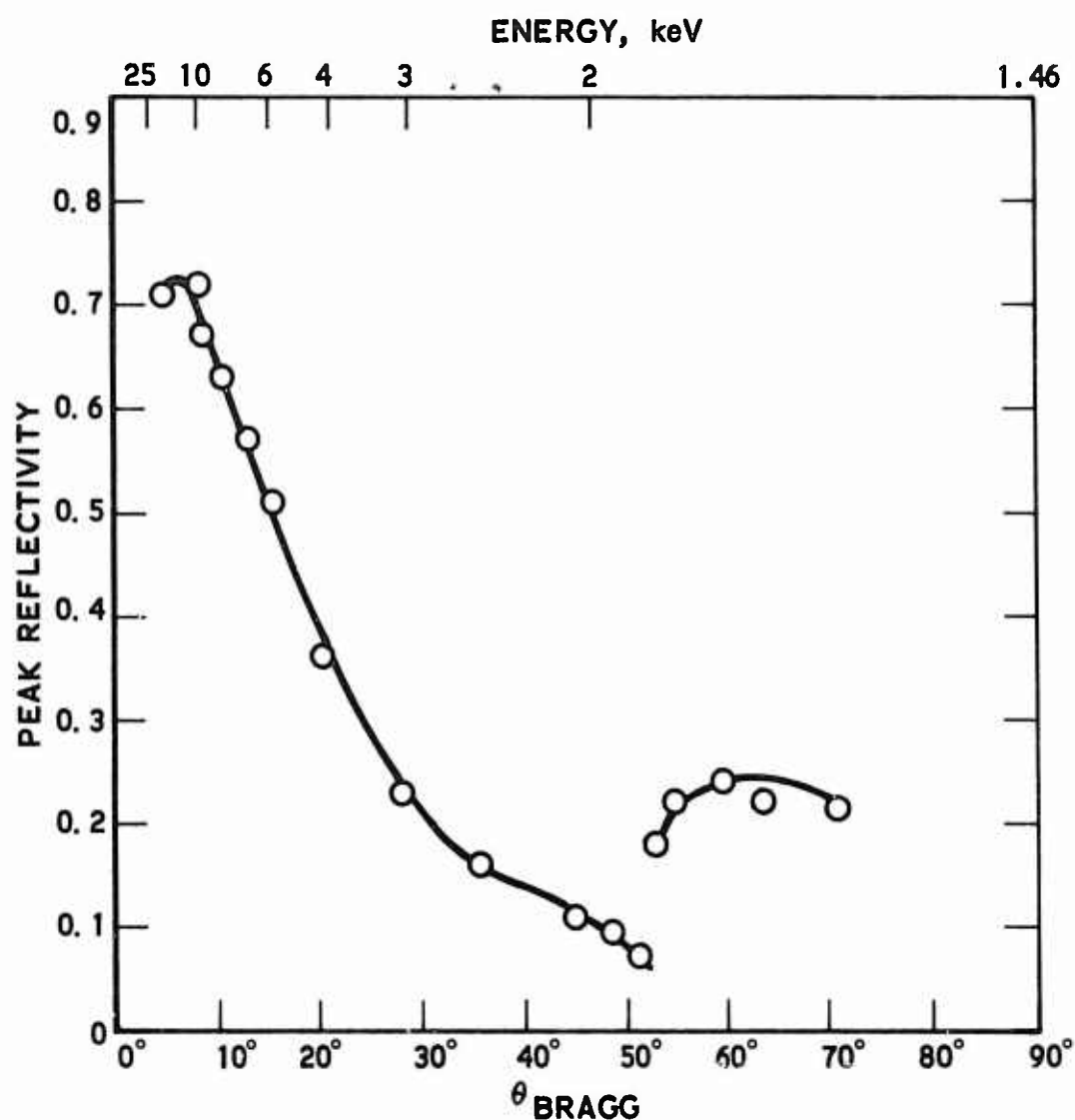


Figure 20. The peak reflectivity of $(10\bar{1}0)$ quartz as a function of the Bragg angle (bottom) or as a function of x-ray energy (top). The experimental data are reported by G. Brogren.⁽⁹⁾

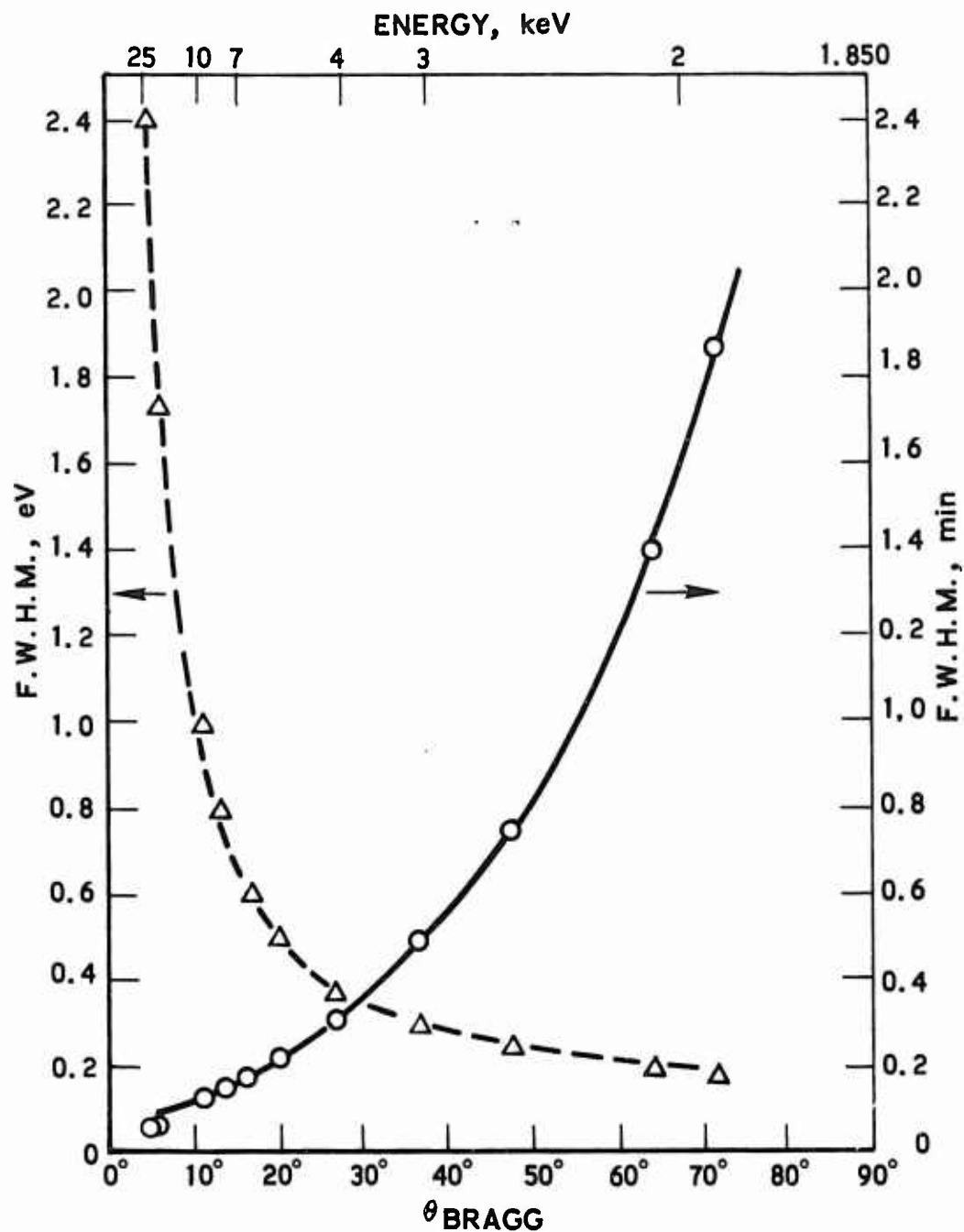


Figure 21. $\sqrt{2} \times \text{F.W.H.M.}$ of $(10\bar{1}\bar{1})$ quartz. The experimental data are reported by G. Brogren⁽⁹⁾.

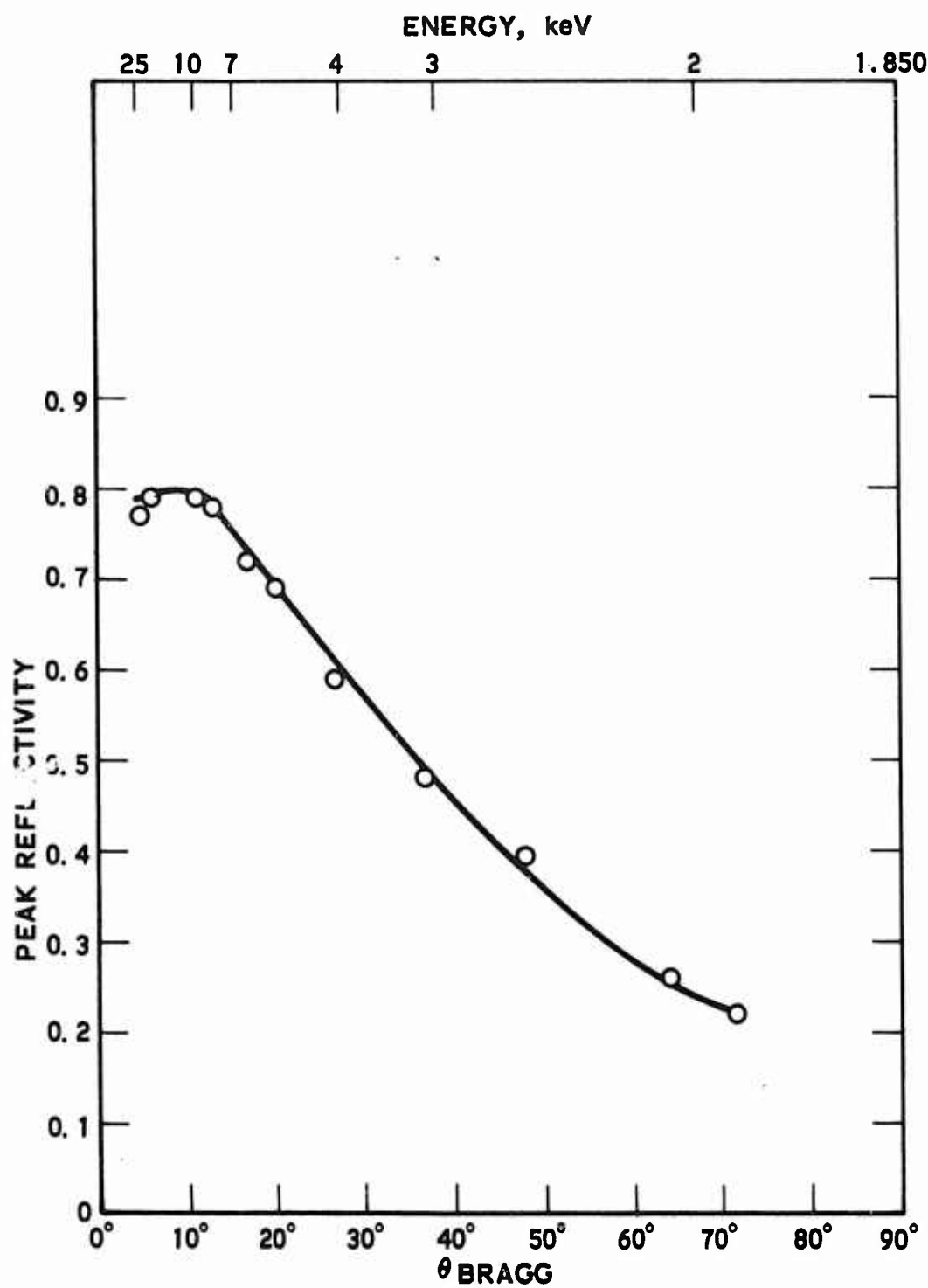


Figure 22. The peak reflectivity of (1011) quartz. The experimental data are reported by G. Brogren⁽⁹⁾.

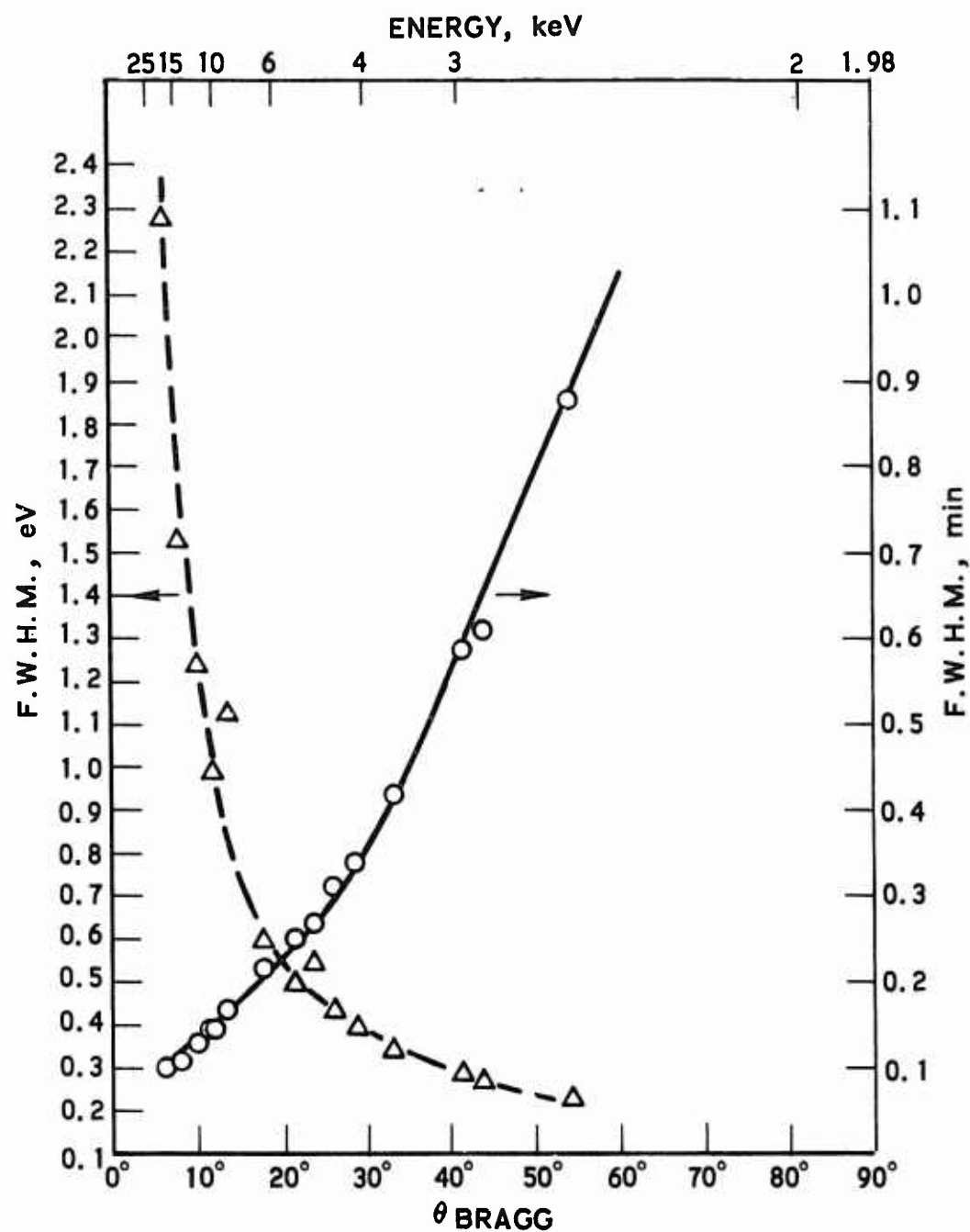


Figure 23. $\sqrt{2} \times \text{F.W.H.M.}$ of (111) silicon. The experimental data are reported by Brogren⁽¹³⁾.

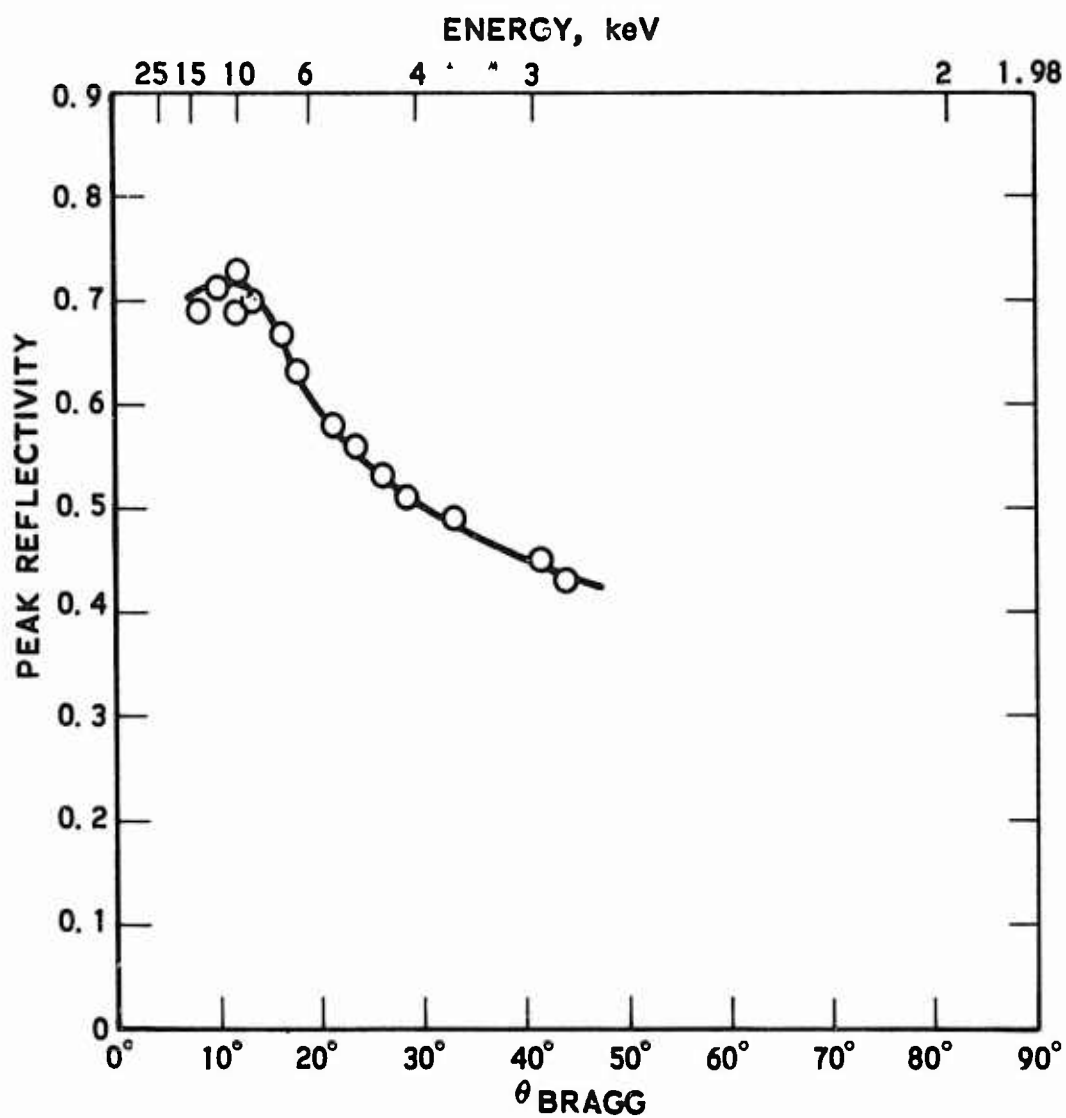


Figure 24. The peak reflectivity of (111) silicon. The experimental data are reported by Brogren et al⁽¹³⁾.

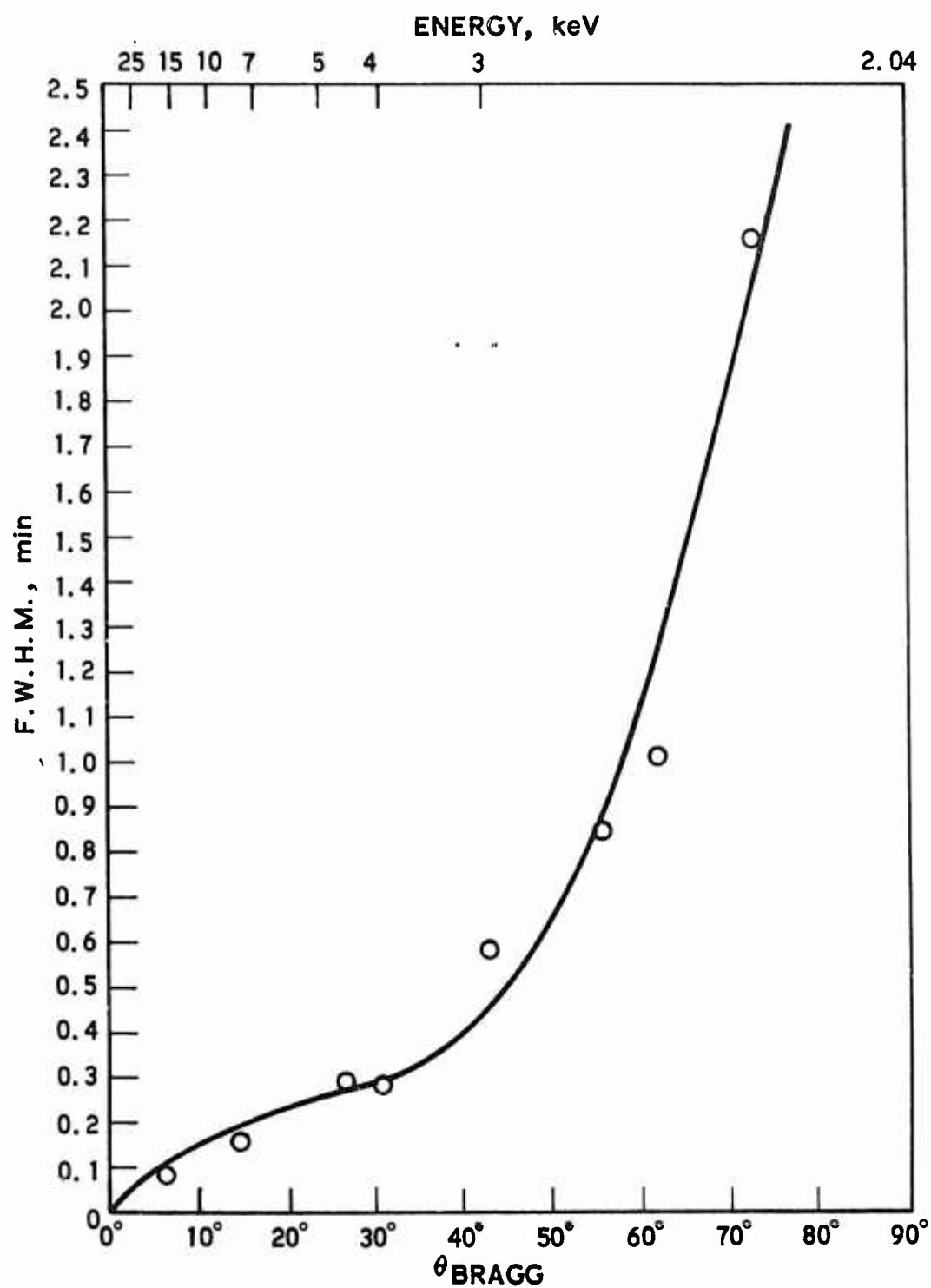


Figure 25. $\sqrt{2} \times \text{F.W.H.M.}$ of (211) calcite in minutes as a function of the Bragg angle (bottom scale) or as a function of the x-ray energy (top) scale. The experimental data are reported by Paratt et al⁽¹⁴⁾.

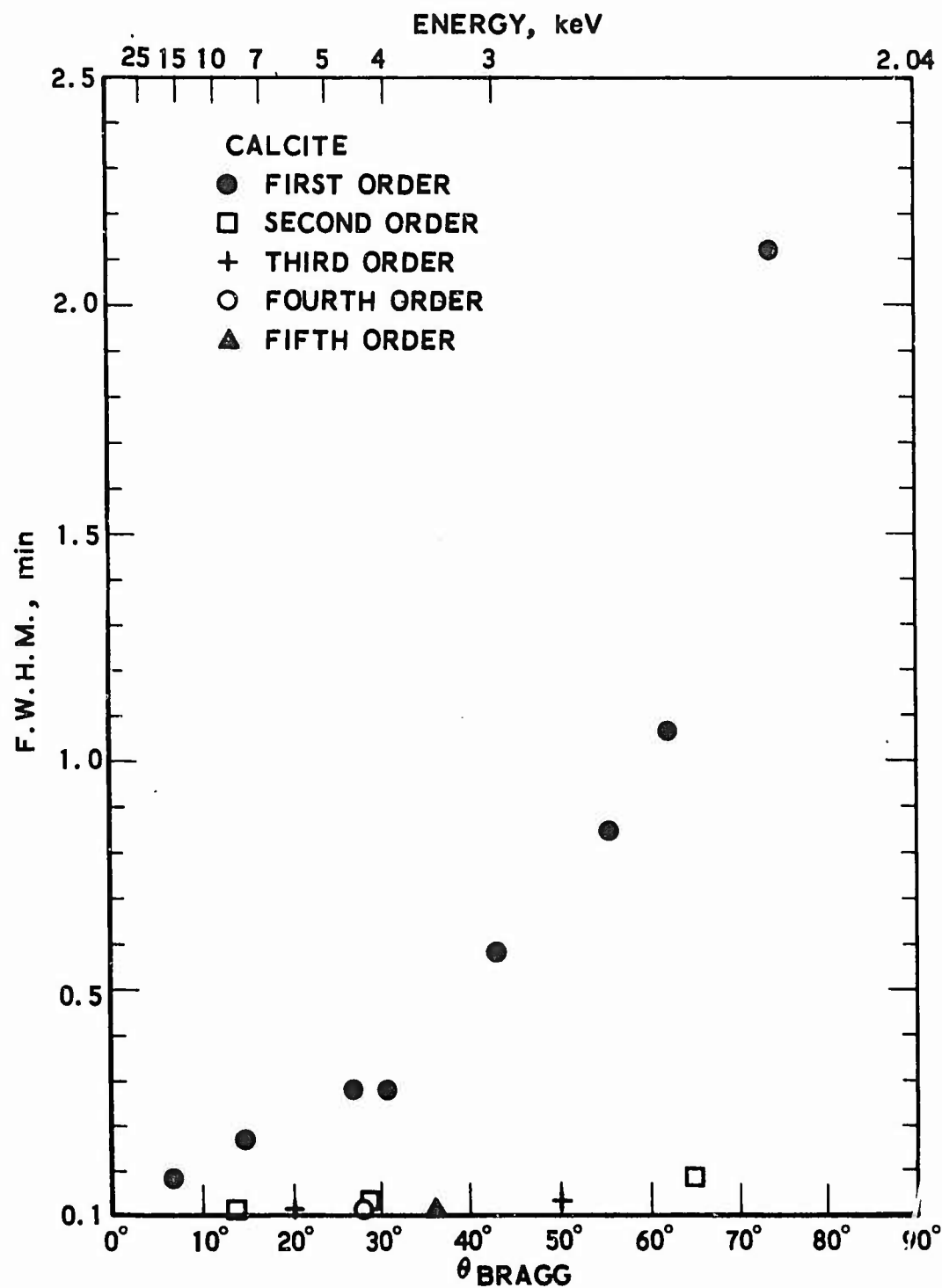


Figure 26. $\sqrt{2} \times \text{F.W.H.M.}$ for calcite (211) at first, second, third, fourth and fifth order of reflection. Notice the decrease in intensity with the increase of the reflection order. Data reported by Parrat et al⁽¹⁴⁾.

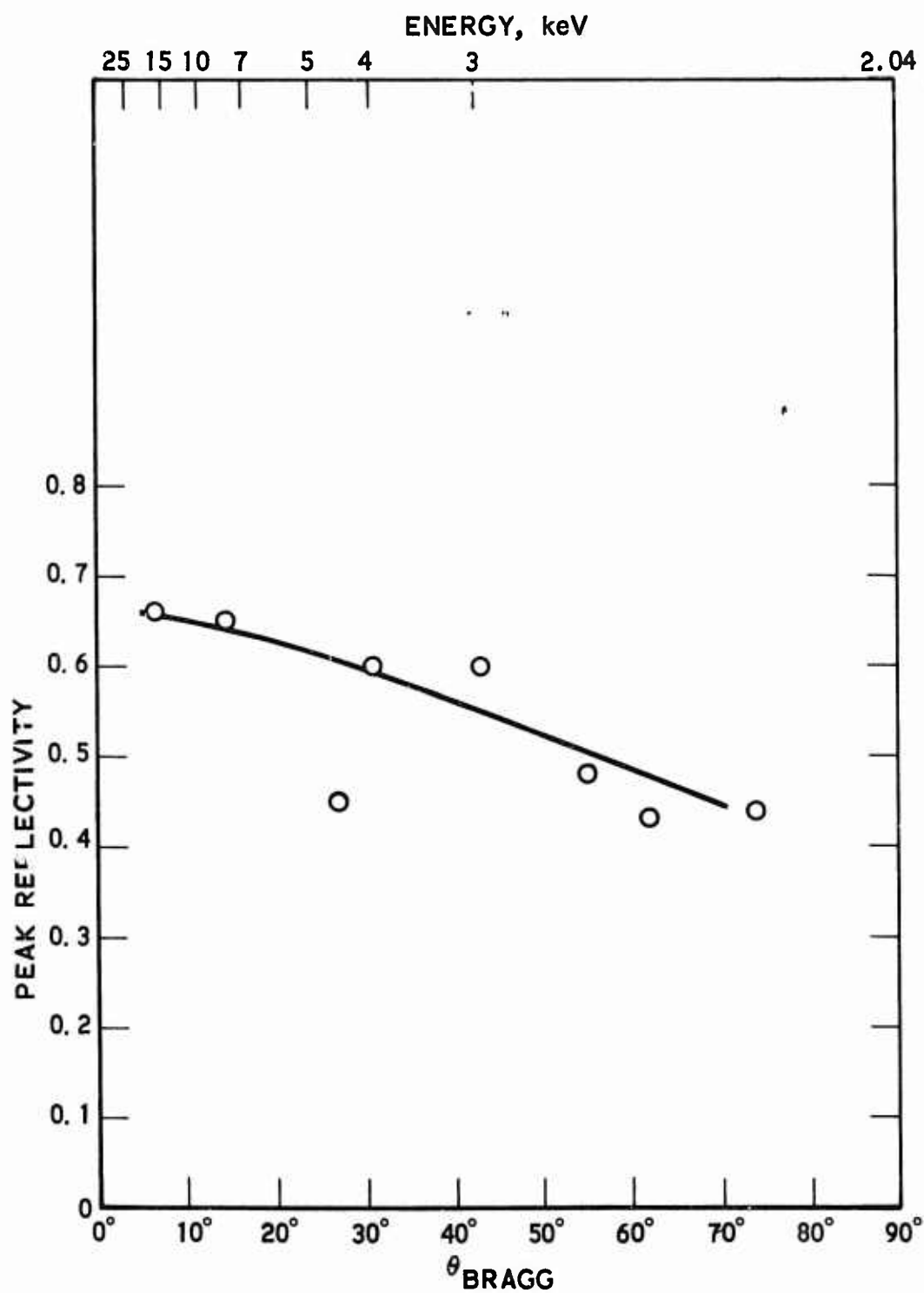


Figure 27. The peak reflectivity of (211) calcite. Data reported by Paratt et al⁽¹⁴⁾.

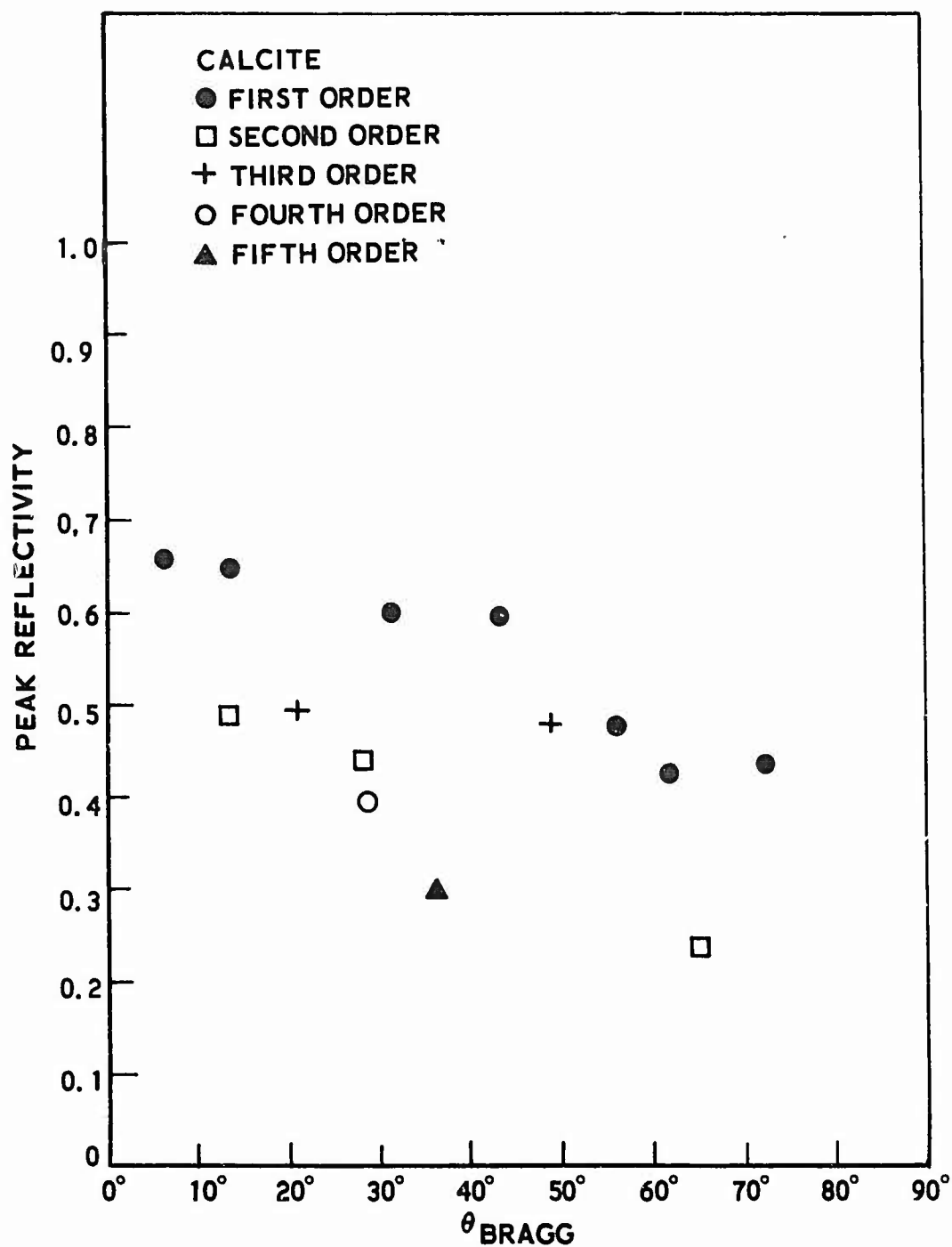


Figure 28. The peak reflectivity of (211) calcite for a number of reflection. Data reported by Paratt et al⁽¹⁴⁾.

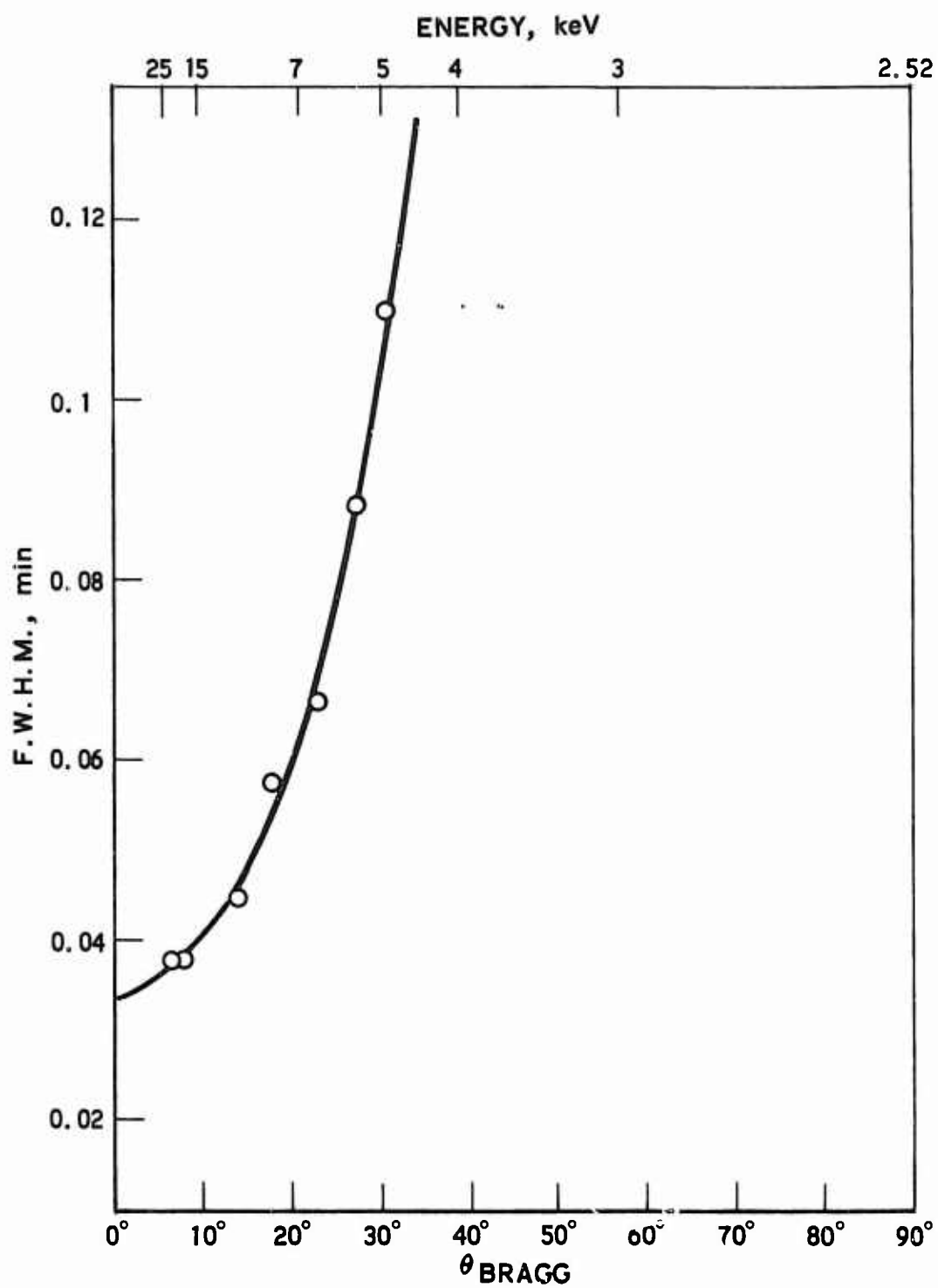


Figure 29. The F.W.H.M. of $(11\bar{2}0)$ quartz. Data are reported by Brogren⁽¹⁰⁾.

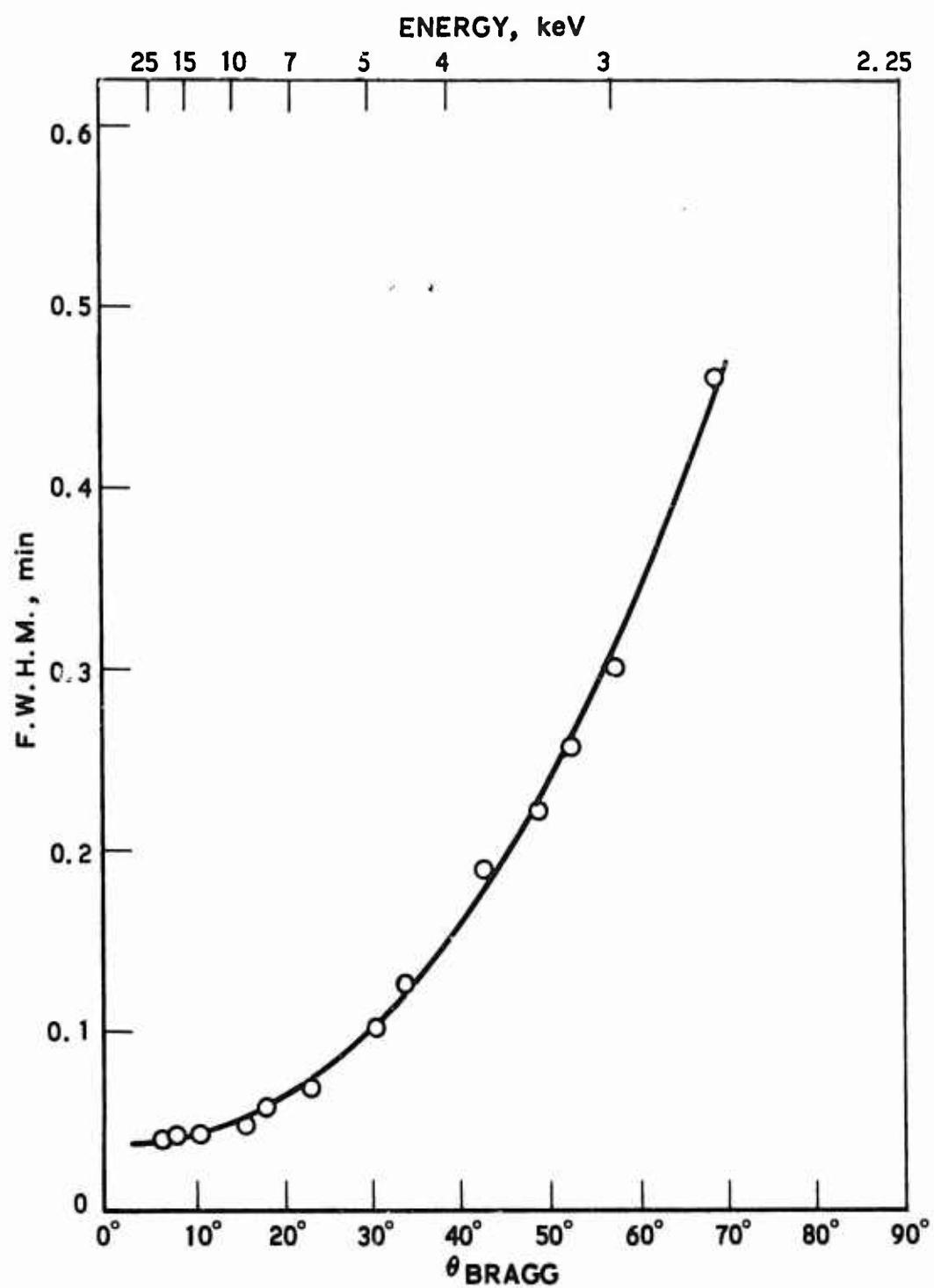


Figure 30. The F.W.H.M. of $(11\bar{2}0)$ quartz. Data are reported by Parratt⁽¹⁵⁾.

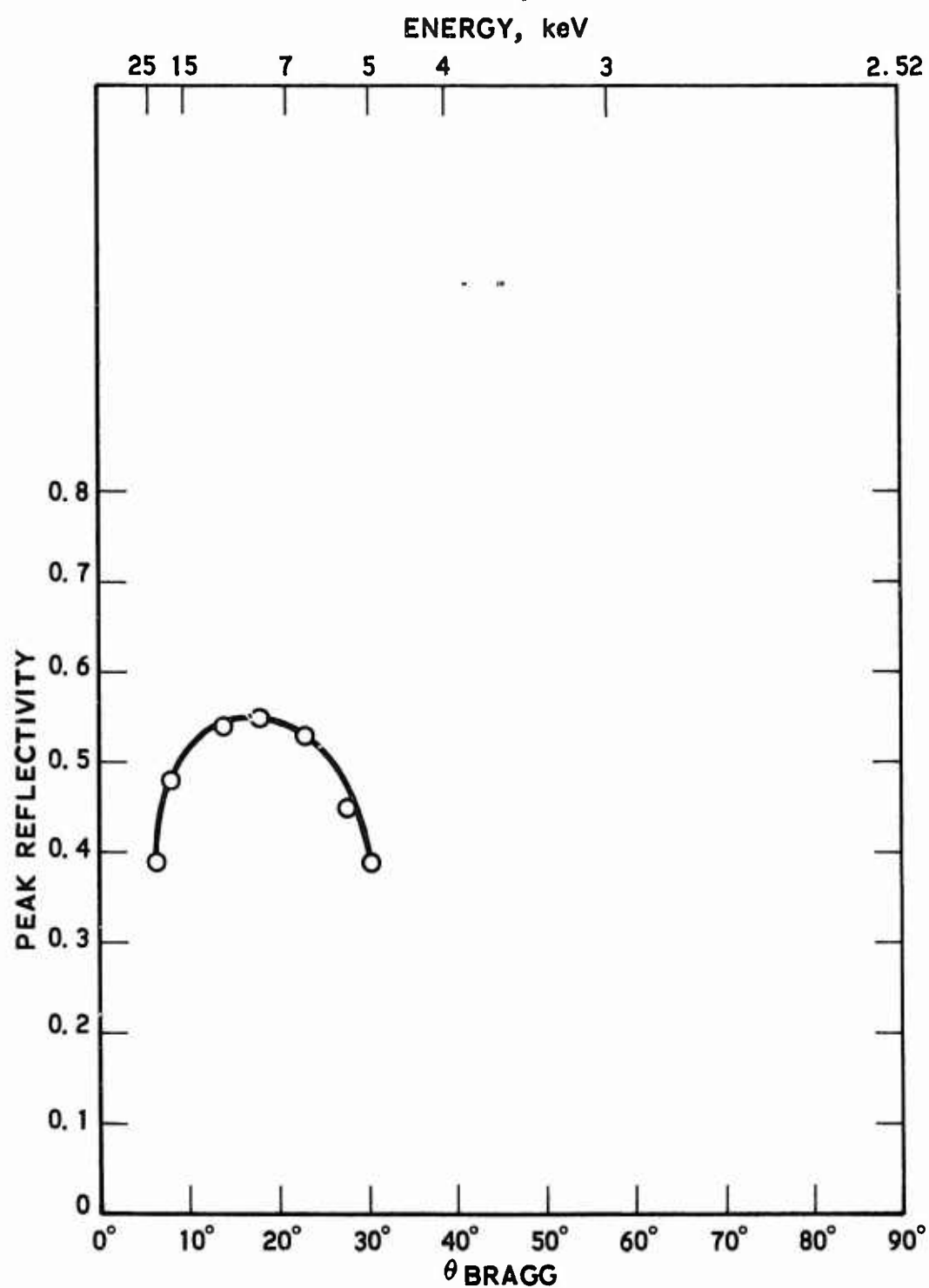


Figure 31. The peak reflectivity of (1120) quartz. Data are reported by Brogren⁽¹⁰⁾.

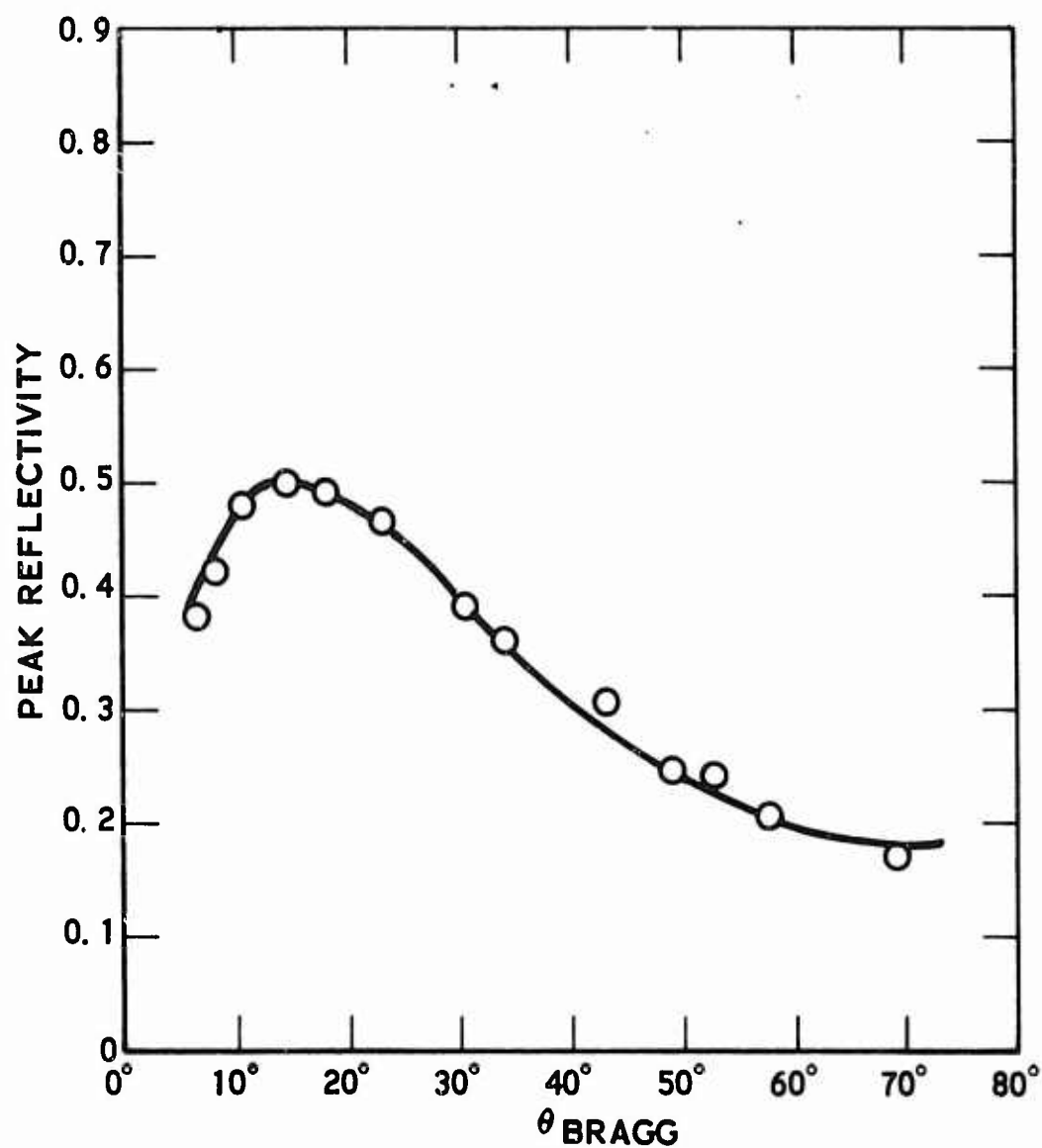


Figure 32. The peak reflectivity of $(11\bar{2}0)$ quartz. The data are reported by Parratt⁽¹⁵⁾.

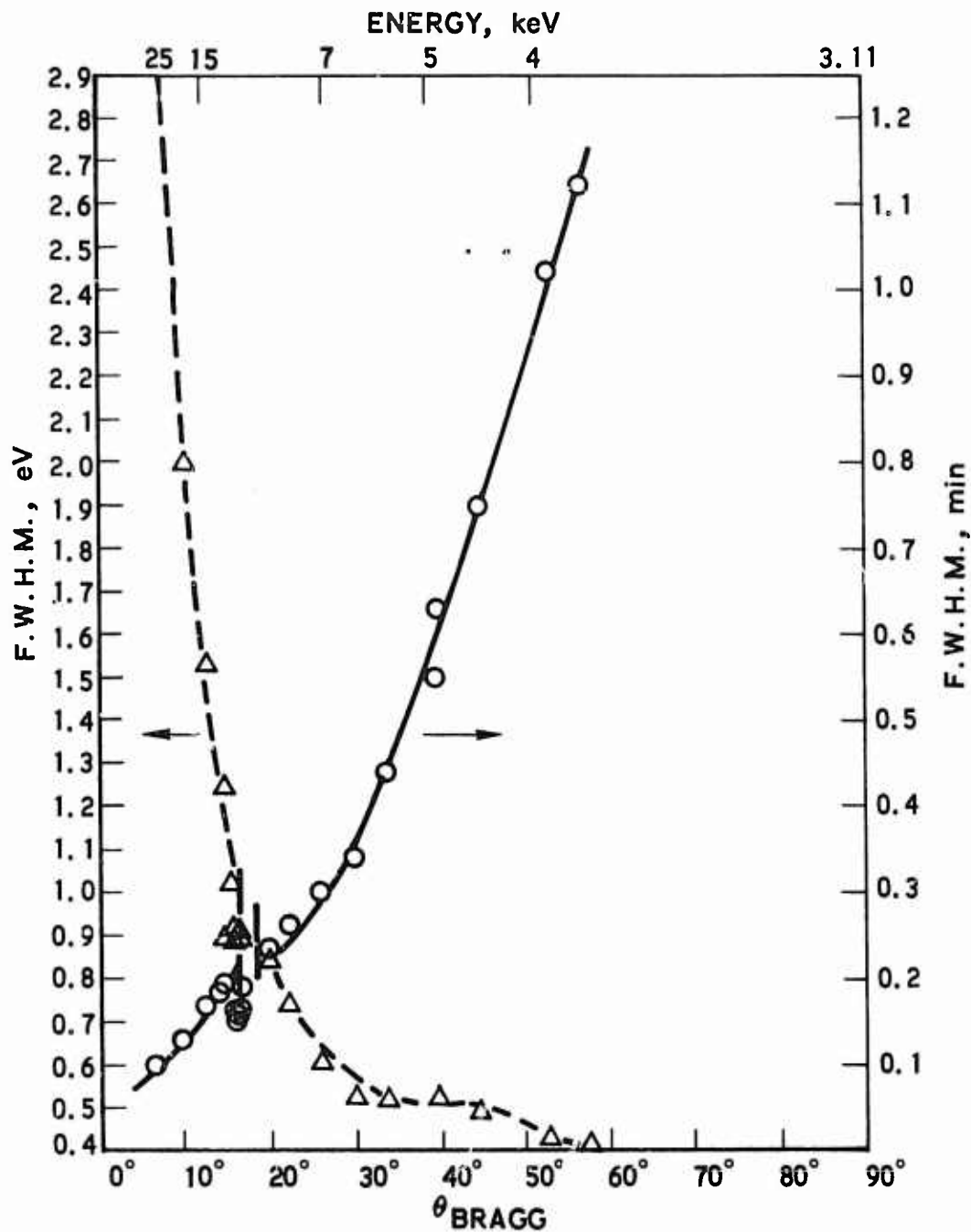


Figure 33. The F.W.H.M. of (220) Germanium. Solid line (F.W.H.M. $\times \sqrt{2}$) in minutes (right-hand scale); dashed line in eV (left-hand scale). The data are reported by Brogren et al⁽¹²⁾.

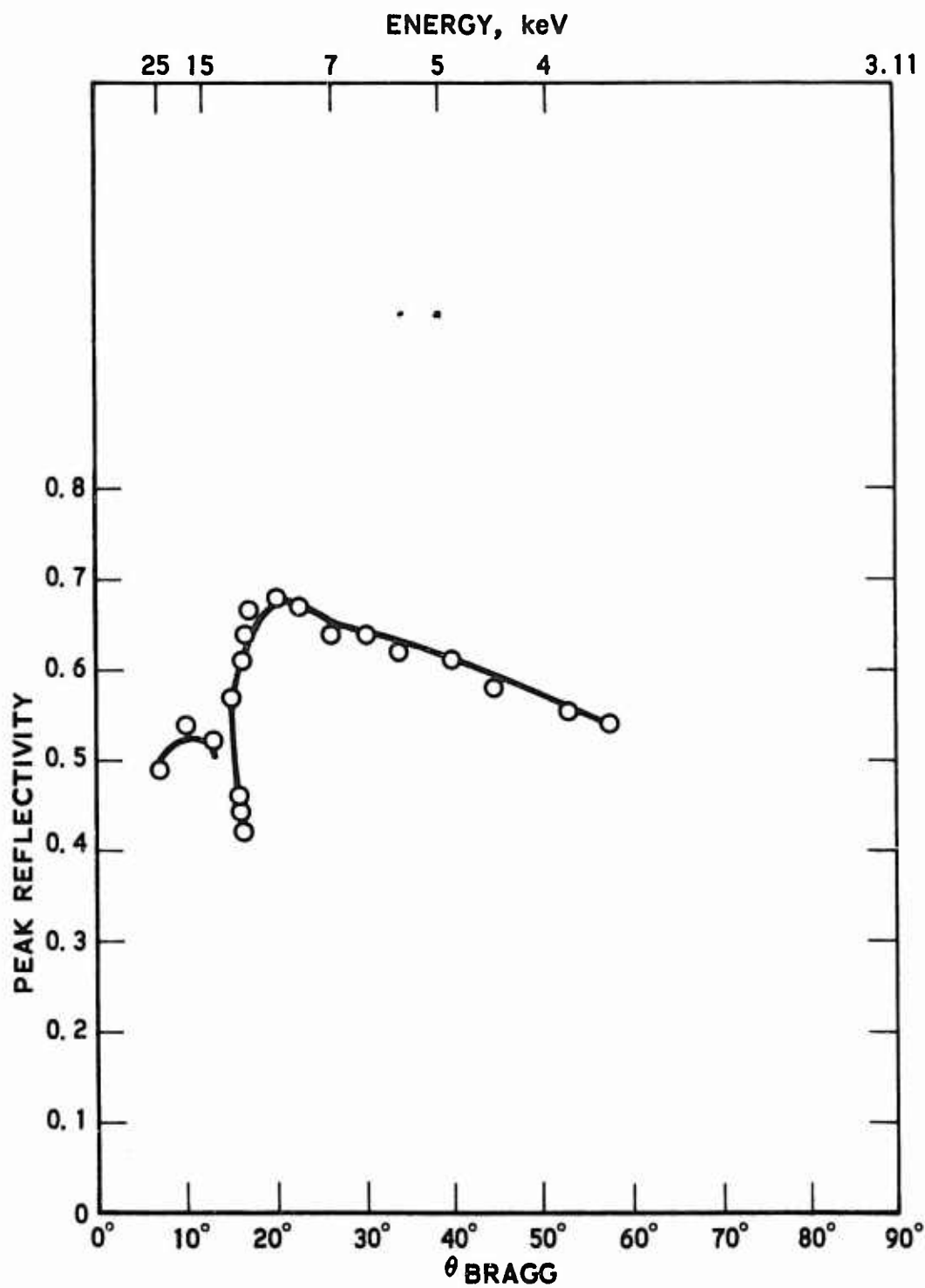


Figure 34. The peak reflectivity of (220) Germanium. The data are reported by Brogren et al⁽¹²⁾.

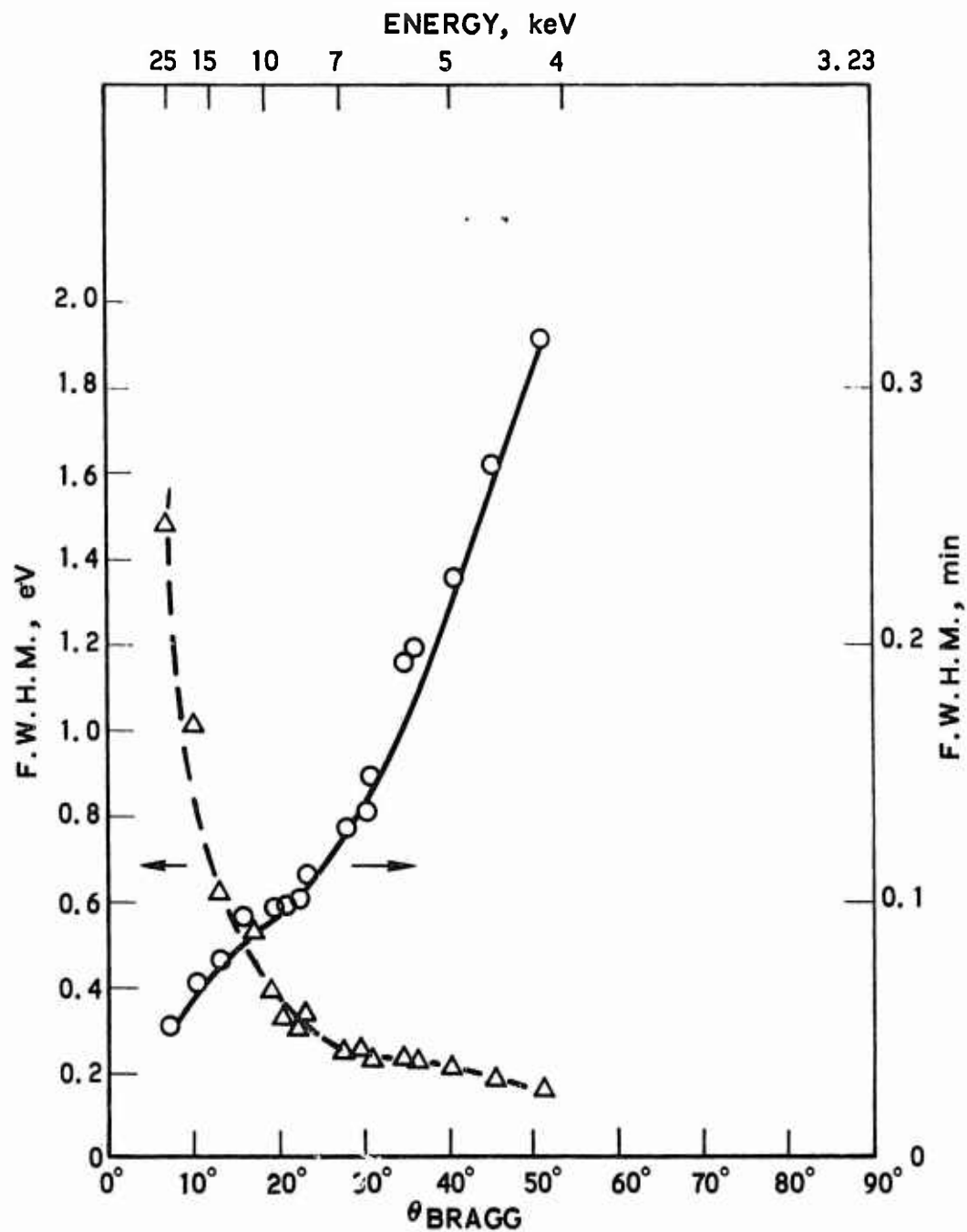


Figure 35. $\sqrt{2} \times$ F.W.H.M. of (220) silicon reported by Brogren et al⁽¹³⁾.

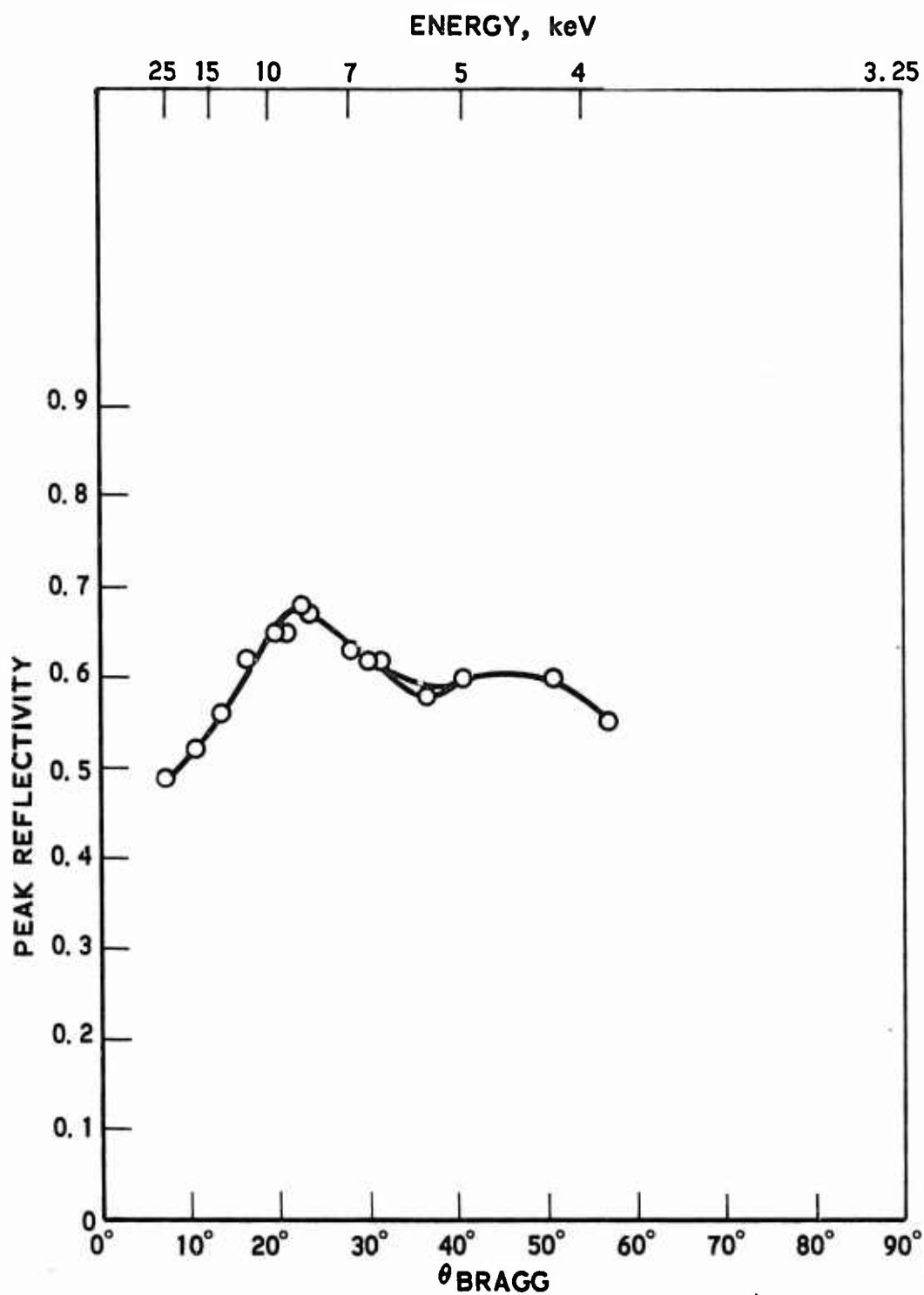


Figure 36. The peak reflectivity of (220) silicon reported by Brogren et al⁽¹³⁾.

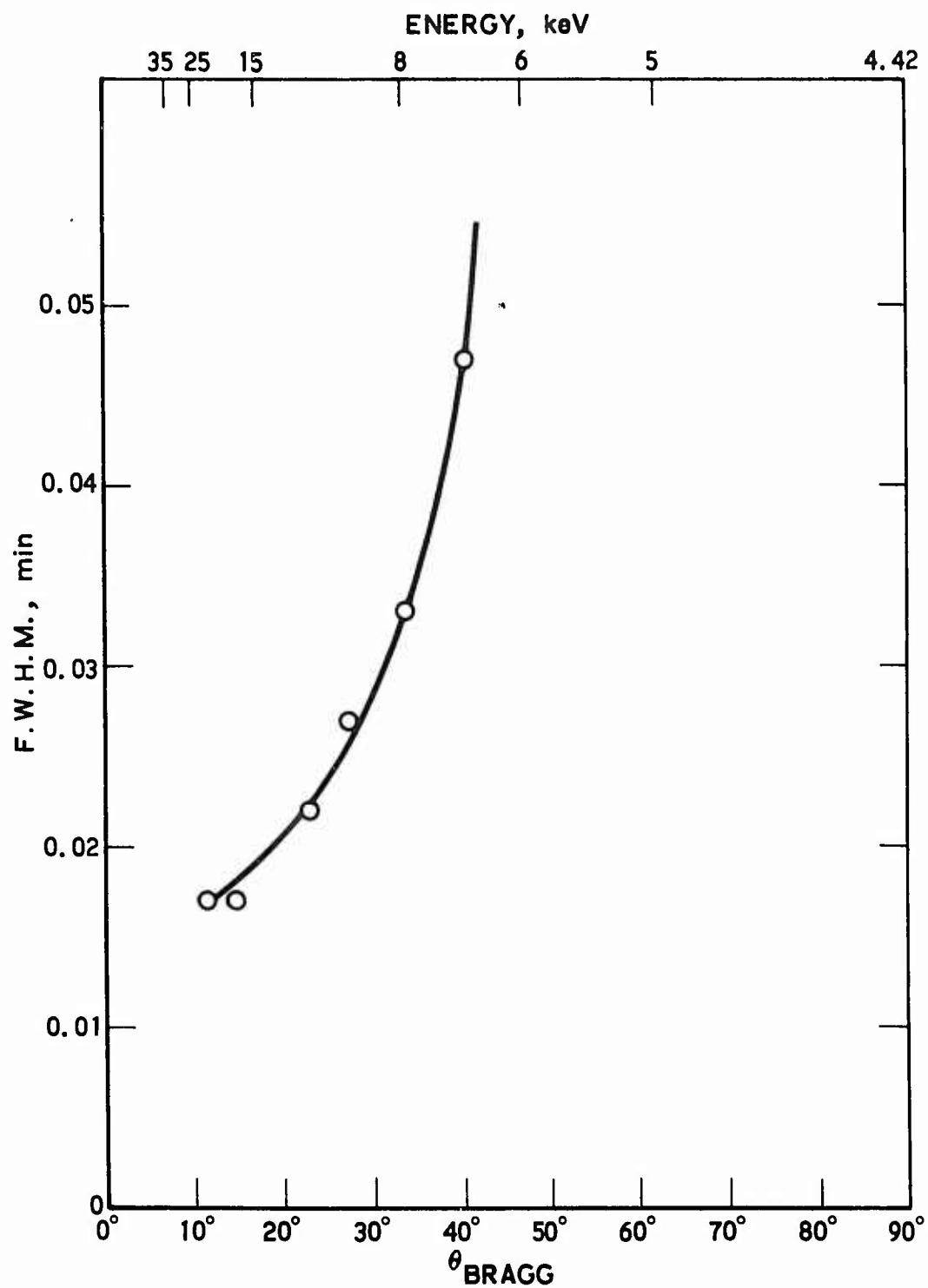


Figure 37. $\sqrt{2} \times \text{F.W.H.M.}$ of $(20\bar{2}\bar{3})$ quartz in minutes reported by Adell et al⁽⁸⁾.

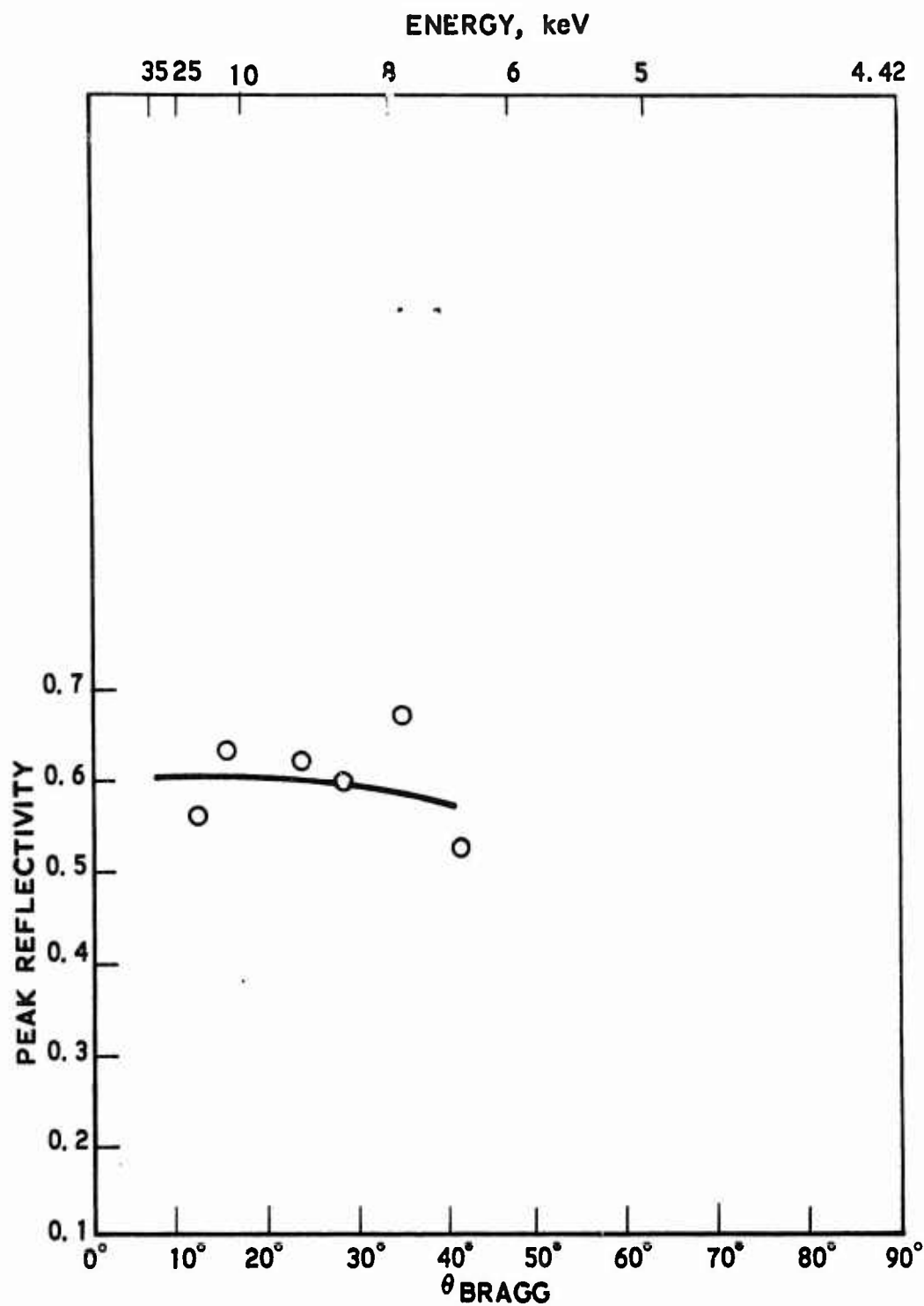


Figure 38. The peak reflectivity of $(20\bar{2}3)$ quartz reported by Adell et al⁽⁸⁾.

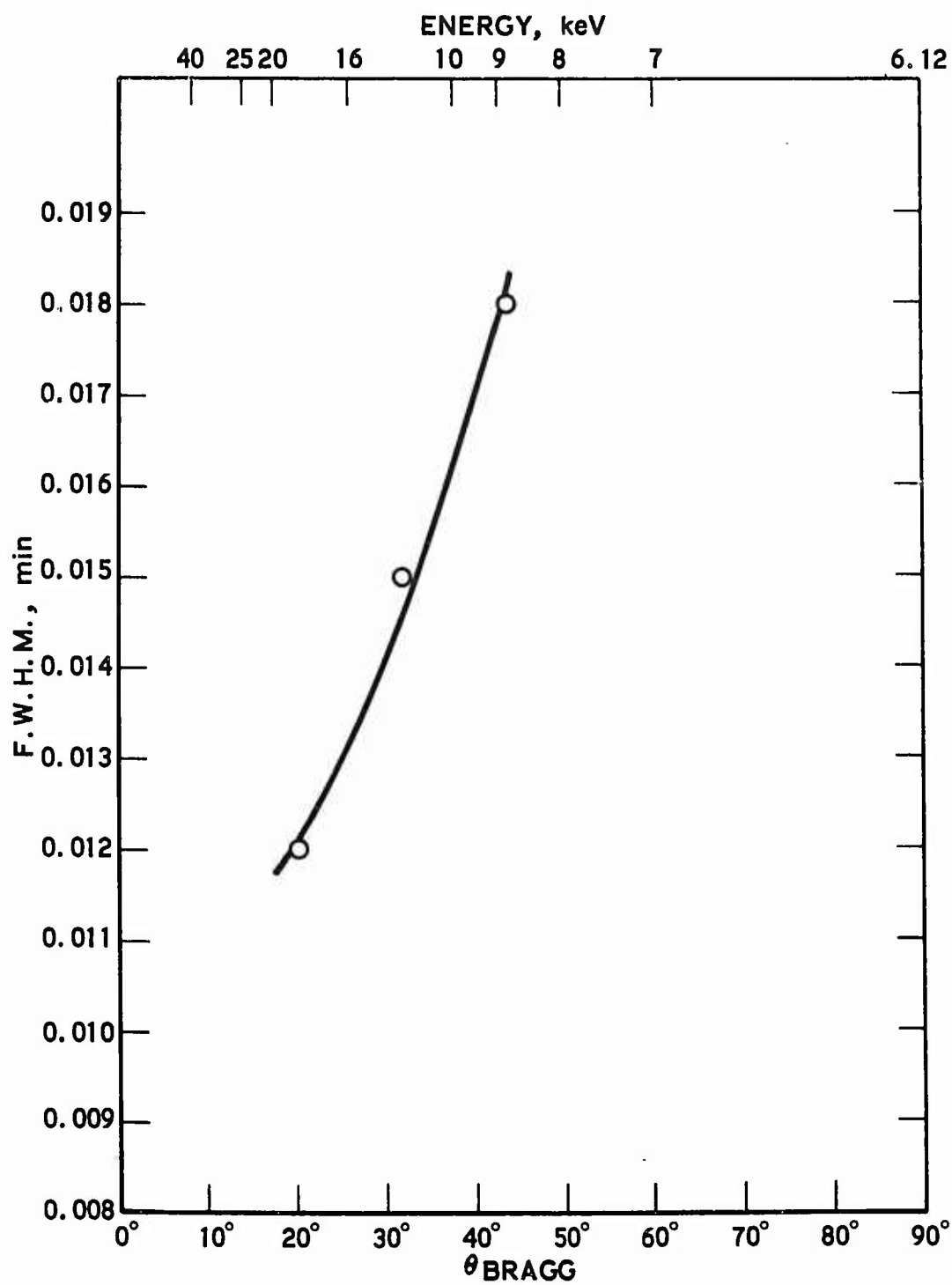


Figure 39. F.W.H.M. $\times \sqrt{2}$ of (2243) quartz in minutes reported by Adell et al⁽⁸⁾.

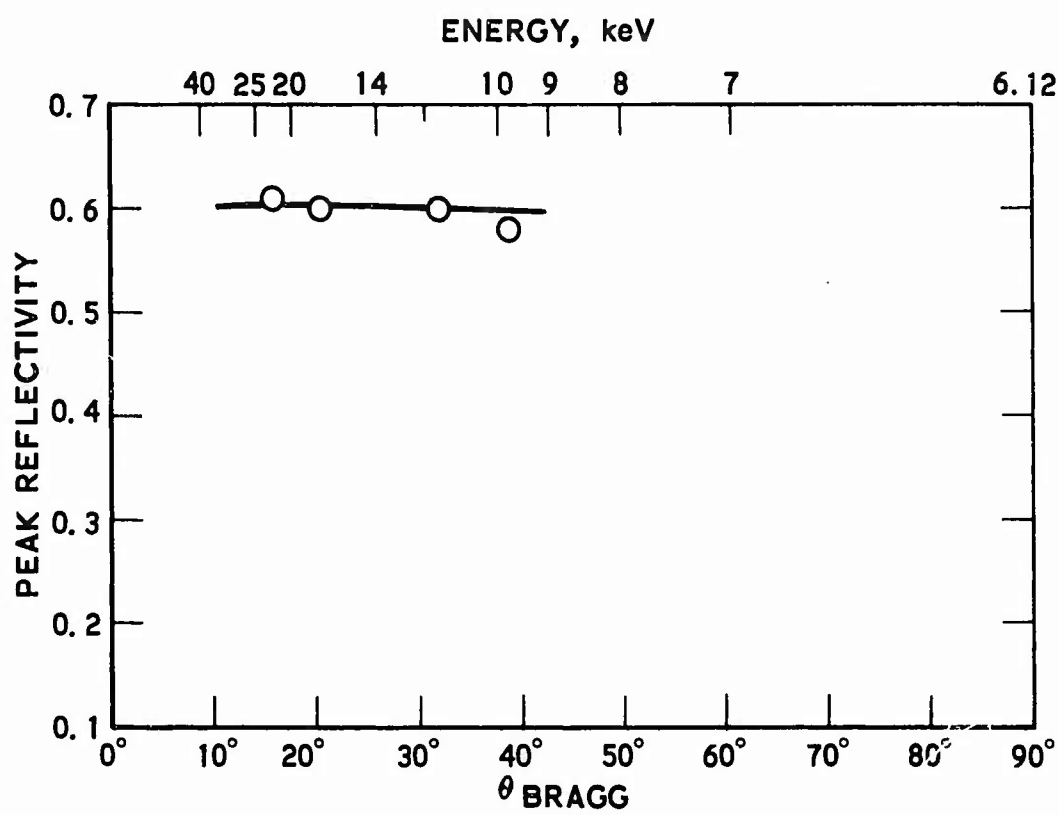


Figure 40. The peak reflectivity of (2243) quartz reported by Adell et al⁽⁸⁾.

REFERENCES

1. N. G. Alexandropoulos, G. G. Cohen, Crystals for Stellar Spectrometers, Appl. Spectrosc. March-April (1973) (Part I of this Report).
2. R. J. Liefeld, S. Hanzely, T. B. Kibby, and D. Mott, X-ray Spectrometric Properties of Potassium Acid Phthalate Crystals, ADV. X-RAY ANAL. 13, 373-381 (1970).
3. B. L. Henke, R. E. Lent, Some Recent Work in Low Energy X-ray and Electron Analysis, ADV. X-RAY ANAL. 12, 480-495 (1969).
4. W. Parrish, B. W. Roberts, Filter and Crystal Monochromator Techniques, International Tables for X-ray Crystallography III, 73-88 (1962), The Kynoch Press, Birmingham.
5. M. A. Blokhin, Methods of X-ray Spectroscopic Research, Pergamon Press (1965).
6. R. O. Muller, Spectrochemical Analysis by X-ray Fluorescence, Plenum Press, New York (1972).
7. R. D. Deslattes, J. L. Torgesen, B. Paretsky and A. T. Horton, Preliminary Studies on the Characterization of Solution-Grown ADP Crystals, ADV. X-RAY ANAL. 8, 315-324 (1965).
8. O. Adell, G. Brogren, and L. E. Haeggbloom, The X-ray Diffraction Quartz, Arkiv for Fysik 7, 197-211 (1953).
9. G. Brogren, The Reflection Properties of the 1010 Plane in Quartz, Arkiv for Fysik 22, 267-275.
10. G. Brogren, The X-ray Diffraction from Quartz and the Influence of the Surface Treatment, Arkiv for Fysik 6, 321-334 (1953).
11. J. Vierling, J. V. Gilfrich, and L. S. Birks, Improving the Diffraction Properties of LiF: Comparison with Graphite, Appl. Spect. 23, 342-345, (1969).
12. G. Brogren, E. Hornstrom, The X-ray Reflection Properties of Germanium Single Crystals, Arkiv for Fysik 23, 81-85 (1962).
13. G. Brogren, E. Linden, The X-ray Diffraction Properties of Silicon Single Crystals, Arkiv for Fysik 22, 535-541 (1962).

Preceding page blank

14. L. G. Parratt, F. Miller, X-ray Diffraction with Calcite in Several Orders of Reflection, Phys. Rev. 49, 280-288 (1936).
15. L. G. Parratt, Practicality of Etched Quartz Crystals for X-ray Spectrometers, Rev. Sci. Inst. 5, 395-400 (1934).
16. R. W. G. Wyckoff, Crystal Structures, 2nd Ed. 1963, Interscience Publishers, Inc., New York.
17. A. T. Bearden, F. N. Huffman, Precision Measurement of the Cleavage Plane Grating Spacing of Potassium Acid Phthalate, Rev. Sci. Inst. 34, 1233-1234 (1963).

PART III. MULTI-PURPOSE TRIPLE CRYSTAL SPECTROMETER

INTRODUCTION

In this third part of this report a triple x-ray crystal spectrometer is described. There exists a considerable literature on the alignment and the theory of double crystal spectrometers, but little information on the alignment and theory of triple crystal spectrometers is available. It is, however, worthwhile to mention a useful graphical method introduced by DuMond. The method is simple and permits the definition, with some degree of accuracy, of the passband and the efficiency of a multi-crystal spectrometer. This approach to the understanding of a triple crystal spectrometer is considerably easier for the beginner than an approach utilizing analytic functions at the outset.

The method basically consists in the construction of a transparency for each crystal and a way to superimpose these transparencies. The transparency consists of a line described by the Bragg equation $2d \sin \theta = n\lambda$. The line thickness is proportional to the F.W.H.M. of the crystal rocking curve at a given wavelength and the line darkness is proportional to the peak reflectivity for the same wavelength. The transparencies of two crystals overlap in such a way that the angle axis is consistent in the parallel position (1-1) the angles increasing in the same direction, while in the antiparallel position they increase in opposite directions. In both cases, the distance between the origins of the two transparencies is equal to the dihedral angle between the crystals. In playing with these transparencies, it is easy to see some of the properties of a multi-crystal spectrometer.

CONSTRUCTION OF A MULTI-CRYSTAL SPECTROMETER

The spectrometer described below is the triple crystal spectrometer built for high resolution measurements making use of commercially available angular orientation devices. It can be used for a number of applications. Fig. 41 is the sideview of the spectrometer without the x-ray tube.

The chassis consists of an aluminum ($40 \times 40 \times 1.5$ in.) plate, P_1 , with two axes A_1 , A_2 attached on. The arm Ar_1 , which rotate around axis A_1 , supports the x-ray tube; the arm Ar_2 supports the second crystal, the axis for the third crystal and the stepping system. The arm's angular position is defined by the verniers $V_{1.1}$, $V_{2.1}$. The $A_{1.1}$ and $A_{2.1}$ supports of the first and second crystal rotate inside the axes of A_1 and A_2 , respectively. The stainless steel plates $P_{1.1}$, $P_{2.1}$, the verniers $V_{1.2}$, $V_{2.2}$ and long arms (for precise rotation) $Ar_{1.1}$, $Ar_{2.1}$ are all screwed on to each of these axes ($A_{1.1}$, $A_{2.1}$). The plates support the Lansing translation stages $L.T.S_1$ and $L.T.S_2$. The Lansing Angular Orientation Device, which is supported by the translation stages, has the crystal holders mounted on its center (not shown in the figure). The axis A_3 is supported on the other end of arm Ar_2 . The arm $Ar_{3.1}$ which is on the A_3 axis supports the detector D. The arm $Ar_{3.2}$, a long arm for precise rotation, and the vernier $V_{3.1}$ are also attached to A_3 . Inside the A_3 axis, the A_3 axis has an assembly similar to that above the other axes A_1 and A_2 , i. e., the plate $P_{3.1}$, the Lansing translation stage $L.T.S_3$, the Lansing Orientation Device $L.A.O.D_3$, the vernier $V_{3.2}$, and the arm $Ar_{3.3}$ are all attached to the $A_{3.1}$ axes. Fig. 42 is a view from the top of the arm Ar_2 and shows the parts attached to it. The detector and the third crystal are rotated in a θ -2 θ motion with the help of the arms $Ar_{3.2}$, $Ar_{3.3}$ the micrometer M_4 and the stepping motor $S.M._1$.

The Fig. 42 shows a top view of the arm Ar_2 with the assembly for the second and third crystal and also the micrometers and the additional arms.

Preceding page blank

APPLICATIONS

High Resolution Spectrometer

The addition of a third crystal to a double crystal spectrometer mainly increases the dispersion and improves resolution to some extent, specifically in the tails of emission lines. However, the instrument has been used thus far as a double crystal spectrometer in the study of the spectra of scattered radiation. Using a set of two perfect crystals (333) planes a resolution of 25000 has been observed. Most of the measurements were carried out using a set of cleaved calcite crystal with a resolution of 5000. The sample under investigation was placed in the first crystal holder which was especially to shield the primary beam.

X-Ray Topography

The system is ideal for accurate topographical work. The crystal under investigation is placed in the third crystal position with the first two crystals functioning as monochromator and collimators. A motor attached on micrometer $M_{3.1}$ provides the crystal translation necessary to obtain a scanning topograph. For an oscillating topograph, the oscillation is provided by the third crystal fine rotation system and the step Motor S.M. $_1$.

Other Uses

A number of measurements can be carried out using the system and supporting the crystal sample in the second crystal holder. Such measurements are: the refractive index, the phonon distribution, Brillouin scattering.

Preceding page blank

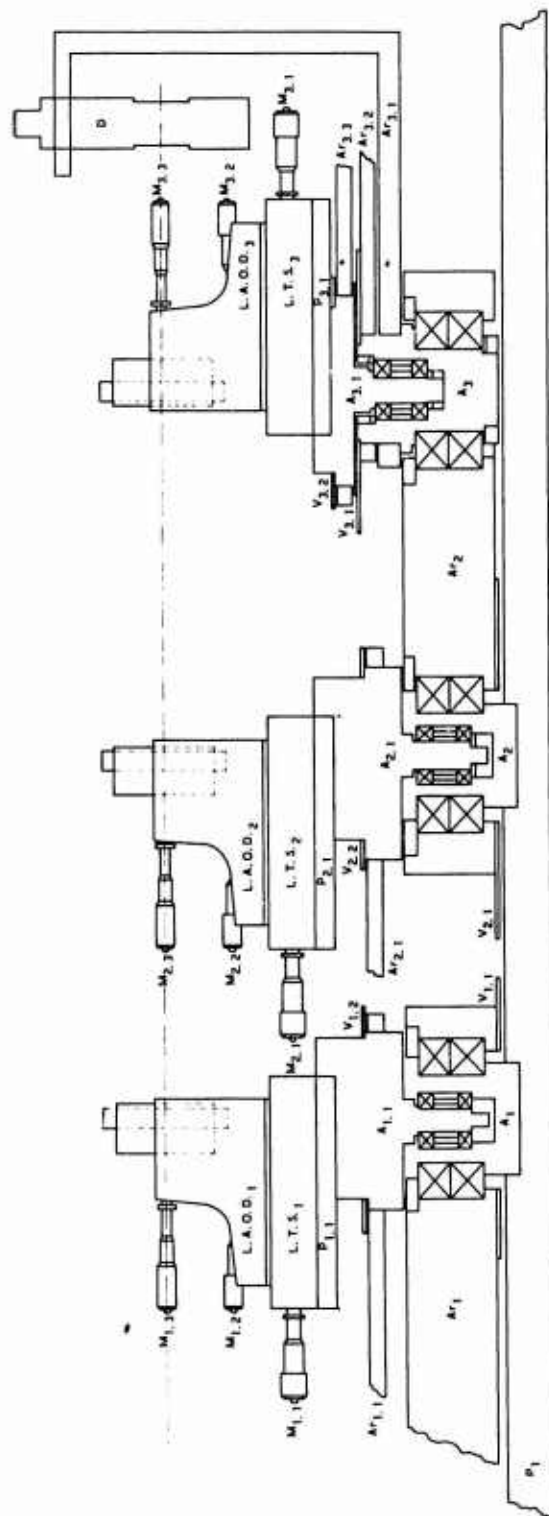


Figure 41. Sideview of the Triple Crystal Multi-Purpose Spectrometer

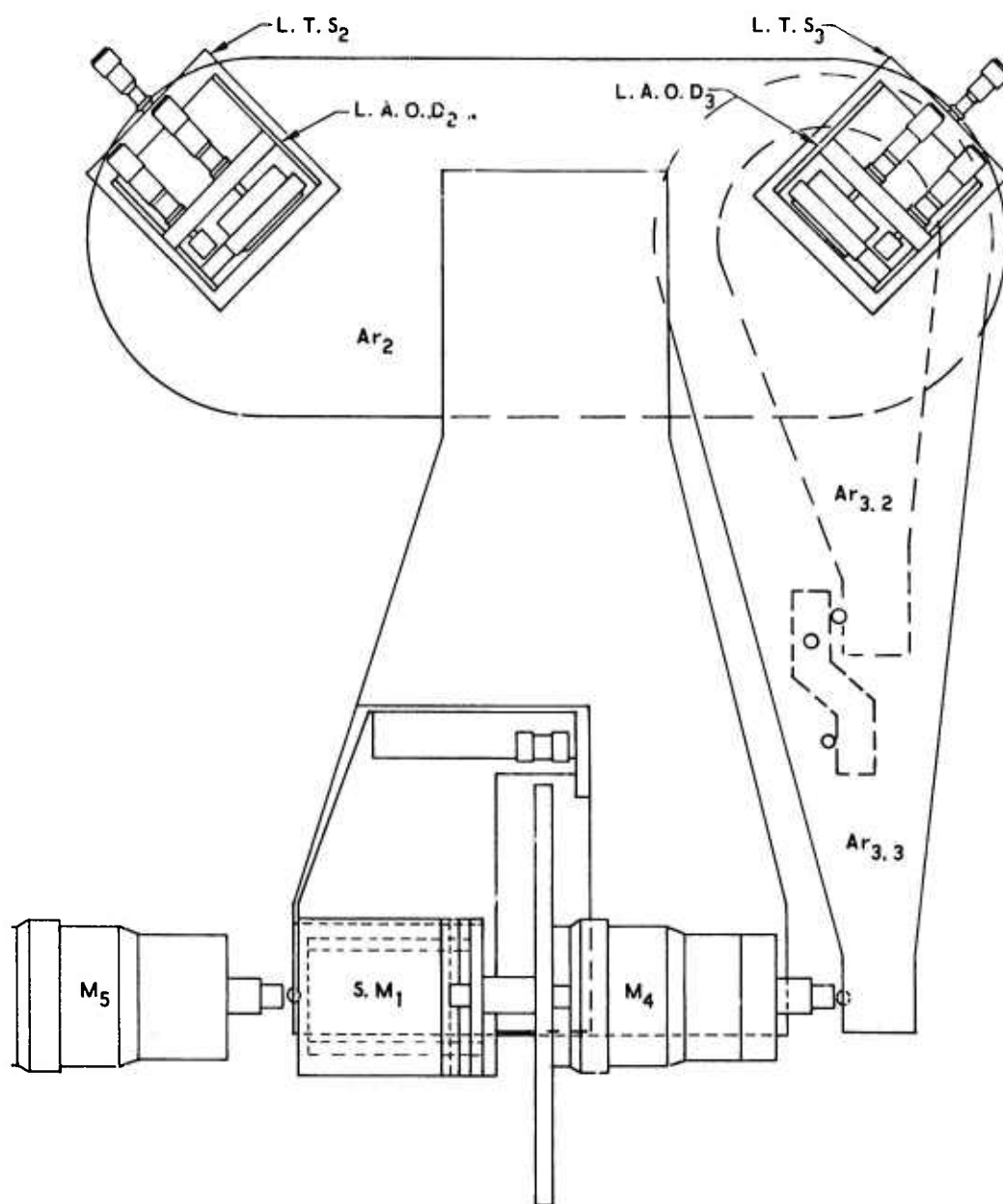


Figure 42. Top View of Arm Ar_2